

New τ -based evaluation of the hadronic contribution to the vacuum polarization piece of the muon anomalous magnetic moment

J. A. Miranda ^{*1} and P. Roig ^{†1}

¹Departamento de Física, Centro de Investigación y de Estudios Avanzados del IPN, Apdo. Postal 14-740,07000 Ciudad de México, México.

Abstract

We revisit the isospin-breaking and electromagnetic corrections to the decay $\tau^- \rightarrow \pi^-\pi^0\nu_\tau$, which allow its use as input in the two-pion contribution to the (leading order) hadronic vacuum polarization part of the muon anomalous magnetic moment. We extend a previous resonance chiral Lagrangian analysis, which included those operators saturating the next-to-leading order chiral low energy constants, by including the contributions appearing at the next order. As a result, we improve agreement between the two-pion tau decay and e^+e^- data and reduce the discrepancy between experiment and the SM prediction of a_μ (using τ input) to the $\sim 2\sigma$ level.

Introduction

The anomalous magnetic moment of the (first electron, and then) muon ($a_\mu \equiv (g_\mu - 2)/2$) has been crucial for the development of quantum field theory and the understanding of radiative corrections within it. Over the years, it has validated those computed in QED at increasing precision and (in the muon case) started probing the other Standard Model sectors, electroweak and QCD, setting also -and more interestingly- stringent constraints on new physics contributions. In the absence of any direct hint for heavy new particles or interactions at the LHC, clean observables both from experiment and theory -among which a_μ stands out- are reinforced as a promising gate for the eagerly awaited further (indirect) discoveries in high-energy physics.

With the forthcoming measurement of a_μ at FNAL [1] we will finally have an experimental update on the long-standing discrepancy (at 3 to 4 sigmas) between the SM prediction of this

^{*}jmiranda@fis.cinvestav.mx

[†]proig@fis.cinvestav.mx

observable (recently refined in [2]) ¹ and its most accurate measurement, at BNL [45]. On the theory side, a tremendous effort driven by the Muon g-2 Theory Initiative ² has been reducing (and making more robust) the SM errors during the last few years, in order to profit maximally from the new data. In the near future, both the FNAL [1] and the J-PARC [46] experiments will shrink the current experimental uncertainty ($63 \cdot 10^{-11}$) by a factor four. A commensurate improvement on the theory error is essential in maximizing the reach on new physics of these measurements.

The SM uncertainty on a_μ ($43 \cdot 10^{-11}$) is saturated by that of the hadronic contributions, where the error of the dominant hadronic vacuum polarization (HVP,LO) part has been reduced to $40 \cdot 10^{-11}$, versus $17 \cdot 10^{-11}$ of the light-by-light piece [2]. In turn, the HVP,LO contribution is dominated by the $\pi\pi$ cut (yielding $\sim 73\%$ of the overall value), where good-quality data of the corresponding e^+e^- hadronic cross-sections [47, 48, 49, 50, 51, 52, 53, 54, 55, 56] enables its computation by dispersive methods [57, 58]. Alternatively, one can also use isospin-rotated $\tau \rightarrow \pi\pi\nu_\tau$ measurements with that purpose, as was put forward in LEP times [59], despite the required IB corrections cannot be computed in a model-independent way presently. Still, while a lattice QCD computation of these is achieved, the authors find convenient testing the consistency of both extractions of $a_\mu^{HVP,LO_{\pi\pi}}$, in light of the tensions between different sets of $e^+e^- \rightarrow \pi^+\pi^-$ data that has not been resolved so far [2].

In addition to the previous data-based determinations of $a_\mu^{HVP,LO}$, lattice QCD is also achieving computations with reduced errors, although not yet competitive with the e^+e^- evaluations [2]. One notable exception to this being the recent very accurate result ($53 \cdot 10^{-11}$ error) of the BMW Coll. [60], according to which the difference with respect to the SM prediction is at the one sigma level.

Concerning the tau based determination, refs. [61, 62] computed the required isospin violating and electromagnetic corrections using Resonance Chiral Theory ($R\chi T$) [63, 64] and refs. [65, 66] using Vector Meson Dominance (VMD). These series of articles were employed by ref. [67] (updated in refs. [68, 69]) which, remarkably, found that the discrepancy of the SM prediction with the measurement is reduced substantially when tau data is employed ³. Notwithstanding, as precise measurements of $\sigma(e^+e^- \rightarrow \text{hadrons})$ became available in the last fifteen years, the e^+e^- based evaluation gained preference over using tau data. Indeed, ref. [2] concludes that ‘at the required precision to match the e^+e^- data, the present understanding of the IB (isospin breaking) corrections to τ data is unfortunately not yet at a level allowing their

¹The SM prediction [2] is based on [3, 4, 5, 6, 7, 8, 9, 10, 11, 12, 13, 14, 15, 16, 17, 18, 19, 20, 21, 22, 23, 24, 25, 26, 27, 28, 29, 30, 31, 32, 33, 34, 35, 36, 37] (see also the last developments in refs. [38, 39, 40, 41, 42, 43, 44]).

²Its website is <https://muon-gm2-theory.illinois.edu/>.

³The difference between the SM prediction of a_μ and the BNL measurement is 3.7σ [2]. If isospin-rotated tau data is employed for $a_\mu^{HVP,LO}$, it amounts to 2.4σ [69], instead. This difference could in principle be due to new physics effects, hinting at a lepton universality violation in the corresponding non-standard vector and/or tensor couplings at low-energies [70, 71, 72]. See the most updated discussions of its connection with α_{QED} in the electroweak fit in refs. [73, 74, 75, 76].

use for the HVP dispersion integrals', despite ref. [77] claiming that (the model-dependent) $\rho - \gamma$ mixing in the neutral channel makes it agree with the results in the charged current. It is the purpose of this work⁴ to extend previous $R\chi T$ analyses [61, 62] of the required IB corrections to di-pion tau decays so that they can again be useful, when combined with $\sigma(e^+e^- \rightarrow \pi^+\pi^-(\gamma))$, to increase the accuracy of the SM prediction of $a_\mu^{HVP,LO}$. In this spirit, we note that F. Jegerlehener [79] indeed combines both sets of data (using the IB corrections of ref. [77]), which reduces the error of $a_\mu^{HVP,LO}$ by $\sim 17\%$ [79].

Within the global effort of the Muon g-2 theory initiative, we revisit in this paper the $R\chi T$ computations including operators that -in the chiral limit- start to contribute at $\mathcal{O}(p^6)$. This is possible by the knowledge acquired after the analyses of Cirigliano *et al.* [61, 62] (where operators contributing at $\mathcal{O}(p^4)$ were considered), through a series of works studying operator product expansion (OPE) restrictions on $R\chi T$ couplings on several relevant 3-point Green functions (and related form factors) [31, 80, 81, 82, 83, 84, 85, 86, 87, 88, 89, 90, 91, 92, 93, 94, 95, 96, 97, 98, 99, 100, 101]^{5 6}. This procedure will also allow us to evaluate an uncertainty for the results by Cirigliano *et al.* [62], which is one of the main outcomes of this work, together with the new results, including operators that start contributing to the $\mathcal{O}(p^6)$ chiral low-energy constants (LECs).

The paper is organized as follows. In section 1 we review the main features of the $\tau^- \rightarrow \pi^-\pi^0\nu_\tau\gamma$ decays and split the model-independent part from the hadron form factors, computed in $R\chi T$ including new terms, subleading in the chiral expansion. We then recall the short-distance (SD) QCD constraints on the Lagrangian couplings, their phenomenological determinations and explain our estimation of the remaining free couplings, based on chiral counting. After that, in section 2 we recap the radiative corrections needed for the tau-based calculation of $a_\mu^{HVP,LO}$ and predict several observables for the processes where the real photon is detected together with the pion pair. Then, in section 3 we evaluate $a_\mu^{HVP,LO|\pi\pi}$ using tau data, which is the main result of this article. Finally, our conclusions are presented in section 4. Several appendices complement the main material, explaining how the coefficients dominating uncertainties were fitted, giving a full account of the kinematics, and providing with the complete expressions for the structure-dependent (axial-)vector form factors of the $\tau^- \rightarrow \pi^-\pi^0\nu_\tau\gamma$ decays.

⁴Currently, a lattice evaluation of IB for using tau data in $a_\mu^{HVP,LO_{\pi\pi}}$ is in progress [78].

⁵See also e.g. refs. [102, 103, 104, 105, 106, 107, 108].

⁶Similar radiative corrections were computed for the $\tau \rightarrow \eta\pi\nu_\tau\gamma$ decays in $R\chi T$ [109], even though part of our contributions here were suppressed (and thus neglected) there because of G-parity.

1 $\tau^- \rightarrow \pi^- \pi^0 \gamma \nu_\tau$ decays

1.1 Amplitude

For the radiative decay $\tau^- (P) \rightarrow \pi^- (p_-) \pi^0 (p_0) \nu_\tau (q) \gamma (k)$, we can split the contribution due to the bremsstrahlung off the initial tau lepton from the one coming from the hadronic part.

We write down the general structure for these processes [110, 62]

$$T = e G_F V_{ud}^* \epsilon^\mu(k)^* \{ F_\nu \bar{u}(q) \gamma^\nu (1 - \gamma_5) (m_\tau + \not{P} - \not{k}) \gamma_\mu u(P) \\ + (V_{\mu\nu} - A_{\mu\nu}) \bar{u}(q) \gamma^\nu (1 - \gamma_5) u(P) \}, \quad (1)$$

where $F_\nu = (p_0 - p_-)_\nu f_+(s) / 2P \cdot k$, with the charged pion vector form factor $f_+(s)$ defined through $\langle \pi^0 \pi^- | \bar{d} \gamma^\mu u | 0 \rangle = \sqrt{2} f_+(s) (p_- - p_0)^\mu$ and $s = (p_- + p_0)^2$. Gauge invariance ($\epsilon_\mu \rightarrow \epsilon_\mu + k_\mu$) implies the Ward identities

$$k_\mu V^{\mu\nu} = (p_- - p_0)^\nu f_+(s), \quad k_\mu A^{\mu\nu} = 0. \quad (2)$$

Imposing eq. (2) and Lorentz invariance, we have the following expression for the vector structure-dependent tensor

$$V^{\mu\nu} = f_+ \left[(P - q)^2 \right] \frac{p_-^\mu (p_- + k - p_0)^\nu}{p_- \cdot k} - f_+ \left[(P - q)^2 \right] g^{\mu\nu} \\ + \frac{f_+ \left[(P - q)^2 \right] - f_+(s)}{(p_0 + p_-) \cdot k} (p_0 + p_-)^\mu (p_0 - p_-)^\nu \\ + v_1 (g^{\mu\nu} p_- \cdot k - p_-^\mu k^\nu) + v_2 (g^{\mu\nu} p_0 \cdot k - p_0^\mu k^\nu) \\ + v_3 (p_0 \cdot k p_-^\mu - p_- \cdot k p_0^\mu) p_-^\nu + v_4 (p_0 \cdot k p_-^\mu - p_- \cdot k p_0^\mu) (p_0 + p_- + k)^\nu, \quad (3)$$

and for the axial one

$$A^{\mu\nu} = i a_1 \epsilon^{\mu\nu\rho\sigma} (p_0 - p_-)_\rho k_\sigma + i a_2 W^\nu \epsilon^{\mu\lambda\rho\sigma} k_\lambda p_{-\rho} p_{0\sigma} \\ + i a_3 \epsilon^{\mu\nu\rho\sigma} k_\rho W_\sigma + i a_4 (p_0 + k)^\nu \epsilon^{\mu\lambda\rho\sigma} k_\lambda p_{-\rho} p_{0\sigma}, \quad (4)$$

where $W \equiv P - q = p_- + p_0 + k$. We could use the basis given in ref. [109] but instead we prefer a modified one that resembles the decomposition in ref. [62] (see also ref. [110]). These tensor structures depend on four vector (v_i) and four axial-vector (a_i) form factors. For the axial structure, the Schouten's identity has been used.

Taking into account that $(P - q)^2 = s + 2(p_0 + p_-) \cdot k$, the Low's theorem [111] is manifestly satisfied

$$V^{\mu\nu} = f_+(s) \frac{p_-^\mu}{p_- \cdot k} (p_- - p_0)^\nu + f_+(s) \left(\frac{p_-^\mu k^\nu}{p_- \cdot k} - g^{\mu\nu} \right) \\ + 2 \frac{df_+(s)}{ds} \left(\frac{p_0 \cdot k}{p_- \cdot k} p_-^\mu - p_0^\mu \right) (p_- - p_0)^\nu + \mathcal{O}(k). \quad (5)$$

1.2 Theoretical framework

We will present in the following the model-dependent contributions to the $V_{\mu\nu}$ and $A_{\mu\nu}$ tensors. We will closely follow ref. [62], extending it to include subleading terms in the chiral expansion. In this reference, a large- N_C [112, 113, 114] inspired computation was carried out. Specifically, it was restricted to the dominant (for $N_C \rightarrow \infty$) tree level diagrams, although the relevant loop corrections for the $\tau^- \rightarrow \pi^-\pi^0\nu_\tau\gamma$ decays –giving the ρ (and a_1 , for completeness) off-shell width ⁷– were taken into account ⁸. Also, given the limited phase space of tau decays and the fact that the region $E \lesssim M_\rho + \Gamma_\rho$ is the most important one for the IB corrections needed for $a_\mu^{HVP,LO_{\pi\pi}}$ [62], the contribution of the $\rho(1450)$ and other heavier resonances was neglected in this reference (despite the fact that, in the large- N_C limit, there is an infinite tower of resonances per channel), as we will also do ⁹. Within this setting, our computation will include all $R\chi T$ operators contributing to the $\mathcal{O}(p^6)$ chiral low-energy constants. Our results agree with those in ref. [62], providing the new contributions with resonance operators that are suppressed by one chiral order in the low-energy limit (where possible, our computations have been checked against the results in ref. [109]).

As explained in ref. [62], this procedure warrants the correct low-energy limit (as given by Chiral Perturbation Theory [126, 127, 128, 129, 130]) and includes consistently the most general pion and photon interactions with the lightest resonances. Demanding the known QCD SD constraints results in relations among the Lagrangian couplings, and chiral counting can be employed to estimate those still unconstrained after using phenomenological information. It should then provide an accurate description of the $\tau^- \rightarrow \pi^-\pi^0\nu_\tau\gamma$ decays for $s \lesssim 1 \text{ GeV}^2$, which gives $\sim 99.8\%$ of the whole $a_\mu^{HVP,LO|_{\pi\pi}}$ contribution.

1.3 Vector Form Factors

Within $R\chi T$ [63, 64, 83, 88], the diagrams contributing to the vector form factors of the $\tau^- \rightarrow \pi^-\pi^0\gamma\nu_\tau$ decays including operators that start contributing to the $\mathcal{O}(p^6)$ LECs are shown in Figs. 1, 2 and 3 ¹⁰. The first three diagrams in fig. 1 and the first diagram in fig. 2 contribute

⁷We will introduce them following ref. [115] for the $\rho(770)$ and refs. [86, 116] for the $a_1(1260)$ resonances.

⁸See refs. [117, 118, 119, 120, 121, 122, 123] for next-to-leading order (NLO) computations in $1/N_C$, allowing to include the scale dependence of the Chiral Perturbation Theory LECs in the low-energy limit of $R\chi T$.

⁹Nevertheless, we will include the dominant effect of the $\rho(1450)$ and $\rho(1700)$ resonances in our dispersive pion form factor [124, 125] and check the negligible impact of heavier resonances in the v_i and a_i form factors in our analysis.

¹⁰The contributions involving scalar and pseudoscalar resonances are discussed at the end of section 1.3.

to the pion vector form factor entering the structure-independent (SI) piece ¹¹

$$f_+(s) = 1 + \frac{G_V F_V}{F^2} \frac{s}{m_\rho^2 - s} + \frac{\sqrt{2} F_V s}{F^2 (m_\rho^2 - s)} [2(2\lambda_8^V + \lambda_9^V + 2\lambda_{10}^V) m_\pi^2 - s\lambda_{21}^V] \\ + \frac{2\sqrt{2} G_V s}{F^2 (m_\rho^2 - s)} [4\lambda_6^V m_\pi^2 - s\lambda_{22}^V] \\ + \frac{4s}{F^2 (m_\rho^2 - s)} [4\lambda_6^V m_\pi^2 - s\lambda_{22}^V] [2(2\lambda_8^V + \lambda_9^V + 2\lambda_{10}^V) m_\pi^2 - s\lambda_{21}^V]. \quad (6)$$

The contribution of both the last diagram in fig. 1 and the last diagram in fig. 2 vanishes for a real photon, as the corresponding ($f_+(0) = 1$ part) contribution is already in the SI piece. We note we are using $F \sim 92$ MeV for the pion decay constant and that QCD OPE constraints $\lambda_{21}^V = \lambda_{22}^V = 0$ [83]. In fact, we will see in sec. 1.5 that all modifications induced by the λ_i^V couplings to $f_+(s)$ (6) vanish once SD QCD constraints are accounted for.

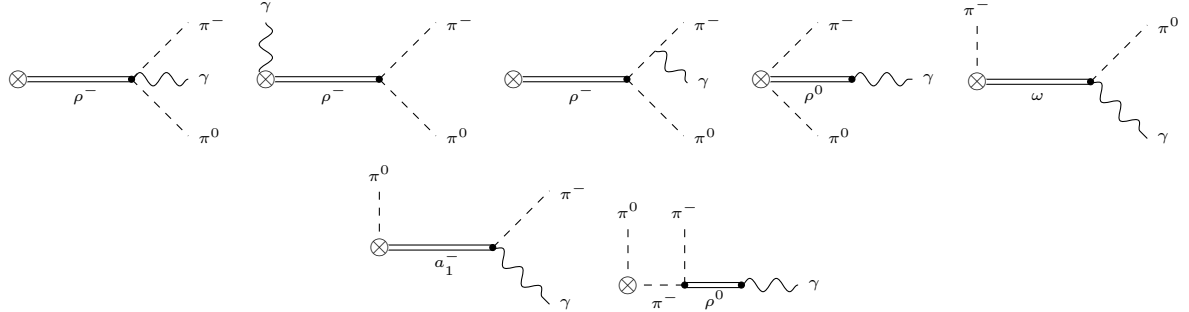


Figure 1: One-resonance exchange contributions from the $R\chi T$ to the vector form factors of the $\tau^- \rightarrow \pi^- \pi^0 \gamma \nu_\tau$ decays.

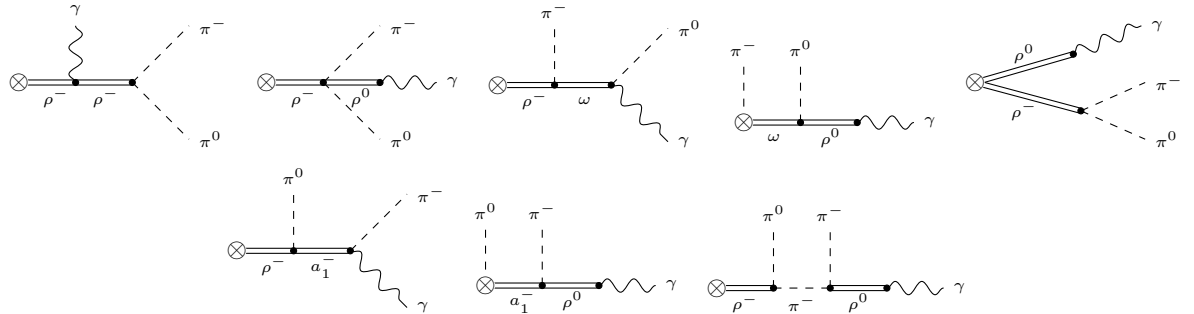


Figure 2: Two-resonance exchange contributions from the $R\chi T$ to the vector form factors of the $\tau^- \rightarrow \pi^- \pi^0 \gamma \nu_\tau$ decays.

¹¹Relevant $R\chi T$ couplings are introduced after eq. (7) and in sec. 1.5 below.

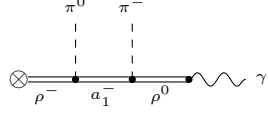


Figure 3: Three-resonance exchange contributions from the $R\chi T$ to the vector form factors of the $\tau^- \rightarrow \pi^-\pi^0\gamma\nu_\tau$ decays.

For the vector form factors, we get

$$v_1 = v_1^0 + v_1^R + v_1^{RR} + v_1^{RRR} + v_{GI1}^{R+RR}, \quad (7a)$$

$$v_2 = v_2^0 + v_2^R + v_2^{RR} + v_2^{RRR} + v_{GI2}^{R+RR}, \quad (7b)$$

$$v_3 = v_3^0 + v_3^R + v_3^{RR} + v_3^{RRR} + v_{GI3}^{R+RR}, \quad (7c)$$

$$v_4 = v_4^0 + v_4^R + v_4^{RR} + v_4^{RRR} + v_{GI4}^{R+RR}, \quad (7d)$$

where v_i^0 is the contribution in ref. [62] (D_R^{-1} stands for the inverse resonance propagator)¹²

$$\begin{aligned} v_1^0 &\equiv \frac{F_V G_V}{F^2 M_\rho^2} \left(2 + 2M_\rho^2 D_\rho^{-1} [(P-q)^2] + s D_\rho^{-1}(s) + s M_\rho^2 D_\rho^{-1}(s) D_\rho^{-1}[(P-q)^2] \right) \\ &+ \frac{F_V^2}{2F^2 M_\rho^2} \left(-1 - M_\rho^2 D_\rho^{-1}[(P-q)^2] + (P-q)^2 D_\rho^{-1}[(P-q)^2] \right) \\ &+ \frac{F_A^2}{F^2 M_{a_1}^2} \left(M_{a_1}^2 - m_\pi^2 + \frac{1}{2}s \right) D_{a_1}^{-1}[(p_- + k)^2], \\ v_2^0 &\equiv \frac{F_V G_V s}{F^2 M_\rho^2} \left(-D_\rho^{-1}(s) - M_\rho^2 D_\rho^{-1}(s) D_\rho^{-1}[(P-q)^2] \right) \\ &+ \frac{F_V^2}{2F^2 M_\rho^2} \left(-1 - M_\rho^2 D_\rho^{-1}[(P-q)^2] - (P-q)^2 D_\rho^{-1}[(P-q)^2] \right) \\ &+ \frac{F_A^2}{F^2 M_{a_1}^2} \left(M_{a_1}^2 - m_\pi^2 - k \cdot p_- \right) D_{a_1}^{-1}[(p_- + k)^2], \\ v_3^0 &\equiv \frac{F_A^2}{F^2 M_{a_1}^2} D_{a_1}^{-1}[(p_- + k)^2], \\ v_4^0 &\equiv -\frac{2F_V G_V}{F^2} D_\rho^{-1}(s) D_\rho^{-1}[(P-q)^2] + \frac{F_V^2}{F^2 M_\rho^2} D_\rho^{-1}[(P-q)^2], \end{aligned}$$

and v_i^R , v_i^{RR} , v_i^{RRR} and v_{GIi}^{R+RR} ¹³ correspond to contributions including operators which do not contribute to the NLO chiral LECs. Due to their length, the expressions for these form factors are in App. C. In writing the new contributions to v_i , the basis given in ref. [83] has been used for the even-intrinsic parity operators (with couplings λ_i^X) and the basis given in ref. [88] has been employed for the odd-intrinsic parity operators (κ_i^X couplings). Both sets of λ_i^X and κ_i^X couplings have dimensions of inverse energy.

¹²We recall that F_R gives the coupling of the $R = V, A$ resonance to the $r = v, a$ external current and the $\rho\pi\pi$ vertex receives contributions both from F_V and G_V .

¹³In general, diagrams are gauge-invariant by themselves. Those giving the contribution v_{GIi}^{R+RR} need to be summed to achieve gauge invariance. These are the first three diagrams in fig. 1 and the first diagram in fig. 2.

Including operators with at most one resonance, only the contribution from the exchange of ρ and a_1 resonances on the vector form factor appeared [62]. Allowing for multi-resonance operators we also have contributions with ω exchange, coming from the odd-intrinsic parity sector, for both vector and axial-vector form factors (as well as resonance contributions on the axial form factor, absent in ref. [62]). Apparently, such ω contributions were responsible for the larger effect of the IB corrections obtained in refs. [65, 66] with respect to refs. [61, 62]. As a result, ref. [67] (and later evaluations by this group) ascribed an error to these corrections covering both contradictory evaluations. As we include (among others) contributions with an $\omega - \rho - \pi$ vertex in this work, closer agreement with the VMD evaluation should, in principle, be expected.

We have verified that all diagrams including scalar mesons vanish in the isospin symmetry limit. We point out that all contributions involving pseudoscalar mesons can be obtained from those with an axial-vector resonance by replacing it by a pseudoscalar resonance. Then, at leading chiral order, the saturation of the LECs by spin-one mesons [63] shows that diagrams including pseudoscalar resonances are suppressed. If we assume that this feature also holds at the next chiral order, then pseudoscalar resonance exchanges could be safely neglected ¹⁴.

1.4 Axial-Vector Form Factors

The axial form factors at chiral $\mathcal{O}(p^4)$ get contributions from the Wess-Zumino-Witten functional [131, 132]:

$$a_1^0 \equiv \frac{1}{8\pi^2 F^2}, \quad a_2^0 \equiv \frac{-1}{4\pi^2 F^2 \left[(P-q)^2 - m_\pi^2 \right]}. \quad (8)$$

The diagrams that receive contributions due to the anomaly are shown in fig. 4 ¹⁵.

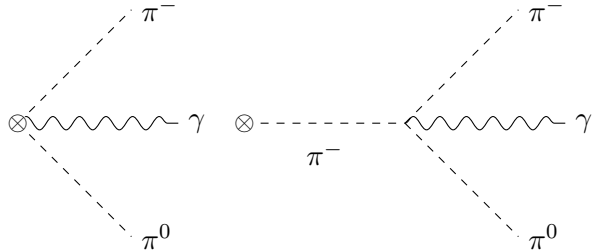


Figure 4: Anomalous diagrams contributing to the axial tensor amplitude $A^{\mu\nu}$ at $\mathcal{O}(p^4)$.

¹⁴Since contributions from scalar and pseudoscalar resonances are suppressed, we will neglect them for the axial form factors in the next section.

¹⁵The first diagram, when coupled to a vector current, contributes to the SI piece in $V^{\mu\nu}$.

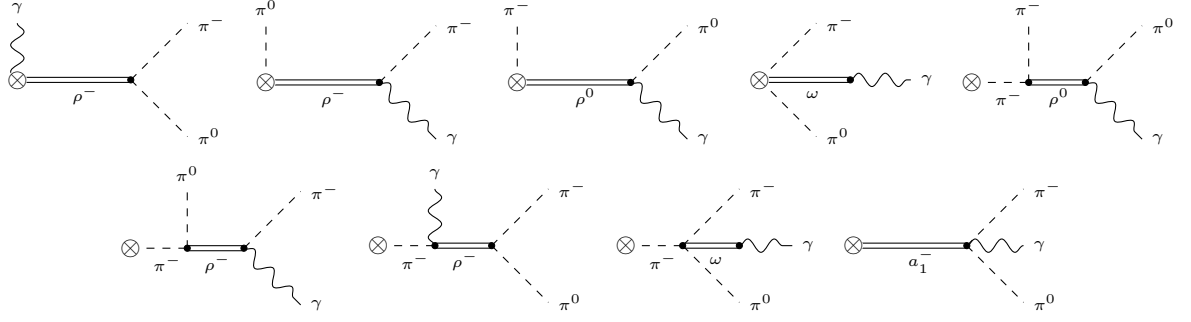


Figure 5: One-resonance exchange contributions from the $R\chi T$ to the axial-vector form factors of the $\tau^- \rightarrow \pi^- \pi^0 \gamma \nu_\tau$ decays.

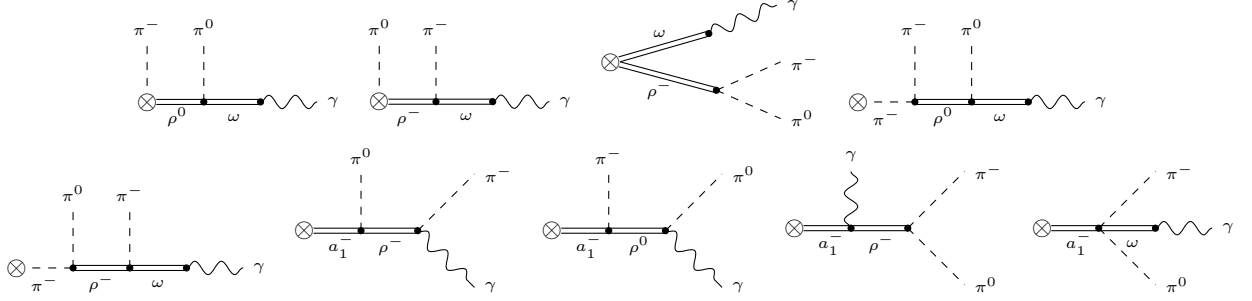


Figure 6: Two-resonance exchange contributions from the $R\chi T$ to the axial-vector form factors of the $\tau^- \rightarrow \pi^- \pi^0 \gamma \nu_\tau$ decays.

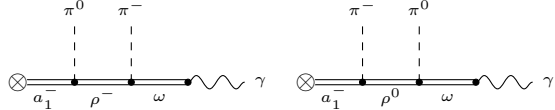


Figure 7: Three-resonance exchange contributions from the $R\chi T$ to the axial-vector form factors of the $\tau^- \rightarrow \pi^- \pi^0 \gamma \nu_\tau$ decays.

For the axial form factors, we get

$$a_1 = a_1^0 + a_1^R + a_1^{RR} + a_1^{RRR}, \quad (9a)$$

$$a_2 = a_2^0 + a_2^R + a_2^{RR} + a_2^{RRR}, \quad (9b)$$

$$a_3 = a_3^R + a_3^{RR} + a_3^{RRR}, \quad (9c)$$

$$a_4 = a_4^R + a_4^{RR} + a_4^{RRR}, \quad (9d)$$

where a_i^R , a_i^{RR} and a_i^{RRR} include $\mathcal{O}(p^6)$ vertices. Due to their length, the expressions for these form factors appear in App. D.

1.5 SD constraints

Including operators which start contributing to the $\mathcal{O}(p^6)$ LECs, we have now so many parameters (see Table 1) allowed by the discrete symmetries of QCD and chiral symmetry that, in practice, prevent making phenomenological predictions. It is possible to find relations between these couplings by means of SD properties of QCD and its OPE. We summarize these results in this section.

For the parameters contributing to 2-point Green Functions (and related form factors), the constraints [63, 64, 133, 134, 135, 136, 137]:

$$\begin{aligned} F_V G_V &= F^2, & F_V^2 - F_A^2 &= F^2, \\ F_V^2 M_V^2 &= F_A^2 M_A^2, & 4c_d c_m &= F^2, \\ 8(c_m^2 - d_m^2) &= F^2, & c_m = c_d &= \sqrt{2}d_m = F/2 \end{aligned} \quad (10)$$

are set, respectively, by the known asymptotic behaviour of: the pion vector form factor, the $V - A$ correlator (yielding the Weinberg sum rules), the scalar form factor and the $S - P$ correlator.

We note that the vanishing of the axial pion form factor (giving the π -to- γ matrix element) at infinite momentum transfer demands -if only the original $R\chi T$ Lagrangian [64] is used- $2F_V G_V = F_V^2$. This, together with the two first eqs. in (10), determine

$$F_V = \sqrt{2}F, \quad G_V = \frac{F}{\sqrt{2}}, \quad F_A = F, \quad (11)$$

all in terms of the pion decay constant. These relations were employed in ref. [62]. We emphasize that -once operators contributing to the NLO chiral LECs are considered [83, 88]-, the relations (11) no longer hold true (see ref. [94]). Seen from another perspective, consistent sets of SD relations on n -point Green functions vary with n . For $n = 2$ one has the set (11) [63]. We shall also consider the set obtained for $n = 3$ [83, 88, 94] (where operators with more than one resonance field start to appear) in the following. We will come back to discussing the actual values of the F_V , G_V and F_A couplings before closing this section, as they are essential to assess the error associated to the IB corrections computed in ref. [62].

Now, we consider $R\chi T$ operators which do not contribute to the NLO chiral LECs. For the even intrinsic parity sector [83, 98]¹⁶:

$$\begin{aligned} \lambda_{13}^P &= 0, & \lambda_{17}^S &= \lambda_{18}^S = 0, \\ \lambda_{17}^A &= 0, & \lambda_6^V &= \lambda_{21}^V = \lambda_{22}^V = 0, \end{aligned} \quad (12)$$

using these SD constraints in eq. (6) and the Brodsky-Lepage behaviour [138, 139] of $f_+(s)$, we get:

$$2\lambda_8^V + \lambda_9^V + 2\lambda_{10}^V = 0. \quad (13)$$

¹⁶The corresponding coefficients are denoted λ_i^R , with the upper index showing the resonance fields involved.

The study of the $\langle VAP \rangle$ and $\langle SPP \rangle$ Green functions yield the following restrictions on the resonance couplings [83, 81, 82] (the Weinberg sum rules in eq. (10) were used below):

$$\begin{aligned}\sqrt{2}\lambda_0 &= -4\lambda_1^{VA} - \lambda_2^{VA} - \frac{\lambda_4^{VA}}{2} - \lambda_5^{VA} = \frac{1}{2\sqrt{2}}(\lambda' + \lambda''), \\ \sqrt{2}\lambda' &= \lambda_2^{VA} - \lambda_3^{VA} + \frac{\lambda_4^{VA}}{2} + \lambda_5^{VA} = \frac{F_V}{2\sqrt{F_V^2 - F^2}}, \\ \sqrt{2}\lambda'' &= \lambda_2^{VA} - \frac{\lambda_4^{VA}}{2} - \lambda_5^{VA} = \frac{2F^2 - F_V^2}{2F_V\sqrt{F_V^2 - F^2}}, \\ \lambda_1^{PV} &= -4\lambda_2^{PV} = -\frac{F^2}{4\sqrt{2}d_m F_V}, \quad \lambda_1^{PA} = \frac{F^2}{16\sqrt{2}d_m\sqrt{F_V^2 - F^2}}.\end{aligned}\tag{14}$$

For the odd-intrinsic parity sector [88]¹⁷:

$$\begin{aligned}\kappa_{14}^V &= \frac{N_C}{256\sqrt{2}\pi^2 F_V}, \quad 2\kappa_{12}^V + \kappa_{16}^V = -\frac{N_C}{32\sqrt{2}\pi^2 F_V}, \quad \kappa_{17}^V = -\frac{N_C}{64\sqrt{2}\pi^2 F_V}, \quad \kappa_5^P = 0, \\ \kappa_2^{VV} &= \frac{F^2 + 16\sqrt{2}d_m F_V \kappa_3^{PV}}{32F_V^2} - \frac{N_C M_V^2}{512\pi^2 F_V^2}, \quad 8\kappa_2^{VV} - \kappa_3^{VV} = \frac{F^2}{8F_V^2}.\end{aligned}\tag{15}$$

The analysis of the $\langle VAS \rangle$ Green's function yields [88]:

$$\begin{aligned}\kappa_2^S &= \kappa_{14}^A = 0, \quad \kappa_4^V = 2\kappa_{15}^V, \quad \kappa_6^{VA} = \frac{F^2}{32F_A F_V}, \\ F_V(2\kappa_1^{SV} + \kappa_2^{SV}) &= 2F_A \kappa_1^{SA} = \frac{F^2}{16\sqrt{2}c_m},\end{aligned}\tag{16}$$

and through the study of the $\langle VVA \rangle$ Green's function in ref. [31]:

$$F_V \kappa_5^{VA} = -\frac{N_C M_V^2}{64\pi^2 F_A}.\tag{17}$$

A comparison between two basis for the odd-intrinsic operators [80, 88] was given in ref. [94], which is consistent with those in eq. (15)¹⁸

$$\begin{aligned}M_V(2\kappa_{12}^V + 4\kappa_{14}^V + \kappa_{16}^V - \kappa_{17}^V) &= 4c_3 + c_1 = 0, \\ M_V(2\kappa_{12}^V + \kappa_{16}^V - 2\kappa_{17}^V) &= c_1 - c_2 + c_5 = 0, \\ -M_V \kappa_{17}^V &= c_5 - c_6 = \frac{N_C M_V}{64\sqrt{2}\pi^2 F_V}, \\ M_V \kappa_{15}^V &= c_4, \\ 8\kappa_2^{VV} &= d_1 + 8d_2 = \frac{F^2}{8F_V^2} - \frac{N_C M_V^2}{64\pi^2 F_V^2}, \\ \kappa_3^{VV} &= d_3 = -\frac{N_C M_V^2}{64\pi^2 F_V^2}, \\ 1 + \frac{32\sqrt{2}F_V d_m \kappa_3^{PV}}{F^2} &= 0, \\ F_V^2 &= 3F^2,\end{aligned}\tag{18}$$

For the even- and odd-intrinsic parity sectors, there are 115 (EIP)+67 (OIP)=182 operators saturating the $\mathcal{O}(p^6)$ LECs but only a few of them contribute to a given process. The form factors of the $\tau^- \rightarrow \pi^-\pi^0\gamma\nu_\tau$ decays at $\mathcal{O}(p^6)$ are given by 32 (EIP)+23(OIP)=55 operators (Table 1). Taking into account the relations in eqs. (12)-(18) we get 24 (EIP)+17 (OIP)=41 undetermined couplings.

In order to estimate the unknown parameters, we basically followed (but for the results in

¹⁷The corresponding coefficients are denoted κ_i^R , with the upper index showing the resonance fields involved.

¹⁸We note, particularly, the last of these eqs., which is at odds with (11).

Even-intrinsic parity (EIP)[83]	
\hat{O}_i^V	6,7,8,9,10,12,13,14,15,16,17,18,19,20,21,22
\hat{O}_i^A	4,12,13,15,16,17
\hat{O}_i^{VV}	2,3,4,5,7
\hat{O}_i^{VA}	1,2,3,4,5
Odd-intrinsic parity (OIP)[88]	
$\hat{O}_{i\mu\nu\alpha\beta}^V$	1,2,3,6,7,8,9,10,11,12,14,16,17
$\hat{O}_{i\mu\nu\alpha\beta}^A$	5,6,7
$\hat{O}_{i\mu\nu\alpha\beta}^{VV}$	2,3,4
$\hat{O}_{i\mu\nu\alpha\beta}^{VA}$	2,3,4,5

Table 1: Operators contributing at $\mathcal{O}(p^6)$ to the vector and axial-vector form factors.

appendix A) the strategy devised in ref. [109]. We will restore to the available phenomenological information on these couplings and estimate -based on chiral counting- those for which we lack it.

Eq. (14) leaves two λ_i^{VA} couplings undetermined, the numerical values of the restricted combinations (see their definitions in terms of the λ_i^{VA} in [81]) are:

$$\lambda' \sim 0.4, \quad \lambda'' \sim -0.14, \quad \lambda_0 \sim 0.07. \quad (19)$$

Since the same linear combination of λ_4^{VA} and λ_5^{VA} is in all couplings in eq. (19), we choose λ_4^{VA} as independent. By similar reasons we take λ_2^{VA} as the other independent coupling. Based on eq. (19), we conservatively estimate $|\lambda_2^{VA}| \sim |\lambda_4^{VA}| \leq 0.4$.

According to ref. [83] the λ_i^X couplings can be estimated from low energy couplings C_i^R of the $\mathcal{O}(p^6)$ χPT Lagrangian as ¹⁹

$$\begin{aligned} |\lambda_i^V| &\sim \frac{3M_V^2}{2F} C_i^R \sim 0.025 \text{ GeV}^{-1}, \\ |\lambda_i^{VV}| &\sim \frac{M_V^4}{2F^2} C_i^R \sim 0.1, \end{aligned} \quad (20)$$

where we take the relation $|C_i^R| \sim \frac{1}{F^2(4\pi)^4}$ linked to $|L_i^R| \sim \frac{1}{(4\pi)^2} \sim 5 \cdot 10^{-3}$ which corresponds to the typical size of the $\mathcal{O}(p^4)$ LECs. This sets a reasonable upper bound on $|\lambda_i^V| \sim |\lambda_i^A| \lesssim 0.025 \text{ GeV}^{-1}$ and $|\lambda_i^{VV}| \sim |\lambda_i^{VA}| \lesssim 0.1$.

For the anomalous sector, we have the following predictions from the eq. (18): $-M_V \kappa_{17}^V = c_5 - c_6 \sim 0.016$, $8\kappa_2^{VV} = d_1 + 8d_2 \sim -0.070$ and $\kappa_3^{VV} = d_3 \sim -0.112$. There is a sign ambiguity on the determination of c_3 from $\tau^- \rightarrow \eta\pi^-\pi^0\nu_\tau$ decays [89]. We will take $c_3 = 0.007_{-0.012}^{+0.020}$ according to the determinations by Y. H. Chen *et al.* in refs. [90, 95, 140] (which is also in agreement with the most elaborated $e^+e^- \rightarrow (\eta/\pi^0)\pi^+\pi^-$ fit [92]). Although c_4 was first evaluated by studying $\sigma(e^+e^- \rightarrow KK\pi)$ in ref. [86], this yielded an inconsistent result for $\tau^- \rightarrow K^-\gamma\nu_\tau$ branching ratio [87], so we will use $c_4 = -0.0024 \pm 0.0006$ [95] as the most reliable

¹⁹Couplings of operators with two resonance fields are dimensionless [83, 88].

estimation. In view of all these results, we will take $|c_i| \lesssim 0.015$ as a reasonable estimate, which is translated to $|\kappa_i^V| \lesssim 0.025 \text{ GeV}^{-1}$. Since there is not enough information on κ_i^A , we will take $|\kappa_i^A| \sim |\kappa_i^V| \lesssim 0.025 \text{ GeV}^{-1}$. We will see in the following sections that the observables that we consider and the IB corrections for $a_\mu^{HVP,LO|\pi\pi}$ depend mostly on the κ_i^V couplings (besides F_V , G_V and F_A) for this reason we perform a global fit to better bind these couplings (see App. A) ²⁰.

We turn now to the remaining couplings. We will employ $d_2 = 0.08 \pm 0.08$, which has been determined simultaneously with c_3 [90, 95, 140, 92]. For d_4 we will assume $|d_4| < 0.15$, or in terms of κ_i^{VV} , we get $|\kappa_i^{VV}| \lesssim 0.1$. Again we will adopt $|\kappa_i^{VA}| \sim |\kappa_i^{VV}| \lesssim 0.1$, which agrees with the prediction $\kappa_5^{VA} \sim -0.14$ in eq. (17).

Using only operators contributing to the $\mathcal{O}(p^4)$ LECs we have the consistent set for 2-point Green functions (11). However, including operators which start contributing at $\mathcal{O}(p^6)$, we shall use the relations for 2 and 3-point Green functions (eq. (10) and eqs. (12) to (18)). In particular, $F_V = \sqrt{3}F$, which implies (via (10)) $G_V = F/\sqrt{3}$ and $F_A = \sqrt{2}F$. Therefore, we will also be showing the Cirigliano *et al.* results [62] with the latter set of constraints (inconsistent for 2-point Green functions) so that the impact of the change of F_V , F_A and G_V between these two cases is appreciated.

We will refer to the original [62] constraints (11) as ‘ $F_V = \sqrt{2}F$ ’ and by ‘ $F_V = \sqrt{3}F$ ’ to their consistent set of values ($F_V = \sqrt{3}F$, $G_V = F/\sqrt{3}$, $F_A = \sqrt{2}F$) up to 3-point Green functions. In this last way, we stress that the consistent set of SD constraints in both parity sectors [81, 83, 88, 94] determines the $F_V = \sqrt{3}F$ relations (among many others, reviewed in this section).

2 Radiative corrections for hadronic vacuum polarization

The four-body differential decay width is given by [62] ²¹

$$d\Gamma = \frac{(2\pi)^4}{2m_\tau} \overline{|\mathcal{M}|^2} \delta^4(P - p_- - p_0 - k - q) \frac{d^3 p_-}{(2\pi)^3 2E_-} \frac{d^3 p_0}{(2\pi)^3 2E_0} \frac{d^3 q}{(2\pi)^3 2E_\nu} \frac{d^3 k}{(2\pi)^3 2E_\gamma}, \quad (21)$$

using the relation $\frac{d^3 p_-}{2E_-} \frac{d^3 p_0}{2E_0} = \frac{\pi^2}{4m_\tau^2} ds du dx$ and integrating over the three-momentum of the photon and neutrino ²², we get

$$d\Gamma = \frac{1}{32(2\pi)^6 m_\tau^3} \left[\int \frac{d^3 q}{2E_\nu} \frac{d^3 k}{2E_\gamma} \overline{|\mathcal{M}|^2} \delta^4(P - p_- - p_0 - k - q) \right] ds du dx, \quad (22)$$

²⁰The results obtained assuming $|\kappa_i^V| \lesssim 0.025 \text{ GeV}^{-1}$ can be found in <https://arxiv.org/abs/2007.11019v1>. While both results agree remarkably, the errors are reduced in the current procedure.

²¹Although the analytical results in this section were presented in the quoted reference, we include them here given their importance in the evaluation of the relevant IB corrections, and take advantage to add a few explanations to previous discussions of this subject [62, 66].

²²The kinematics for these decays are in App. B.

working at leading order in the Low expansion and in the isospin limit $m_u = m_d$, we have

$$\mathcal{M} = e \epsilon^{*\mu}(k) \mathcal{M}_{\pi\pi}^{(0)} \left(\frac{p_{-\mu}}{p_- \cdot k} - \frac{P_\mu}{P \cdot k} \right) + \mathcal{O}(k^0), \quad (23)$$

where $\mathcal{M}_{\pi\pi}^{(0)} = G_F V_{ud}^* \sqrt{S_{EW}} f_+(s) (p_- - p_0)_\nu \bar{u}(q) \gamma^\nu (1 - \gamma_5) u(P)$ is the amplitude at leading order for the non-radiative decay that includes the SD electroweak radiative corrections (S_{EW}). At $\mathcal{O}(k^{-1})$, the amplitude for the radiative decay is proportional to the amplitude of the non-radiative decay according to the Low's theorem [111].

The unpolarized spin-averaged squared amplitude is given by

$$\begin{aligned} \overline{|\mathcal{M}|^2} &= 4\pi\alpha \overline{|\mathcal{M}_{\pi\pi}^{(0)}|^2} \sum_\gamma \epsilon^{*\mu}(k) \epsilon^\nu(k) \left(\frac{p_{-\mu}}{p_- \cdot k + \frac{1}{2}M_\gamma^2} - \frac{P_\mu}{P \cdot k - \frac{1}{2}M_\gamma^2} \right) \\ &\quad \times \left(\frac{p_{-\nu}}{p_- \cdot k + \frac{1}{2}M_\gamma^2} - \frac{P_\nu}{P \cdot k - \frac{1}{2}M_\gamma^2} \right) + \mathcal{O}(k^{-1}), \end{aligned} \quad (24)$$

using the relation $\sum_\gamma \epsilon^{*\mu}(k) \epsilon^\nu(k) = -g^{\mu\nu}$ and massive photons ($k^\mu k_\mu = M_\gamma^2$). The sum over photon polarizations should include the longitudinal part, since our photon has mass and the amplitude is no longer gauge invariant. We do not take into account this contribution because it will vanish in the limit $M_\gamma \rightarrow 0$.

Thus, eq. (24) becomes

$$\begin{aligned} \overline{|\mathcal{M}|^2} &= 4\pi\alpha \overline{|\mathcal{M}_{\pi\pi}^{(0)}|^2} \left(\frac{2P \cdot p_-}{(p_- \cdot k + \frac{1}{2}M_\gamma^2)(P \cdot k - \frac{1}{2}M_\gamma^2)} - \frac{m_\pi^2}{(p_- \cdot k + \frac{1}{2}M_\gamma^2)^2} \right. \\ &\quad \left. - \frac{m_\pi^2}{(P \cdot k - \frac{1}{2}M_\gamma^2)^2} \right) + \mathcal{O}(k^{-1}), \end{aligned} \quad (25)$$

where

$$\overline{|\mathcal{M}_{\pi\pi}^{(0)}|^2} = 4G_F^2 |V_{ud}|^2 S_{EW} |f_+(s)|^2 (D(s, u) + \mathcal{O}(k)), \quad (26)$$

with $D(s, u) = \frac{1}{2}m_\tau^2(m_\tau^2 - s) + 2m_\pi^4 - 2u(m_\tau^2 - s + 2m_\pi^2) + 2u^2$. Eq. (25) does not contribute at $\mathcal{O}(k^{-1})$, these terms are canceled out by those in eq. (26) according to the Burnett-Kroll theorem [141].

Replacing eqs. (25) and (26) in eq. (22), we get

$$\begin{aligned} d\Gamma &= \frac{\alpha G_F^2 |V_{ud}|^2 S_{EW}}{4(2\pi)^4 m_\tau^3} |f_+(s)|^2 D(s, u) (2P \cdot p_- I_{11}(s, u, x) - m_\pi^2 I_{02}(s, u, x) \\ &\quad - m_\tau^2 I_{20}(s, u, x)) ds du dx + \mathcal{O}(k^0), \end{aligned} \quad (27)$$

the $I_{mn}(s, u, x)$ is defined as

$$I_{mn}(s, u, x) = \frac{1}{2\pi} \int \frac{d^3 q}{2E_\nu} \frac{d^3 k}{2E_\gamma} \frac{\delta^4(P - p_- - p_0 - k - q)}{(P \cdot k - \frac{1}{2}M_\gamma^2)^m (p_- \cdot k + \frac{1}{2}M_\gamma^2)^n}, \quad (28)$$

performing an integration over x , we can split the decay width according to the integration region

$$\frac{d^2\Gamma}{ds du} = \frac{d^2\Gamma}{ds du}\Big|_{\mathcal{D}_{III}} + \frac{d^2\Gamma}{ds du}\Big|_{\mathcal{D}_{IV/III}} + \mathcal{O}(k^0), \quad (29)$$

where

$$\begin{aligned} \frac{d^2\Gamma}{ds du}\Big|_{\mathcal{D}_{III}} &= \frac{\alpha G_F^2 |V_{ud}|^2 S_{EW}}{4(2\pi)^4 m_\tau^3} |f_+(s)|^2 D(s, u) \times \\ &\quad (J_{11}(s, u, M_\gamma) + J_{02}(s, u, M_\gamma) + J_{20}(s, u, M_\gamma)), \end{aligned} \quad (30)$$

and

$$\begin{aligned} \frac{d^2\Gamma}{ds du}\Big|_{\mathcal{D}_{IV/III}} &= \frac{\alpha G_F^2 |V_{ud}|^2 S_{EW}}{4(2\pi)^4 m_\tau^3} |f_+(s)|^2 D(s, u) \times \\ &\quad (K_{11}(s, u) + K_{02}(s, u) + K_{20}(s, u)), \end{aligned} \quad (31)$$

with

$$J_{mn}(s, u, M_\gamma) = c_{mn} \int_{M_\gamma^2}^{x_+(s, u)} dx I_{mn}(s, u, x), \quad (32)$$

$$K_{mn}(s, u) = c_{mn} \int_{x_-(s, u)}^{x_+(s, u)} dx I_{mn}(s, u, x), \quad (33)$$

and

$$c_{mn} = \begin{cases} 2P \cdot p_- & m = n = 1, \\ -m_\tau^2 & m = 2, n = 0, \\ -m_{\pi^-}^2 & m = 0, n = 2. \end{cases} \quad (34)$$

Eq. (28) is an invariant, so we can evaluate it in any reference frame in order to simplify the integration, working in the $\gamma - \nu_\tau$ center of mass, we have

$$I_{mn}(s, u) = \frac{1}{2^3(2\pi)} \int \frac{x - M_\gamma^2}{x(P \cdot k - \frac{1}{2}M_\gamma^2)^m (p_- \cdot k + \frac{1}{2}M_\gamma^2)^n} d\cos\theta_\nu d\phi_-. \quad (35)$$

Integrating this equation over x in $\mathcal{D}_{IV/III}$ and \mathcal{D}_{III} , as in refs. [62, 142] we get ($\text{Li}_2(x) = -\int_0^1 \frac{dt}{t} \log(1 - xt)$)

$$\begin{aligned} J_{11}(s, u) &= \log\left(\frac{2x_+(s, u)\bar{\gamma}}{M_\gamma}\right) \frac{1}{\bar{\beta}} \log\left(\frac{1 + \bar{\beta}}{1 - \bar{\beta}}\right) \\ &\quad + \frac{1}{\bar{\beta}} (Li_2(1/Y_2) - Li_2(Y_1) + \log^2(-1/Y_2)/4 - \log^2(-1/Y_1)/4), \end{aligned} \quad (36)$$

$$J_{20}(s, u) = \log\left(\frac{M_\gamma(m_\tau^2 - s)}{m_\tau^- x_+(s, u)}\right), \quad (37)$$

$$J_{02}(s, u) = \log\left(\frac{M_\gamma(m_\tau^2 + m_{\pi^0}^2 - s - u)}{m_\pi^- x_+(s, u)}\right), \quad (38)$$

$$K_{20}(s, u) = K_{0,2}(s, u) = \log \left(\frac{x_-(s, u)}{x_+(s, u)} \right), \quad (39)$$

where the expressions in eq. (36) are given by

$$Y_{1,2} = \frac{1 - 2\bar{\alpha} \pm \sqrt{(1 - 2\bar{\alpha})^2 - (1 - \bar{\beta}^2)}}{1 + \bar{\beta}}, \quad (40)$$

with

$$\begin{aligned} \bar{\alpha} &= \frac{(m_\tau^2 - s)(m_\tau^2 + m_{\pi^0}^2 - s - u)}{(m_{\pi^-}^2 + m_\tau^2 - u)} \cdot \frac{\lambda(u, m_{\pi^-}^2, m_\tau^2)}{2\bar{\delta}}, \\ \bar{\beta} &= -\frac{\sqrt{\lambda(u, m_{\pi^-}^2, m_\tau^2)}}{m_{\pi^-}^2 + m_\tau^2 - u}, \\ \bar{\gamma} &= \frac{\sqrt{\lambda(u, m_{\pi^-}^2, m_\tau^2)}}{2\sqrt{\bar{\delta}}}, \\ \bar{\delta} &= -m_{\pi^0}^4 m_\tau^2 + m_{\pi^-}^2 (m_\tau^2 - s)(m_{\pi^0}^2 - u) - su(-m_\tau^2 + s + u) \\ &\quad + m_{\pi^0}^2 (-m_\tau^4 + su + m_\tau^2 s + m_\tau^2 u). \end{aligned}$$

Experimentally, it is impossible to measure the full photon spectrum because of acceptances, efficiencies and cuts. For this reason, we need to calculate the inclusive decay width, since we can not distinguish the radiative decay from the non-radiative decay for low-energy (or collinear) photons.

For the non-radiative decay, we have

$$\frac{d^2\Gamma}{ds du} = \frac{G_F^2 |V_{ud}|^2 S_{EW}}{64\pi^3 m_\tau^3} |f_+(s)|^2 (1 + f_{loop}^{elm}(u, M_\gamma))^2 D(s, u), \quad (42)$$

that includes isospin violation and photonic corrections according to ref. [61], where $f_{loop}^{elm}(u, M_\gamma)$ is given by

$$\begin{aligned} f_{loop}^{elm}(u, M_\gamma) &= \frac{\alpha}{4\pi} \left((u - m_\pi^2) \mathcal{A}(u) + (u - m_\pi^2 - m_\tau^2) \mathcal{B}(u) \right. \\ &\quad \left. + 2(m_\pi^2 + m_\tau^2 - u) \mathcal{C}(u, M_\gamma) + 2 \log \frac{m_\pi m_\tau}{M_\gamma^2} \right), \end{aligned} \quad (43)$$

with

$$\begin{aligned}\mathcal{A}(u) &= \frac{1}{u} \left(-\frac{1}{2} \log r_\tau + \frac{2-y_\tau}{\sqrt{r_\tau}} \frac{x_\tau}{1-x_\tau^2} \log x_\tau \right), \\ \mathcal{B}(u) &= \frac{1}{u} \left(\frac{1}{2} \log r_\tau + \frac{2r_\tau-y_\tau}{\sqrt{r_\tau}} \frac{x_\tau}{1-x_\tau^2} \log x_\tau \right), \\ \mathcal{C}(u, M_\gamma) &= \frac{1}{m_\tau m_\pi} \frac{x_\tau}{1-x_\tau^2} \left(-\frac{1}{2} \log^2 x_\tau + 2 \log x_\tau \log(1-x_\tau^2) - \frac{\pi^2}{6} + \frac{1}{8} \log^2 r_\tau \right. \\ &\quad \left. + Li_2(x_\tau^2) + Li_2\left(1 - \frac{x_\tau}{\sqrt{r_\tau}}\right) + Li_2(1 - x_\tau \sqrt{r_\tau}) - \log x_\tau \log \frac{M_\gamma^2}{m_\tau m_\pi} \right),\end{aligned}$$

in terms of the variables

$$r_\tau = \frac{m_\tau^2}{m_\pi^2}, \quad y_\tau = 1 + r_\tau - \frac{u}{m_\pi^2}, \quad x_\tau = \frac{1}{2\sqrt{r_\tau}} \left(y_\tau - \sqrt{y_\tau^2 - 4r_\tau} \right),$$

Thus, the inclusive decay width is

$$\frac{d^2\Gamma}{ds du} \Big|_{\pi\pi(\gamma)} = \frac{G_F^2 |V_{ud}|^2 S_{EW}}{64\pi^3 m_\tau^3} |f_+(s)|^2 D(s, u) \Delta(s, u), \quad (45)$$

where

$$\Delta(s, u) = 1 + 2f_{loop}^{elm}(u, M_\gamma) + g_{rad}(s, u, M_\gamma). \quad (46)$$

In the previous expression we neglected the quadratic term for $f_{loop}^{elm}(u, M_\gamma)$, and

$$g_{rad}(s, u, M_\gamma) = g_{brems}(s, u, M_\gamma) + g_{rest}(s, u), \quad (47)$$

with

$$g_{brems}(s, u, M_\gamma) = \frac{\alpha}{\pi} (J_{11}(s, u, M_\gamma) + J_{20}(s, u, M_\gamma) + J_{02}(s, u, M_\gamma)), \quad (48a)$$

$$g_{rest}(s, u) = \frac{\alpha}{\pi} (K_{11}(s, u) + K_{20}(s, u) + K_{02}(s, u)). \quad (48b)$$

Integrating eq. (45) over u , and using

$$\int_{u_-(s)}^{u_+(s)} D(s, u) du = \frac{m_\tau^6}{6} \left(1 - \frac{s}{m_\tau^2} \right)^2 \left(1 - \frac{4m_\pi^2}{s} \right)^{3/2} \left(1 + \frac{2s}{m_\tau^2} \right),$$

we have

$$\begin{aligned}\frac{d\Gamma}{ds} \Big|_{\pi\pi(\gamma)} &= \frac{G_F^2 |V_{ud}|^2 m_\tau^3 S_{EW}}{384\pi^3} |f_+(s)|^2 \left(1 - \frac{s}{m_\tau^2} \right)^2 \left(1 - \frac{4m_\pi^2}{s} \right)^{3/2} \times \\ &\quad \left(1 + \frac{2s}{m_\tau^2} \right) G_{EM}(s),\end{aligned} \quad (49)$$

for this we follow the same notation as in ref. [62],

$$G_{EM}(s) = \frac{\int_{\mathcal{R}^{IV}} D(s, u) \Delta(s, u) du}{\int_{u_-(s)}^{u_+(s)} D(s, u) du}. \quad (50)$$

We can split the electromagnetic correction factor ($G_{EM}(s)$) in two parts, $G_{EM}^{(0)}(s)$ and $G_{EM}^{rest}(s)$, the first one corresponds to taking $g_{rest}(s, u) \rightarrow 0$ and the second one is the remainder of $G_{EM}(s)$,

$$G_{EM}^{(0)}(s) = \frac{\int_{\mathcal{R}^{III}} D(s, u) \left(1 + 2f_{loop}^{elm}(u, M_\gamma) + g_{brems}(s, u, M_\gamma) \right) du}{\int_{u_-(s)}^{u_+(s)} D(s, u) du}, \quad (51a)$$

$$G_{EM}^{rest}(s) = \frac{\int_{\mathcal{R}^{IV/III}} D(s, u) g^{rest}(s, u) du}{\int_{u_-(s)}^{u_+(s)} D(s, u) du}. \quad (51b)$$

In eq. (51a), the term $2f_{loop}^{elm}(u, M_\gamma) + g_{brems}(s, u, M_\gamma)$ is finite when $M_\gamma \rightarrow 0$,

$$\begin{aligned} 2f_{loop}^{elm}(u, M_\gamma) + g_{brems}(s, u, M_\gamma) &= \frac{\alpha}{4\pi} \left((u - m_\pi^2) \mathcal{A}(u) + (u - m_\pi^2 - m_\tau^2) \mathcal{B}(u) \right. \\ &\quad \left. + 2(m_\pi^2 + m_\tau^2 - u) \mathcal{C}(u) \right) \\ &\quad + \frac{\alpha}{\pi} (J_{11}(s, u) + J_{20}(s, u) + J_{02}(s, u)). \end{aligned} \quad (52)$$

In this limit, we have

$$\begin{aligned} \mathcal{C}(u) &= \frac{1}{m_\tau m_\pi} \frac{x_\tau}{1 - x_\tau^2} \left(-\frac{1}{2} \log^2 x_\tau + 2 \log x_\tau \log(1 - x_\tau^2) - \frac{\pi^2}{6} + \frac{1}{8} \log^2 r_\tau \right. \\ &\quad \left. + Li_2(x_\tau^2) + Li_2\left(1 - \frac{x_\tau}{\sqrt{r_\tau}}\right) + Li_2(1 - x_\tau \sqrt{r_\tau}) \right), \end{aligned} \quad (53)$$

$$\begin{aligned} J_{11}(s, u) &= \frac{1}{2} \log \left(\frac{4x_+^2(s, u)\bar{\gamma}^2}{m_\pi m_\tau} \right) \frac{1}{\bar{\beta}} \log \left(\frac{1 + \bar{\beta}}{1 - \bar{\beta}} \right) \\ &\quad + \frac{1}{\bar{\beta}} (Li_2(1/Y_2) - Li_2(Y_1) + \log^2(-1/Y_2)/4 - \log^2(-1/Y_1)/4), \end{aligned} \quad (54)$$

$$J_{20}(s, u) = \log \left(\frac{m_\tau^2 - s}{x_+(s, u)} \right), \quad (55)$$

$$J_{02}(s, u) = \log \left(\frac{m_\tau^2 + m_\pi^2 - s - u}{x_+(s, u)} \right), \quad (56)$$

where $x_+(s, u)$ is defined in eq. (104).

The leading Low approximation for $G_{EM}^{(0)}(s)$ is plotted in fig. 8. This function has two poles, one at $s = 4m_\pi^2$ and the other at $s = m_\tau^2$.

We will use the same conventions as ref. [62], so we denote as ‘complete Bremsstrahlung’

the amplitude where the structure-dependent ('SD') part vanishes, i.e. $v_1 = v_2 = v_3 = v_4 = a_1 = a_2 = a_3 = a_4 = 0$. For convenience, we will refer in the following simply as $\mathcal{O}(p^4)$ and $\mathcal{O}(p^6)$ to the contributions from $R\chi T$ including operators that contribute up to $\mathcal{O}(p^4)$ and up to $\mathcal{O}(p^6)$ chiral LECs, respectively²³.

In $G_{EM}(s)$, the difference between using the $F_V = \sqrt{2}F$ or $F_V = \sqrt{3}F$ constraints at $\mathcal{O}(p^4)$ is only appreciated for $s \lesssim 0.35$ GeV², with the latter set producing the largest deviation with respect to the SI result (fig. 8). It is important to note that -as put forward in ref. [62]- with $F_V = \sqrt{2}F$ constraints (those consistent for 2-point Green functions) the impact of the 'SD' corrections on $G_{EM}(s)$ is negligible and the evaluation with *SI* gives already an excellent approximation. On the contrary, we find that using the $F_V = \sqrt{3}F$ set this is no longer true, which will increase the $G_{EM}(s)$ correction in $a_\mu^{HVP,LO|\pi\pi}$ using τ data (even before adding the $\mathcal{O}(p^6)$ contributions).

In fig. 8 several contributions to the $G_{EM}(s)$ function are shown: the $G_{EM}^{(0)}$ part by a dashed blue line and the complete Bremsstrahlung (SI) contribution with a solid black line. The full amplitude including all $R\chi T$ operators which contribute at $\mathcal{O}(p^4)$ ($\mathcal{O}(p^6)$) are represented by black dashed/dotted (red dashed-dotted) lines in fig. 8. For the $\mathcal{O}(p^4)$ contribution we distinguish between using $F_V = \sqrt{2}F$ ($F_V = \sqrt{3}F$), represented by dashed (dotted) lines. Compared to previous results [61, 62, 65, 66], we note the appearance of a bump near the end of the phase space on $G_{EM}(s)$ due to the inclusion of the $\rho(1450)$ and the $\rho(1700)$ resonances in the dispersive representation of the vector form factor [124, 125]. The blue band in fig. 8 shows the uncertainty of the $\mathcal{O}(p^6)$ contribution, evaluated according to that on the couplings which were determined phenomenologically or estimated from chiral counting in section 1.5 (see also appendix A)²⁴. While the central values of the $\mathcal{O}(p^6)$ corrections change mildly the results obtained at $\mathcal{O}(p^4)$ ²⁵, their huge uncertainty band suggests that our estimate of the $R\chi T$ couplings which start contributing at $\mathcal{O}(p^6)$ was very conservative (one naively expects a $\sim 1/N_C$ uncertainty for a large- N_C expansion²⁶). Lacking a better way for this estimation, we consider this uncertainty band as a conservative upper limit on the corresponding uncertainties. Therefore, our error bands at $\mathcal{O}(p^6)$ should be regarded accordingly in the following. On the contrary, the small modification induced by those $\mathcal{O}(p^6)$ couplings fixed by SD constraints (with all remaining ones vanishing) with respect to the $\mathcal{O}(p^4)$ [62] results, suggests that the difference

²³The different SD constraints applying in each case were discussed at length in section 1.5.

²⁴These were varied assuming Gaussian errors, and the band was generated so as to cover all data points obtained in 100 spectrum simulations. Results were stable upon increasing statistics. The corresponding blue bands were obtained similarly in Figs. 12 to 14.

²⁵This is reasonable, since *SI* is basically unchanged by the $\mathcal{O}(p^4)$ contributions.

²⁶This rough estimate of the parametric uncertainty is supported by the computation of χPT LECs including such corrections (see e. g. refs. [119, 121, 123]). We note that in this work resonance widths (dominant next-to-leading order effect in the large- N_C expansion for the considered decays) are included. Also the uncertainty corresponding to including excited resonances (an infinite number of them appears for $N_C \rightarrow \infty$) was checked to be negligible.

between those is a realistic estimate of the missing subdominant terms in ref. [62]²⁷ and will be given as such in the remainder of the paper.

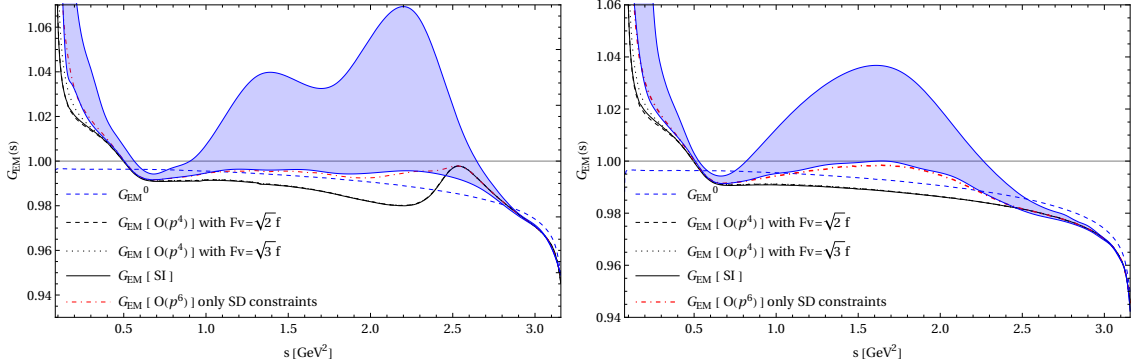


Figure 8: Correction function $G_{EM}^{(0)}(s)$ in eq. (51a) (blue dashed line). The solid line shows the $G_{EM}(s)$ function neglecting the structure-dependent part (SI), i.e. by taking $v_1 = v_2 = v_3 = v_4 = a_1 = a_2 = a_3 = a_4 = 0$, the dashed and dotted lines are the $\mathcal{O}(p^4)$ $G_{EM}(s)$ function (with either $F_V = \sqrt{2}F$ or $F_V = \sqrt{3}F$ constraints). The blue shaded region is the full $\mathcal{O}(p^6)$ contribution, including (overestimated) uncertainties. The left-hand side plot corresponds to the dispersive parametrization [124] while the right-hand side corresponds to the Guerrero-Pich parametrization [143] of the form factor (the latter was used in ref. [62]).

2.1 Radiative decay

The differential decay width [142] is given by

$$d\Gamma = \frac{\lambda^{1/2}(s, m_{\pi^0}^2, m_{\pi^-}^2)}{2(4\pi)^6 m_\tau^2 s} \overline{|\mathcal{M}|^2} dE_\gamma dx ds d\cos\theta_- d\phi_-, \quad (57)$$

where $\overline{|\mathcal{M}|^2}$ is the unpolarized spin-averaged squared amplitude that corresponds to the $\tau^- \rightarrow \pi^-\pi^0\gamma\nu_\tau$ decays, and E_γ is the photon energy in the τ rest frame. It is not worth to quote here the full analytical expression for $\overline{|\mathcal{M}|^2}$.

For these decays, we have the following integration region

$$\begin{aligned} \mathcal{D} = \{ & E_\gamma^{min} \leq E_\gamma \leq E_\gamma^{max}, x_{min} \leq x \leq x_{max}, s_{min} \leq s \leq s_{max}, \\ & -1 \leq \cos\theta_- \leq +1, 0 \leq \phi_- \leq 2\pi \}, \end{aligned} \quad (58)$$

with boundaries

$$\begin{aligned} \frac{(m_\tau^2 - s + x)}{4m_\tau^2} - \frac{\lambda^{1/2}(s, x, m_\tau^2)}{4m_\tau} &\leq E_\gamma(s, x) \leq \frac{(m_\tau^2 - s + x)}{4m_\tau} + \frac{\lambda^{1/2}(s, x, m_\tau^2)}{4m_\tau}, \\ 4m_\pi^2 &\leq s(x) \leq (m_\tau - \sqrt{x})^2, \\ 0 &\leq x \leq (m_\tau - 2m_\pi)^2, \end{aligned} \quad (59)$$

²⁷These were not estimated in ref. [62] as SI was already an excellent approximation to the result up to $\mathcal{O}(p^4)$ (using the $F_V = \sqrt{2}F$ set).

or interchanging the last two limits,

$$\begin{aligned} 0 \leq x(s) &\leq (m_\tau - \sqrt{s})^2, \\ 4m_\pi^2 \leq s &\leq m_\tau^2. \end{aligned} \tag{60}$$

There are other ways to write these,

$$\begin{aligned} 4m_\pi^2 \leq s(x, E_\gamma) &\leq \frac{(m_\tau - 2E_\gamma)(2m_\tau E_\gamma - x)}{2E_\gamma}, \\ 0 \leq x(E_\gamma) &\leq \frac{2E_\gamma(m_\tau^2 - 4m_\pi^2 - 2m_\tau E_\gamma)}{m_\tau - 2E_\gamma}, \\ E_\gamma^{cut} \leq E_\gamma &\leq \frac{m_\tau^2 - 4m_\pi^2}{2m_\tau}, \end{aligned} \tag{61}$$

or exchanging $x \leftrightarrow E_\gamma$,

$$\begin{aligned} \frac{(m_\tau^2 + x - 4m_\pi^2)}{4m_\tau} - \frac{\lambda^{1/2}(x, m_\tau^2, 4m_\pi^2)}{4m_\tau} &\leq E_\gamma(s) \leq \frac{(m_\tau^2 + x - 4m_\pi^2)}{4m_\tau} + \frac{\lambda^{1/2}(x, m_\tau^2, 4m_\pi^2)}{4m_\tau}, \\ 0 \leq x &\leq (m_\tau - 2m_\pi)^2, \end{aligned} \tag{62}$$

and

$$\begin{aligned} 0 \leq x(s, E_\gamma) &\leq \frac{2E_\gamma(m_\tau^2 - s - 2E_\gamma m_\tau)}{m_\tau - 2E_\gamma} \\ 4m_\pi^2 \leq s(E_\gamma) &\leq m_\tau(m_\tau - 2E_\gamma), \\ E_\gamma^{cut} \leq E_\gamma &\leq \frac{m_\tau^2 - 4m_\pi^2}{2m_\tau}. \end{aligned} \tag{63}$$

Further, interchanging $s \leftrightarrow E_\gamma$, we get

$$\begin{aligned} E_\gamma^{cut} \leq E_\gamma(s) &\leq \frac{m_\tau^2 - s}{2m_\tau}, \\ 4m_\pi^2 \leq s &\leq m_\tau(m_\tau - 2E_\gamma^{cut}). \end{aligned} \tag{64}$$

We recall that this amplitude has IR divergences due to soft photons, i.e. $E_\gamma \rightarrow 0$, which is the same problem with $M_\gamma \rightarrow 0$ outlined in the previous section. Correspondingly, the experiment is not able to measure photons with energies smaller than some E_γ^{cut} (which is related with the experimental resolution).

Concerning the $\mathcal{O}(p^6)$ contributions, once we employ the relations obtained from the SD behaviour of QCD and its OPE, it is seen that observables are basically insensitive (at the percent level of precision) to $\mathcal{O}(1)$ changes of all the couplings but κ_i^V (the $\rho - \omega - \pi$ vertex is described by these couplings), which will saturate the (overestimated) uncertainty of our predictions at this order.

If we integrate eq. (57) using the limits in eq. (64) and the dispersive vector form factor [124, 125], we get the $\pi^- \pi^0$ invariant mass distribution, the photon energy distribution and the branching ratios as a function of E_γ^{cut} , shown in Figs. 10, 11, 12, 13 and 14 and summarized in Table 2. In these figures, the dotdashed red line corresponds to taking the limit where all the couplings at $\mathcal{O}(p^6)$ vanish except for those constrained by SD and the band overestimates the corresponding uncertainties.

E_γ^{cut}	$\text{BR}(\text{Brems})$	$\text{BR}(F_V = \sqrt{2}F) [\mathcal{O}(p^4)]$	$\text{BR}(F_V = \sqrt{3}F) [\mathcal{O}(p^4)]$
100 MeV	8.6×10^{-4}	9.0×10^{-4}	9.5×10^{-4}
300 MeV	1.7×10^{-4}	1.9×10^{-4}	2.3×10^{-4}
500 MeV	2.8×10^{-5}	3.9×10^{-5}	5.4×10^{-5}

Table 2: Branching ratios $\text{Br}(\tau^- \rightarrow \pi^-\pi^0\gamma\nu_\tau)$ for different values of E_γ^{cut} . The second column corresponds to the complete Bremsstrahlung and the third and fourth to the $\mathcal{O}(p^4)$ contributions.

E_γ^{cut}	$\text{BR}(\text{SD}) [\mathcal{O}(p^6)]$	$\text{BR} [\mathcal{O}(p^6)]$
100 MeV	1.3×10^{-3}	$(1.9 \pm 0.3) \times 10^{-3}$
300 MeV	5.1×10^{-4}	$(1.1 \pm 0.3) \times 10^{-3}$
500 MeV	2.4×10^{-4}	$(0.6 \pm 0.2) \times 10^{-3}$

Table 3: Branching ratios $\text{Br}(\tau^- \rightarrow \pi^-\pi^0\gamma\nu_\tau)$ for different E_γ^{cut} values at $\mathcal{O}(p^6)$.

As it can be observed from Table 2 and fig. 14, the main contribution at $\mathcal{O}(p^4)$ corresponds to the complete Bremsstrahlung (SI) amplitude (in agreement with ref. [62]), and the value for the branching ratio becomes smaller with larger values of E_γ^{cut} . The values in Table 2 are slightly different from those reported in ref. [62], this effect is mainly due to the parametrization of the pion vector form factor (see fig. 9). The form factor obtained from the dispersion relation [124] is above the one obtained using the Guerrero-Pich parametrization [143] at $s \simeq M_\rho^2$, and also the former includes the $\rho(1450)$ and $\rho(1700)$ resonances.

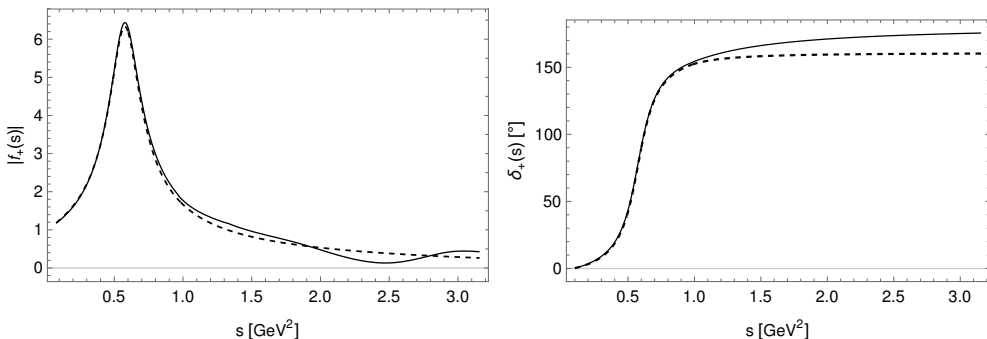


Figure 9: Modulus and phase of the pion vector form factor, $f_+(s)$. The solid line corresponds to the dispersive representation used in ref. [124] while the dashed line corresponds to the Guerrero-Pich parametrization [143] employed by ref. [62].

According to our discussion on error estimation of the $\mathcal{O}(p^4)$ result (including the uncertainty coming from missing higher-order terms from the result at $\mathcal{O}(p^6)$ when only SD constraints are used), we have -for $E_\gamma^{cut} = 300$ MeV- $\text{BR}(\tau^- \rightarrow \pi^-\pi^0\nu_\tau) = (1.9_{-0.0}^{+3.2}) \cdot 10^{-4}$.

The spectrum for these decays with $v_i = a_i = 0$ is plotted in fig. 10, the dominant peak

corresponds to bremsstrahlung off the π^- , and the secondary receives two contributions: one from bremsstrahlung off the τ lepton and another from a resonance exchange in $V_{\mu\nu}$ (for $E_\gamma^{cut} \leq 100$ MeV, these two are merged into one single peak). The rate and spectrum are dominated by the complete bremsstrahlung (SI) contribution.

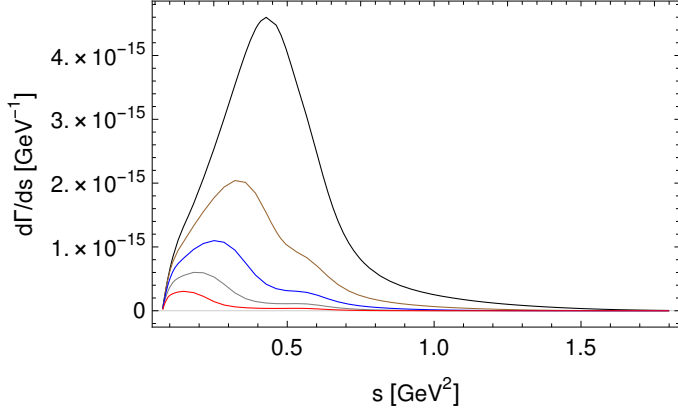


Figure 10: The $\pi^-\pi^0$ hadronic invariant mass distribution for the $\tau^-\rightarrow\pi^-\pi^0\gamma\nu_\tau$ decays for $E_\gamma^{cut} = 100$ MeV (black), $E_\gamma^{cut} = 200$ MeV (brown), $E_\gamma^{cut} = 300$ MeV (blue), $E_\gamma^{cut} = 400$ MeV (gray) and $E_\gamma^{cut} = 500$ MeV (red) using only the Bremsstrahlung (SI) contribution.

In fig. 11, we show the distribution for $E_\gamma^{cut} = 300$ MeV taking into account the SI contribution (dotted line) and the $\mathcal{O}(p^4)$ amplitude obtained using $F_V = \sqrt{2}F$ (dashed line) and $F_V = \sqrt{3}F$ (solid line), the most important contribution corresponds to the ρ resonance exchange at $s \sim 0.6$ GeV². The main difference between these two approaches is seen in fig. 11, where up to $s \sim 0.4$ GeV² the dashed line is below and the solid line is above the bremsstrahlung (SI) contribution (dotted line). The dashed line is quite similar to the distribution in fig. 2 of ref. [62] while the solid line resembles closely the distribution in fig. 4.6 of ref. [142] obtained from the vector meson dominance (VMD) model [144] neglecting the ω -resonance contribution.

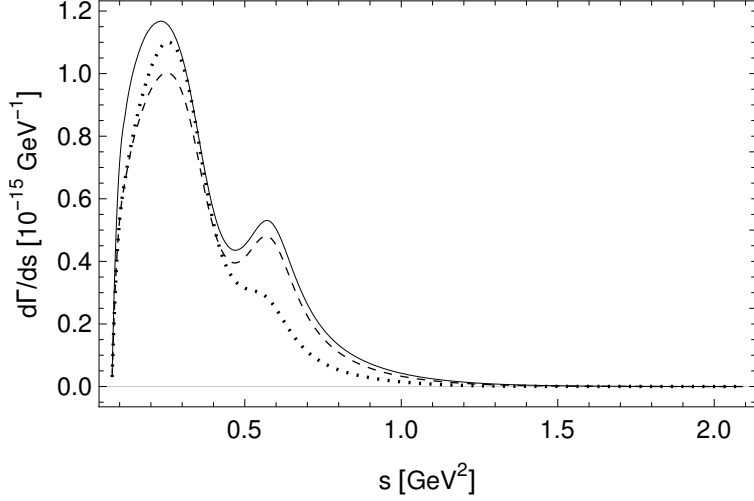


Figure 11: The $\pi^-\pi^0$ hadronic invariant mass distributions for $E_\gamma^{cut} = 300$ MeV. The solid and dashed lines represent the $\mathcal{O}(p^4)$ corrections using $F_V = \sqrt{3}F$ and $F_V = \sqrt{2}F$, respectively. The dotted line stands for the Bremsstrahlung contribution (SI).

In fig. 12 we show a comparison between the di-pion distribution at different orders. As we can see, the inclusion of the corrections at $\mathcal{O}(p^6)$ gives a noticeable enhancement at low s .

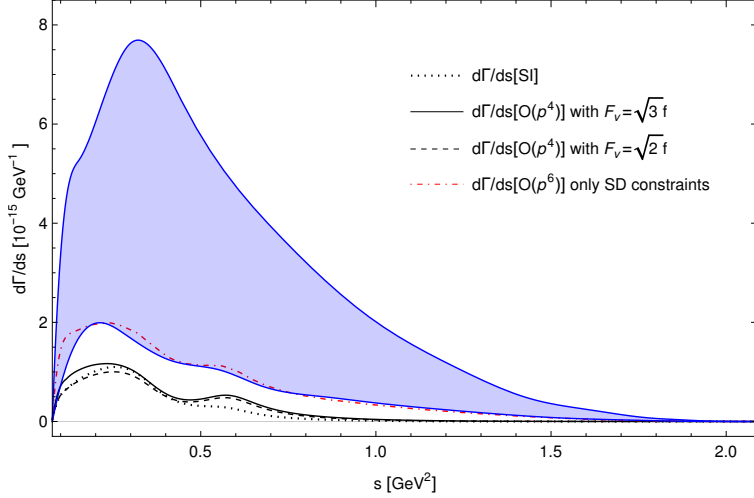


Figure 12: The $\pi^-\pi^0$ hadronic invariant mass distributions for $E_\gamma^{cut} = 300$ MeV. The solid and dashed line represent the $\mathcal{O}(p^4)$ corrections using $F_V = \sqrt{3}F$ and $F_V = \sqrt{2}F$, respectively. The dotted line represents the Bremsstrahlung contribution (SI). The dotdashed red line corresponds to using only SD constraints at $\mathcal{O}(p^6)$ and the blue shaded region overestimates the corresponding uncertainties.

For the photon energy distribution, fig. 13, we can differentiate between the full amplitude (solid, dashed lines up to $\mathcal{O}(p^4)$ and dotdashed red line up to $\mathcal{O}(p^6)$) and the bremsstrahlung contribution (dotted line) but, as in the case of the branching fraction, the distribution decreases for high-energies. In the case of the $\mathcal{O}(p^6)$ distribution there is an enhancement at middle and

high photon energies.

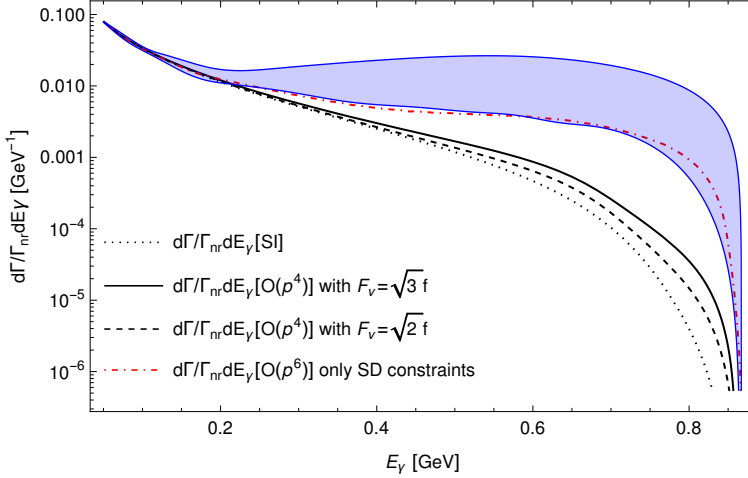


Figure 13: Photon energy distribution for the $\tau^- \rightarrow \pi^-\pi^0\gamma\nu_\tau$ decays normalized with the non-radiative decay width. The dotted line represents the Bremsstrahlung contribution. The solid and dashed lines represent the $\mathcal{O}(p^4)$ corrections using $F_V = \sqrt{3}F$ and $F_V = \sqrt{2}F$, respectively. The dotdashed red line corresponds to using only SD constraints at $\mathcal{O}(p^6)$ (with overestimated uncertainties in the blue shaded area).

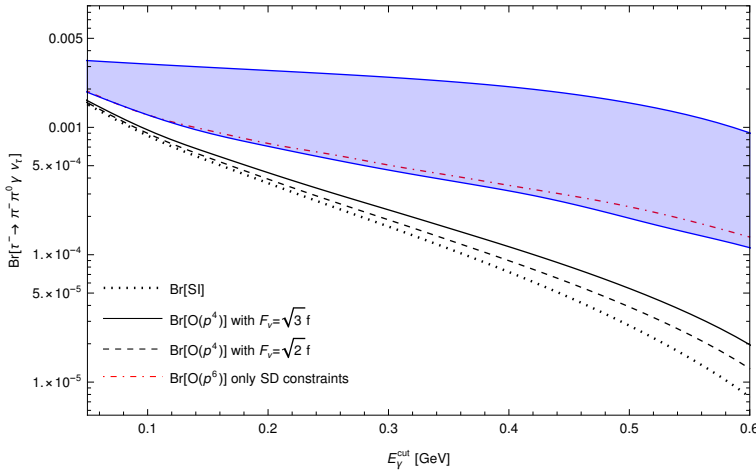


Figure 14: Branching ratio for the $\tau^- \rightarrow \pi^-\pi^0\gamma\nu_\tau$ decays as a function of E_γ^{cut} . The dotted line represents the Bremsstrahlung contribution, the solid line and dashed line represent the $\mathcal{O}(p^4)$ corrections using $F_V = \sqrt{3}F$ and $F_V = \sqrt{2}F$, respectively. The dotdashed red line is the $\mathcal{O}(p^6)$ contribution using only SD constraints and neglecting all other couplings. The blue shaded region overestimates the $\mathcal{O}(p^6)$ uncertainties.

According to Figs. 11 to 14, measurements of the $\pi\pi$ invariant mass, of the photon spectrum and the partial decay width, for a reasonable cut on E_γ (at low enough energies the inner bremmstrahlung contribution hides completely any structure-dependent effect), could decrease substantially the uncertainty of the $\mathcal{O}(p^6)$ computation. This was already emphasized in ref.

[62] but remained unmeasured at BaBar and Belle. We hope these data can finally be acquired and analyzed at Belle-II.

In fig. 15, we show the branching ratio for $E_\gamma^{cut} = 100, 300$, and 500 MeV from top to bottom. The outcomes were summarized in Table 3.

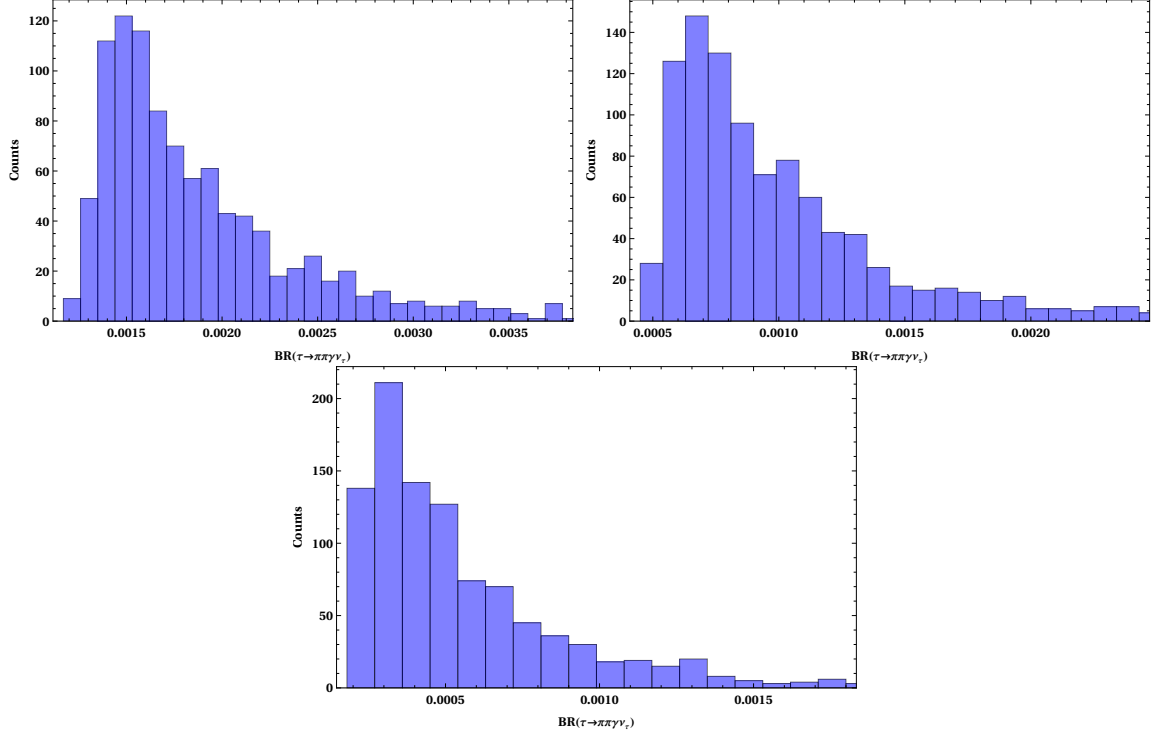


Figure 15: Predictions for the branching ratio at $\mathcal{O}(p^6)$ for a sample of 1000 points, with $E_{cut} = 100, 300$, and 500 MeV from top to bottom.

3 IB corrections to $a_\mu^{HVP,LO\pi\pi}$

We can evaluate the leading contributions to the hadronic vacuum polarization (HVP) by means of the dispersion relation [145],

$$a_\mu^{HVP,LO} = \frac{1}{4\pi^3} \int_{s_{thr}}^\infty ds K(s) \sigma_{e^- e^+ \rightarrow hadrons}^0(s), \quad (65)$$

where $K(s)$ is a smooth QED kernel concentrated at low energies, which increases the $E \lesssim M_\rho$ contribution,

$$K(s) = \frac{x^2}{2}(2-x^2) + \frac{(1+x^2)(1+x)^2}{x^2} \left(\ln(1+x) - x + \frac{x^2}{2} \right) + \frac{(1+x)}{(1-x)} x^2 \ln(x), \quad (66)$$

with

$$x = \frac{1-\beta_\mu}{1+\beta_\mu}, \quad \beta_\mu = \sqrt{1-4m_\mu^2/s},$$

and $\sigma_{e^- e^+ \rightarrow hadrons}^0(s)$ is the bare hadronic cross section²⁸. We can relate the hadronic spectral function from τ decays to the $e^+ e^-$ hadronic cross section by including the radiative corrections and the IB effects. For the $\pi\pi$ final state, we have [61, 62]:

$$\sigma_{\pi\pi}^0 = \left[\frac{K_\sigma(s)}{K_\Gamma(s)} \frac{d\Gamma_{\pi\pi[\gamma]}}{ds} \right] \frac{R_{IB}(s)}{S_{EW}}, \quad (67)$$

where

$$K_\Gamma(s) = \frac{G_F^2 |V_{ud}|^2 m_\tau^3}{384\pi^3} \left(1 - \frac{s}{m_\tau^2}\right)^2 \left(1 + \frac{2s}{m_\tau^2}\right), \quad (68)$$

$$K_\sigma(s) = \frac{\pi\alpha^2}{3s},$$

and the IB corrections

$$R_{IB}(s) = \frac{FSR(s)}{G_{EM}(s)} \frac{\beta_{\pi^+\pi^-}^3}{\beta_{\pi^+\pi^0}^3} \left| \frac{F_V(s)}{f_+(s)} \right|^2. \quad (69)$$

The S_{EW} term encodes the SD electroweak corrections [146, 147, 148, 149, 150, 151, 152, 153] and $FSR(s)$ accounts for the radiation from the final-state pions [154, 155]. The $G_{EM}(s)$ term was already discussed at length in section 2, the $\beta_{\pi^+\pi^-}^3/\beta_{\pi^+\pi^0}^3$ term is a phase space factor and the last term in $R_{IB}(s)$ is a ratio between the neutral ($F_V(s)$) and the charged ($f_+(s)$) pion form factor.

In order to study the effect of the radiative correction $G_{EM}(s)$ on $a_\mu^{HVP,LO}[\pi\pi]$, we have evaluated the following expression [62]

$$\Delta a_\mu^{HVP,LO} = \frac{1}{4\pi^3} \int_{s_1}^{s_2} ds K(s) \left[\frac{K_\sigma(s)}{K_\Gamma(s)} \frac{d\Gamma_{\pi\pi[\gamma]}}{ds} \right] \left(\frac{R_{IB}(s)}{S_{EW}} - 1 \right), \quad (70)$$

taking $S_{EW} = 1$, $\frac{\beta_{\pi^+\pi^-}^3}{\beta_{\pi^+\pi^0}^3} = 1$ and $\left| \frac{F_V(s)}{f_+(s)} \right|^2 = 1$. The results are summarized in Table 4 using DR form factor. The results obtained for the $G_{EM}^{(0)}$ and the complete $\mathcal{O}(p^4)$ contribution (with $F_V = \sqrt{2}F$) agree with those in [62], which are $+16 \cdot 10^{-11}$ and $-10 \cdot 10^{-11}$, respectively (for the whole integral). In Table 5, we summarized the results obtained using the Guerrero-Pich [143] parametrization of the form factor (which only accounts for the completely dominant ρ exchange), which are in nice agreement with those found with the dispersive form factor (that also includes the $\rho(1450)$ and $\rho(1700)$ effects). This checks, a posteriori, that excited resonance contributions make a negligible effect in the $G_{EM}(s)$ corrections to $a_\mu^{HVP,LO}$ ²⁹.

The values in the last column of Tables 4 and 5 were obtained evaluating the eq. (70)

²⁸Although final state radiation would belong to HVP,NLO it is always included in HVP,LO (and not in HVP,NLO) as eliminating this radiation from the measured data is unfeasible. Thus, a final state radiation (FSR) factor is also needed in the radiative corrections discussed below.

²⁹By replacing $D_\rho^{-1}(x)$ by $(1 + \beta_{\rho'})^{-1}(D_\rho^{-1}(x) + \beta_{\rho'} D_{\rho'}^{-1}(x))$, with $\beta_{\rho'} \in [0.12, 0.15]$ [125] throughout the v_i and a_i form factors, we have verified that the impact of the ρ' on the $G_{EM}(s)$ correction to $a_\mu^{HVP,LO}[\pi\pi, \tau]$ is negligible. Similarly, the error induced by other excited resonances shall also be irrelevant.

according to the couplings discussed in section 1.5 for a sample of 200 points for each interval of integration (results were stable under increasing this number).

$[s_1, s_2]$	$\Delta a_{\mu, G_{EM}^{(0)}}^{HVP,LO}$	$\Delta a_{\mu, SI}^{HVP,LO}$	$\Delta a_{\mu, [\mathcal{O}(p^4)]}^{HVP,LO}$	$\Delta a_{\mu, [\mathcal{O}(p^4)]}^{HVP,LO}$	$\Delta a_{\mu, [SD]}^{HVP,LO}$	$\Delta a_{\mu, [\mathcal{O}(p^6)]}^{HVP,LO}$
$[4m_{\pi}^2, 1 \text{ GeV}^2]$	+17.8	-11.0	-11.3	-17.0	-32.4	-74.8 ± 44.0
$[4m_{\pi}^2, 2 \text{ GeV}^2]$	+18.3	-10.1	-10.3	-16.0	-31.9	-75.9 ± 45.5
$[4m_{\pi}^2, 3 \text{ GeV}^2]$	+18.4	-10.0	-10.2	-15.9	-31.9	-75.9 ± 45.6
$[4m_{\pi}^2, m_{\tau}^2]$	+18.4	-10.0	-10.2	-15.9	-31.9	-75.9 ± 45.6

Table 4: Contributions to $\Delta a_{\mu}^{HVP,LO}$ in units of 10^{-11} using the dispersive representation of the form factor. From the two evaluations labelled $\mathcal{O}(p^4)$, the left(right) one corresponds to $F_V = \sqrt{2}F$ ($F_V = \sqrt{3}F$).

$[s_1, s_2]$	$\Delta a_{\mu, G_{EM}^{(0)}}^{HVP,LO}$	$\Delta a_{\mu, SI}^{HVP,LO}$	$\Delta a_{\mu, [\mathcal{O}(p^4)]}^{HVP,LO}$	$\Delta a_{\mu, [\mathcal{O}(p^4)]}^{HVP,LO}$	$\Delta a_{\mu, [SD]}^{HVP,LO}$	$\Delta a_{\mu, [\mathcal{O}(p^6)]}^{HVP,LO}$
$[4m_{\pi}^2, 1 \text{ GeV}^2]$	+17.3	-10.2	-10.4	-15.9	-28.3	-63.2 ± 16.5
$[4m_{\pi}^2, 2 \text{ GeV}^2]$	+17.7	-9.4	-9.6	-15.2	-28.1	-58.1 ± 12.2
$[4m_{\pi}^2, 3 \text{ GeV}^2]$	+17.8	-9.3	-9.5	-15.1	-28.0	-67.8 ± 17.5
$[4m_{\pi}^2, m_{\tau}^2]$	+17.8	-9.3	-9.5	-15.1	-28.0	-64.9 ± 13.4

Table 5: Contributions to $\Delta a_{\mu}^{HVP,LO}$ in units of 10^{-11} using the GP parametrization of the form factor. From the two evaluations labelled $\mathcal{O}(p^4)$, the left(right) one corresponds to $F_V = \sqrt{2}F$ ($F_V = \sqrt{3}F$).

The other contributions are summarized in Table 6.

- The S_{EW} contribution $S_{EW} = 1.0201$ gives $\Delta a_{\mu}^{HVP,LO} = -103.1 \times 10^{-11}$, consistent with earlier determinations (using slightly different values of S_{EW}) and with a negligible error.
- The phase space (PS) correction induces $\Delta a_{\mu}^{HVP,LO} = -74.5 \times 10^{-11}$ (trivially in agreement with previous computations), again with tiny uncertainties.
- The final state radiation (FSR, which is formally NLO) yields $\Delta a_{\mu}^{HVP,LO} = +45.5(4.6) \times 10^{-11}$, in accord with ref. [67] (its value was not quoted in ref. [62]).
- The correction due to the ratio of the form factors (fig. 16) is harder to evaluate. We have considered two alternatives, labelled FF1 and FF2, that we explain next. We use the following numerical inputs for the $\rho - \omega$ mixing parameter $\theta_{\rho\omega} = (-3.5 \pm 0.7) \times 10^{-3} \text{ GeV}^2$ [62] and $\Gamma_{\rho^0} - \Gamma_{\rho^+} = 0.3 \pm 1.3 \text{ MeV}$, $m_{\rho^\pm} - m_{\rho^0} = 0.7 \pm 0.8 \text{ MeV}$ and $m_{\rho^0} = 775.26 \pm 0.25 \text{ MeV}$ from PDG [156].

In FF1, as in ref. [62], we include the measurement of the $\pi\pi\gamma$ channel of the ρ^0 $\Gamma_{\rho^0 \rightarrow \pi^+\pi^-\gamma} = 1.5 \pm 0.2 \text{ MeV}$, and the measurement of $\Gamma_{\rho^0 \rightarrow \pi^0\gamma}$ and $\Gamma_{\rho^+ \rightarrow \pi^+\gamma}$ which are approximately 0.1 MeV [157]. Thus, we estimate $\Gamma_{\rho^0 \rightarrow \pi^+\pi^-\gamma} - \Gamma_{\rho^\pm \rightarrow \pi^\pm\pi^0\gamma} = 1.5 \pm 1.3 \text{ MeV}$. In this way, we get a positive correction of $\Delta a_{\mu}^{HVP,LO} = +40.9(48.9) \times 10^{-11}$. The uncertainty on the third column of Table 6 (FF1) corresponds to sum the errors due to

uncertainties of $\rho - \omega$ mixing (8.5), the $\rho^+ - \rho^0$ mass difference (15.9), and the $\rho^+ - \rho^0$ width difference (45.5) in quadrature (in units of 10^{-11}).

On the other hand, in FF2 we use the same numerical inputs for $\Gamma_{\rho^0 \rightarrow \pi^+ \pi^- \gamma} - \Gamma_{\rho^\pm \rightarrow \pi^\pm \pi^0 \gamma} = 0.45 \pm 0.45$ MeV as in ref. [62] (and all the others as we did before), we obtain a positive correction of $\Delta a_\mu^{HVP,LO} = +77.6(24.0) \times 10^{-11}$. The uncertainty on the fourth column Table 6 (FF2) corresponds to sum the errors due to uncertainties of $\rho - \omega$ mixing (8.6), the $\rho^+ - \rho^0$ mass difference (15.9), and the $\rho^+ - \rho^0$ width difference (15.8) in quadrature (in units of 10^{-11}).

This correction was $+(61 \pm 26 \pm 3) \cdot 10^{-11}$ in [62] and $+(86 \pm 32 \pm 7) \cdot 10^{-11}$ in [67], in agreement (despite the big errors) with our FF2 and FF1 determinations, respectively.

- Finally, we get $(-15.9^{+5.7}_{-16.0}) \cdot 10^{-11}$ ($(-76 \pm 46) \cdot 10^{-11}$) for the $G_{EM}(s)$ correction at $\mathcal{O}(p^4)$ ($\mathcal{O}(p^6)$), versus $-10 \cdot 10^{-11}$ in [62] and $-37 \cdot 10^{-11}$ in [65] (from the last two results, $(-19.2 \pm 9.0) \cdot 10^{-11}$ was used in [67]). As explained before, the previous uncertainty on the $\mathcal{O}(p^6)$ can only be taken as an upper bound on it. Also interesting is the $G_{EM}(s)$ correction when only the couplings restricted by SD are used (with all others at this order set to zero), which allows us to estimate the effect of missing higher-order terms on the $\mathcal{O}(p^4)$ result quoted above. This $\mathcal{O}(p^4)$ result, which is our reference value, is consistent with both the earlier $R\chi T$ [62] and the VMD [67] evaluations, albeit with a larger (asymmetric) error.

$[s_1, s_2]$	SEW	PS	FSR	FF1	FF2	EM
$[4m_\pi^2, 1 \text{ GeV}^2]$	-101.1	-74.1	+44.7	$+41.8 \pm 49.0$	$+78.4 \pm 24.5$	$-17.0^{+5.7}_{-15.4}$
$[4m_\pi^2, 2 \text{ GeV}^2]$	-103.1	-74.4	+45.5	$+40.9 \pm 48.9$	$+77.6 \pm 24.0$	$-16.0^{+5.7}_{-15.9}$
$[4m_\pi^2, 3 \text{ GeV}^2]$	-103.1	-74.5	+45.5	$+40.9 \pm 48.9$	$+77.6 \pm 24.0$	$-15.9^{+5.7}_{-16.0}$
$[4m_\pi^2, m_\tau^2]$	-103.1	-74.5	+45.5	$+40.9 \pm 48.9$	$+77.6 \pm 24.0$	$-15.9^{+5.7}_{-16.0}$

$[s_1, s_2]$	$\Delta a_\mu(\text{FF1})$	$\Delta a_\mu(\text{FF2})$
$[4m_\pi^2, 1 \text{ GeV}^2]$	$-105.7^{+49.5}_{-51.6}$	$-69.1^{+25.6}_{-29.3}$
$[4m_\pi^2, 2 \text{ GeV}^2]$	$-107.1^{+49.4}_{-51.6}$	$-70.4^{+25.1}_{-29.2}$
$[4m_\pi^2, 3 \text{ GeV}^2]$	$-107.1^{+49.4}_{-51.7}$	$-70.4^{+25.1}_{-29.2}$
$[4m_\pi^2, m_\tau^2]$	$-107.1^{+49.4}_{-51.7}$	$-70.4^{+25.1}_{-29.2}$

Table 6: Contributions to $\Delta a_\mu^{HVP,LO}$ in units of 10^{-11} using the DR form factor as the reference one.

In fig. 17, we show the full IB correction factor $R_{IB}(s)$ for the different orders of approximation in the $G_{EM}(s)$ factor using the DR parametrization of the form factor. As we can see, there is a difference between the contributions at $\mathcal{O}(p^4)$ and those at $\mathcal{O}(p^6)$ for energies below $\sim 0.5 \text{ GeV}^2$ and above $\sim 0.7 \text{ GeV}^2$.

An important cross-check is the branching fraction $B_{\pi\pi^0} = \Gamma(\tau \rightarrow \pi\pi^0\nu_\tau)/\Gamma_\tau$ which is a directly measured quantity. It can also be evaluated from the $I = 1$ component of the $e^+e^- \rightarrow \pi^+\pi^-(\gamma)$ cross section after taking into account the IB corrections. The branching

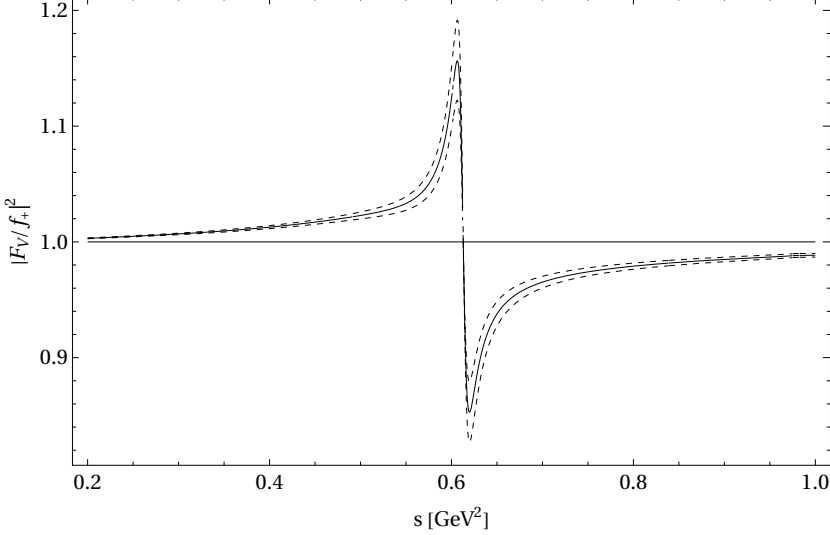


Figure 16: Ratio of the form factors (FF1) for $\theta_{\rho\omega} = (-3.5 \pm 0.7) \times 10^{-3} \text{ GeV}^2$. The solid line represents the mean value.

fraction is given by

$$B_{\pi\pi^0}^{CVC} = B_e \int_{4m_\pi^2}^{m_\tau^2} ds \sigma_{\pi^+\pi^-(\gamma)}(s) \mathcal{N}(s) \frac{S_{EW}}{R_{IB}(s)}, \quad (71)$$

where

$$\mathcal{N}(s) = \frac{3|V_{ud}|^2}{2\pi\alpha_0^2 m_\tau^2} s \left(1 - \frac{s}{m_\tau^2}\right)^2 \left(1 + \frac{2s}{m_\tau^2}\right). \quad (72)$$

Using the most recent data obtained from BaBar [54]³⁰ for the $e^+e^- \rightarrow \pi^+\pi^-(\gamma)$ cross section and taking the same numerical inputs as we did for FF1, we get

$$B_{\pi\pi^0}^{CVC} = \begin{cases} (24.76 \pm 0.11 \pm 0.25 \pm 0.01 \pm 0.01 \pm 0.02)\%, & \text{SI}, \\ (24.77 \pm 0.11 \pm 0.25 \pm 0.01 \pm 0.01 \pm 0.02)\%, & F_V = \sqrt{2}F, \\ (24.77 \pm 0.11 \pm 0.25 \pm 0.01 \pm 0.01 \pm 0.02)\%, & F_V = \sqrt{3}F, \\ (24.80 \pm 0.11 \pm 0.25 \pm 0.01 \pm 0.01 \pm 0.02)\%, & \text{SD}, \end{cases} \quad (73)$$

where ‘SI’, ‘ $F_V = \sqrt{2}F$ ’, ‘ $F_V = \sqrt{3}F$ ’ and ‘SD’ correspond to the different approximations of the $G_{EM}(s)$ factor. The result for $F_V = \sqrt{2}F$ is our reference one, with a negligible uncertainty from the missing higher-order terms starting at $\mathcal{O}(p^6)$.

On the other hand, when we use the same numerical inputs as in the case of FF2, we get

³⁰We thank to Alex Keshavarzi and Bogdan Malaescu for providing us tables with the measurement of the $e^+e^- \rightarrow \pi^+\pi^-(\gamma)$ cross section.

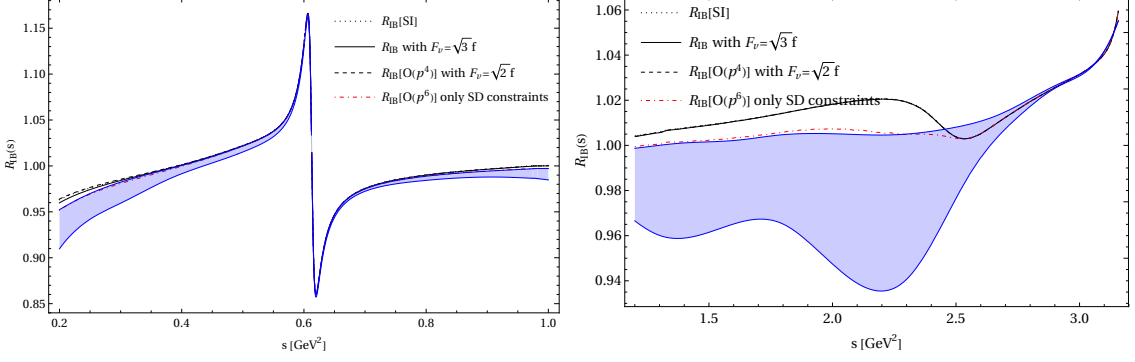


Figure 17: Full IB correction factor $R_{IB}(s)$ for the different orders of approximation in $G_{EM}(s)$ using the central values given in (FF1). The blue region corresponds to the (overestimated) corrections at $\mathcal{O}(p^6)$ in $G_{EM}(s)$.

(again our reference result is the $F_V = \sqrt{2}F$ one, with the uncertainties quoted below)

$$B_{\pi\pi^0}^{CVC} = \begin{cases} (24.57 \pm 0.11 \pm 0.08 \pm 0.01 \pm 0.01 \pm 0.02)\%, & \text{SI}, \\ (24.57 \pm 0.11 \pm 0.08 \pm 0.01 \pm 0.01 \pm 0.02)\%, & F_V = \sqrt{2}F, \\ (24.58 \pm 0.11 \pm 0.08 \pm 0.01 \pm 0.01 \pm 0.02)\%, & F_V = \sqrt{3}F, \\ (24.61 \pm 0.11 \pm 0.08 \pm 0.01 \pm 0.01 \pm 0.01 \pm 0.02)\%, & \text{SD}. \end{cases} \quad (74)$$

In both cases, the first error corresponds to the statistical experimental uncertainty on $\sigma_{\pi\pi(\gamma)}$, the second is related to uncertainty on the $\rho^+ - \rho^0$ width difference, the third to the uncertainty in the $\rho^+ - \rho^0$ mass difference and the fourth to the uncertainty of the $\rho - \omega$ mixing. The last error corresponds to the corrections induced by FSR on $B_{\pi\pi^0}^{CVC}$, which reduces $\sim -0.20(2)\%$ the $\pi\pi$ branching fraction.

If we include all the couplings contributing to $G_{EM}(s)$ at $\mathcal{O}(p^6)$ according to section 1.5 we have an additional error associated to the EM contributions. Thus, we get

$$B_{\pi\pi^0}^{CVC} = (24.80 \pm 0.11 \pm 0.25 \pm 0.01 \pm 0.01 \pm 0.02^{+0.21}_{-0.01})\%, \quad (75)$$

for FF1, and

$$B_{\pi\pi^0}^{CVC} = (24.61 \pm 0.11 \pm 0.08 \pm 0.01 \pm 0.01 \pm 0.02^{+0.21}_{-0.01})\%. \quad (76)$$

for FF2. Both previous results match perfectly our reference determinations obtained with $F_V = \sqrt{2}F$.

These results are in good agreement (though better for FF1) with the value reported by the Belle [158] collaboration,

$$B_{\pi\pi^0}^\tau = (25.24 \pm 0.01 \pm 0.39)\%, \quad (77)$$

where the first uncertainty is statistical and the second is systematic. Nonetheless, they are in

some tension with the very precise ALEPH measurement ($25.471 \pm 0.097 \pm 0.085\%$)% [159].

We show in fig. 18 the prediction for the $e^+e^- \rightarrow \pi^+\pi^-$ cross section using the data reported by Belle [158] (as it is the most precise measurement of this spectrum) for the normalized spectrum $(1/N_{\pi\pi})(dN_{\pi\pi}/ds)$ compared to the last measurements from BaBar [54] and KLOE [160]³¹.

We recall that the $e^+e^- \rightarrow \pi^+\pi^-$ cross section obtained using τ data is given by [158]

$$\sigma_{\pi\pi}^0 = \frac{1}{N(s)} \times \left(\frac{B_{\pi\pi}}{B_e} \right) \times \left(\frac{1}{N_{\pi\pi}} \frac{dN_{\pi\pi}}{ds} \right) \left(\frac{R_{IB}(s)}{S_{EW}} \right). \quad (78)$$

In fig. 18 the τ -based prediction is obtained using the $\mathcal{O}(p^4)$ result for $G_{EM}(s)$, with the estimated uncertainty from missing higher-order corrections given by the result at $\mathcal{O}(p^6)$ (employing only the SD constraints). The blue dotdashed line shown overestimates the error at $\mathcal{O}(p^6)$.

From fig. 18, we observe good agreement between the BaBar data and the τ decays prediction (slightly better for FF1)³². The previous comparisons make us consider our evaluation with FF1 the reference one (so that its difference with FF2 will assess the size of the error induced by IB among the $\rho \rightarrow \pi\pi\gamma$ decay channels)³³.

Using eq. (78) we evaluate the IB-corrected $a_\mu^{HVP,LO}[\pi\pi, \tau]$ from the Belle mass spectrum. We use the PDG values [156] for m_τ , V_{ud} and B_e .

In tables 7 (8) we show IB-corrected $a_\mu^{HVP,LO}[\pi\pi, \tau]$ in units of 10^{-10} using the measured mass spectrum by Belle (ALEPH). For each dataset, results for the different approximations to $G_{EM}(s)$ are shown. We choose showing first the results with both Belle and ALEPH datasets as the first (second) one yields the most accurate spectral function (branching ratio) measurement. As in ref. [67] (and later works by the Orsay group), the contributions are split in two intervals. In the first one, $\sqrt{s} \in [2m_{\pi^\pm}, 0.36 \text{ GeV}]$, (the very scarce) data is not used, as this affects the precision of the integral. Instead, we use the results of the dispersive fits in ref. [125]. We proceed analogously in tables 9 and 10 with the CLEO [166] and OPAL [167]³⁴ measurements.

Taking into account all di-pion tau decay data from the ALEPH [159], Belle [158], CLEO [166] and OPAL [167] Colls. (the latter yielding the largest contribution to $a_\mu^{HVP,LO}[\pi\pi]$ exceeding $\sim 10.7 \cdot 10^{-10}$ the mean, although with the largest errors as well) in tables 11 and 12 at $\mathcal{O}(p^4)$

³¹We have chosen to show in the comparison these two e^+e^- data sets as the results from both Colls. are those deviating the most, and thus mainly responsible from the tension in $\sigma(e^+e^- \rightarrow \pi^+\pi^-)$.

³²One can also check how important the $\rho^+ - \rho^0$ width difference is around $s \simeq M_\rho^2$.

³³We, nevertheless, recall that recent BESIII data [55, 161] and evaluations within the Hidden Local Symmetry model [162, 163, 164, 165] agree better with the KLOE data than with BaBar's.

³⁴We thank to Jorge Portolés for providing us with the OPAL data set.

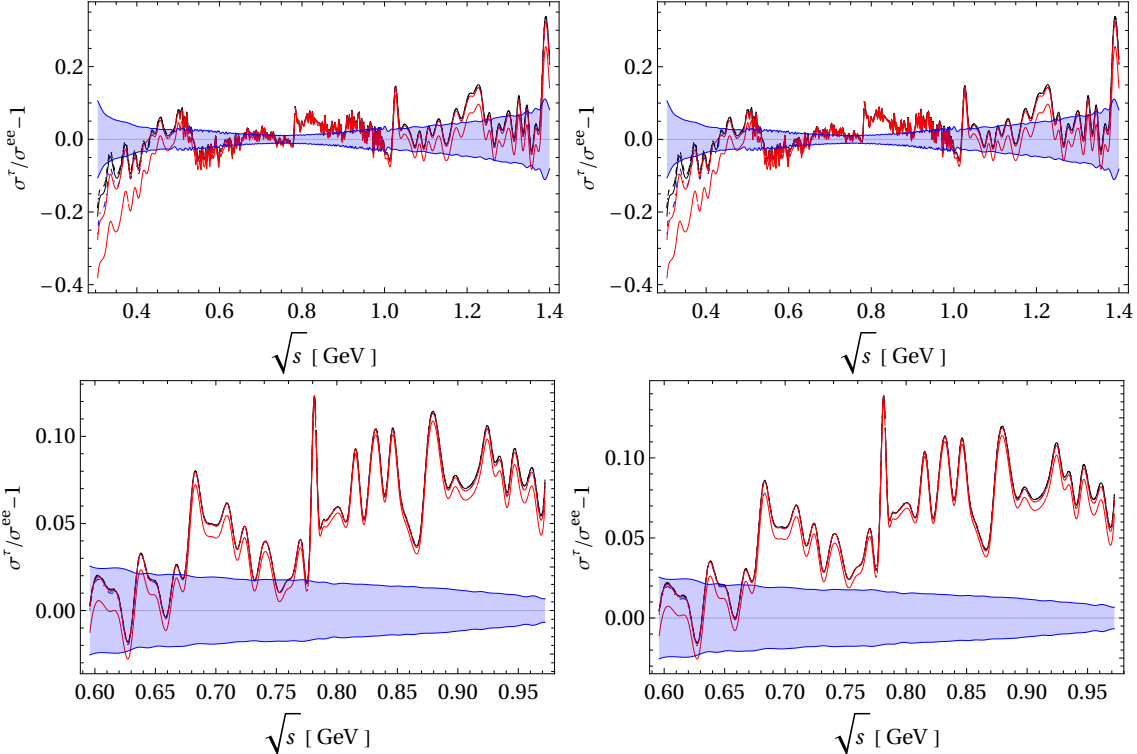


Figure 18: Comparison between the different data sets from BaBar (above) and KLOE (below) with $\Delta\Gamma_{\pi\pi\gamma} = 1.5 \text{ MeV}$ (left-hand) and $\Delta\Gamma_{\pi\pi\gamma} = 0.45 \text{ MeV}$ (right-hand) for FF1 and FF2, respectively. The blue region corresponds to the experimental error on $\sigma_{\pi\pi(\gamma)}$. The solid and dashed lines represent the contributions with $F_V = \sqrt{3}F$ and $F_V = \sqrt{2}F$ at $\mathcal{O}(p^4)$, respectively. The dotted line is the SI contribution. The red line depicts the envelope of $G_{EM}(s)$ at $\mathcal{O}(p^6)$, that overestimates the uncertainty at this order. The blue dotdashed line is the $\mathcal{O}(p^6)$ contribution using only SD constraints.

FF1							
$[s_1, s_2]$	SI	$F_V = \sqrt{2}F$	$F_V = \sqrt{3}F$	SD	min	max	mean
$[0.1296 \text{ GeV}^2, 1 \text{ GeV}^2]$	499.43	499.42	499.05	498.16	492.18	498.41	495.30
$[0.1296 \text{ GeV}^2, 2 \text{ GeV}^2]$	509.47	509.46	509.09	508.14	501.87	508.40	505.13
$[0.1296 \text{ GeV}^2, 3 \text{ GeV}^2]$	509.68	509.67	509.30	508.35	502.08	508.61	505.34
$[0.1296 \text{ GeV}^2, 3.125 \text{ GeV}^2]$	509.72	509.71	509.34	508.40	502.12	508.65	505.39
FF2							
$[s_1, s_2]$	SI	$F_V = \sqrt{2}F$	$F_V = \sqrt{3}F$	SD	min	max	mean
$[0.1296 \text{ GeV}^2, 1 \text{ GeV}^2]$	503.03	503.02	502.65	501.75	495.76	502.01	498.88
$[0.1296 \text{ GeV}^2, 2 \text{ GeV}^2]$	513.08	513.06	512.70	511.75	505.46	512.00	508.73
$[0.1296 \text{ GeV}^2, 3 \text{ GeV}^2]$	513.29	513.28	512.91	511.96	505.66	512.21	508.94
$[0.1296 \text{ GeV}^2, 3.125 \text{ GeV}^2]$	513.33	513.32	512.95	512.01	505.71	512.26	508.98

Table 7: IB-corrected $a_\mu^{HVP,LO}[\pi\pi, \tau]$ in units of 10^{-10} using the measured mass spectrum by Belle with $B_{\pi\pi} = (25.24 \pm 0.01 \pm 0.39)\%$. Different approximation to $G_{EM}(s)$ are displayed in the various columns. The last three of them show the results at $\mathcal{O}(p^6)$ and their differences overestimate the error at this order. The error of the $\mathcal{O}(p^4)$ prediction (obtained with $F_V = \sqrt{2}F$) can be quantified from its difference with the SD value (corresponding to the $\mathcal{O}(p^6)$ contribution using only SD constraints).

FF1							
$[s_1, s_2]$	SI	$F_V = \sqrt{2}F$	$F_V = \sqrt{3}F$	SD	min	max	mean
$[0.1296 \text{ GeV}^2, 1 \text{ GeV}^2]$	495.28	495.27	494.92	494.05	488.25	494.30	491.27
$[0.1296 \text{ GeV}^2, 2 \text{ GeV}^2]$	506.57	506.56	506.21	505.29	499.15	505.53	502.34
$[0.1296 \text{ GeV}^2, 3 \text{ GeV}^2]$	506.82	506.81	506.45	505.53	499.38	505.77	502.58
$[0.1296 \text{ GeV}^2, 3.125 \text{ GeV}^2]$	506.82	506.81	506.46	505.53	499.39	505.78	502.58
FF2							
$[s_1, s_2]$	SI	$F_V = \sqrt{2}F$	$F_V = \sqrt{3}F$	SD	min	max	mean
$[0.1296 \text{ GeV}^2, 1 \text{ GeV}^2]$	498.86	498.85	498.50	497.63	491.81	497.87	494.84
$[0.1296 \text{ GeV}^2, 2 \text{ GeV}^2]$	510.16	510.15	509.80	508.87	502.72	509.12	505.92
$[0.1296 \text{ GeV}^2, 3 \text{ GeV}^2]$	510.41	510.40	510.04	509.12	502.95	509.36	506.16
$[0.1296 \text{ GeV}^2, 3.125 \text{ GeV}^2]$	510.41	510.40	510.05	509.12	502.96	509.36	506.16

Table 8: IB-corrected $a_\mu^{HVP,LO}[\pi\pi, \tau]$ in units of 10^{-10} using the measured mass spectrum by ALEPH with $B_{\pi\pi} = (25.471 \pm 0.097 \pm 0.085)\%$. The rest is as in table 7.

FF1							
$[s_1, s_2]$	SI	$F_V = \sqrt{2}F$	$F_V = \sqrt{3}F$	SD	min	max	mean
$[0.1296 \text{ GeV}^2, 1 \text{ GeV}^2]$	498.51	498.50	498.14	497.27	491.43	497.52	494.47
$[0.1296 \text{ GeV}^2, 2 \text{ GeV}^2]$	508.98	508.97	508.61	507.69	501.54	507.93	504.74
$[0.1296 \text{ GeV}^2, 3 \text{ GeV}^2]$	509.15	509.14	508.79	507.86	501.70	508.11	504.91
$[0.1296 \text{ GeV}^2, 3.125 \text{ GeV}^2]$	509.20	509.18	508.83	507.91	501.75	508.15	504.95
FF2							
$[s_1, s_2]$	SI	$F_V = \sqrt{2}F$	$F_V = \sqrt{3}F$	SD	min	max	mean
$[0.1296 \text{ GeV}^2, 1 \text{ GeV}^2]$	502.10	502.09	501.74	500.86	495.00	501.11	498.06
$[0.1296 \text{ GeV}^2, 2 \text{ GeV}^2]$	512.58	512.57	512.22	511.29	505.12	511.58	508.33
$[0.1296 \text{ GeV}^2, 3 \text{ GeV}^2]$	512.76	512.75	512.39	511.47	505.29	511.71	508.50
$[0.1296 \text{ GeV}^2, 3.125 \text{ GeV}^2]$	512.80	512.79	512.43	511.51	505.33	511.75	508.54

Table 9: IB-corrected $a_\mu^{HVP,LO}[\pi\pi, \tau]$ in units of 10^{-10} using the measured mass spectrum by CLEO with $B_{\pi\pi} = (25.36 \pm 0.44)\%$. The rest is as in table 7.

FF1							
$[s_1, s_2]$	SI	$F_V = \sqrt{2}F$	$F_V = \sqrt{3}F$	SD	min	max	mean
$[0.1296 \text{ GeV}^2, 1 \text{ GeV}^2]$	509.50	509.51	509.07	508.04	501.31	508.34	504.82
$[0.1296 \text{ GeV}^2, 2 \text{ GeV}^2]$	521.29	521.29	520.86	519.77	512.69	520.06	516.34
$[0.1296 \text{ GeV}^2, 3 \text{ GeV}^2]$	521.49	521.49	521.06	519.96	512.88	520.25	516.56
$[0.1296 \text{ GeV}^2, 3.125 \text{ GeV}^2]$	521.49	521.49	521.06	519.97	512.88	520.26	516.57
FF2							
$[s_1, s_2]$	SI	$F_V = \sqrt{2}F$	$F_V = \sqrt{3}F$	SD	min	max	mean
$[0.1296 \text{ GeV}^2, 1 \text{ GeV}^2]$	512.99	512.99	512.56	511.53	504.78	511.82	508.30
$[0.1296 \text{ GeV}^2, 2 \text{ GeV}^2]$	524.79	524.79	524.36	523.27	516.17	523.56	519.86
$[0.1296 \text{ GeV}^2, 3 \text{ GeV}^2]$	524.99	524.99	524.56	523.46	516.36	523.76	520.06
$[0.1296 \text{ GeV}^2, 3.125 \text{ GeV}^2]$	524.99	524.99	524.56	523.46	516.36	523.76	520.06

Table 10: IB-corrected $a_\mu^{HVP,LO}[\pi\pi, \tau]$ in units of 10^{-10} using the measured mass spectrum by OPAL with $B_{\pi\pi} = (25.46 \pm 0.17 \pm 0.29)\%$. The rest is as in table 7.

$a_\mu^{HVP,LO}[\pi\pi, \tau]$			
Experiment	$2m_{\pi^\pm} - 0.36 \text{ GeV}$	$0.36 - 1.8 \text{ GeV}$	TOTAL
Belle	$8.81 \pm 0.00 \pm 0.14^{+0.16}_{-0.34}$	$511.14 \pm 1.94 \pm 7.99^{+1.91}_{-2.09}$	$519.95 \pm 1.94 \pm 7.99^{+1.91}_{-2.12}$
ALEPH	$8.89 \pm 0.00 \pm 0.05^{+0.16}_{-0.34}$	$508.26 \pm 4.48 \pm 2.82^{+1.91}_{-2.09}$	$517.15 \pm 4.48 \pm 2.82^{+1.91}_{-2.12}$
CLEO	$8.85 \pm 0.00 \pm 0.15^{+0.16}_{-0.34}$	$510.63 \pm 3.40 \pm 8.93^{+1.90}_{-2.08}$	$519.48 \pm 3.40 \pm 8.93^{+1.90}_{-2.11}$
OPAL	$8.89 \pm 0.00 \pm 0.12^{+0.15}_{-0.34}$	$522.81 \pm 10.04 \pm 7.00^{+1.87}_{-2.12}$	$531.70 \pm 10.04 \pm 7.00^{+1.87}_{-2.15}$

Table 11: IB-corrected $a_\mu^{HVP,LO}[\pi\pi, \tau]$ in units of 10^{-10} at $\mathcal{O}(p^4)$. The first error is related to the systematic uncertainties on the mass spectrum, and also include contributions from the τ -mass and V_{ud} uncertainties. The second error arises from $B_{\pi\pi^0}$ and B_e , and the third error from the isospin-breaking corrections.

$a_\mu^{HVP,LO}[\pi\pi, \tau]$			
Experiment	$2m_{\pi^\pm} - 0.36 \text{ GeV}$	$0.36 - 1.8 \text{ GeV}$	TOTAL
Belle	$7.77 \pm 0.00 \pm 0.12^{+1.20}_{-0.59}$	$507.18 \pm 1.91 \pm 7.88^{+4.72}_{-3.76}$	$514.95 \pm 1.91 \pm 7.88^{+4.87}_{-3.81}$
ALEPH	$7.84 \pm 0.00 \pm 0.04^{+1.21}_{-0.60}$	$504.37 \pm 4.35 \pm 2.79^{+4.63}_{-3.70}$	$512.21 \pm 4.35 \pm 2.79^{+4.78}_{-3.75}$
CLEO	$7.80 \pm 0.00 \pm 0.14^{+1.21}_{-0.59}$	$506.74 \pm 3.28 \pm 8.84^{+4.63}_{-3.71}$	$514.54 \pm 3.28 \pm 8.84^{+4.78}_{-3.76}$
OPAL	$7.84 \pm 0.00 \pm 0.10^{+1.20}_{-0.60}$	$518.32 \pm 9.69 \pm 6.92^{+5.25}_{-4.12}$	$526.16 \pm 9.69 \pm 6.92^{+5.39}_{-4.16}$

Table 12: IB-corrected $a_\mu^{HVP,LO}[\pi\pi, \tau]$ in units of 10^{-10} at $\mathcal{O}(p^6)$. The rest is as in table 11.

and $\mathcal{O}(p^6)$, respectively, we get the combined tau-data contribution

$$10^{10} \cdot a_\mu^{HVP,LO|_{\pi\pi, \tau \text{ data}}} = 519.6 \pm 2.8_{\text{spectra+BRs}-2.1IB}^{+1.9}, \quad (79)$$

at $\mathcal{O}(p^4)$ and

$$10^{10} \cdot a_\mu^{HVP,LO|_{\pi\pi, \tau \text{ data}}} = 514.6 \pm 2.8_{\text{spectra+BRs}-3.9IB}^{+5.0}, \quad (80)$$

at $\mathcal{O}(p^6)$.

The *IB* errors come from the uncertainty on $\Gamma(\rho \rightarrow \pi\pi\gamma)$ (FF1 vs FF2) and either from the difference between the $F_V = \sqrt{2}F$ and *SD* results (in eq. (79)) or from the difference between the 'mean' and 'min'/'max' results (in eq. (80)).

Contrary to previous estimates [62, 67, 68, 77, 69], the errors in $a_\mu^{HVP,LO|_{\pi\pi, \tau \text{ data}}}$ happen to be dominated by the uncertainty on the *IB* contributions (but for the lower error on eq. (79)).

When eqs. (79) and (80) are supplemented with the four-pion tau decays measurements (up to 1.5 GeV) and with e^+e^- data at larger energies in these modes (and with e^+e^- data in all other channels making up the hadronic cross section), we get [7, 69]

$$10^{10} \cdot a_\mu^{HVP,LO|_{\tau \text{ data}}} = 705.7 \pm 2.8_{\text{spectra+BRs}-2.1IB}^{+1.9} \pm 2.0_{e^+e^-} \pm 0.1_{\text{narrow res}} \pm 0.7_{QCD}, \quad (81)$$

at $\mathcal{O}(p^4)$, and

$$10^{10} \cdot a_{\mu}^{HVP,LO|\tau \text{ data}} = 700.7 \pm 2.8_{spectra+BRs-3.9IB}^{+5.0} \pm 2.0_{e^+e^-} \pm 0.1_{narrow res} \pm 0.7_{QCD}, \quad (82)$$

at $\mathcal{O}(p^6)$ and we have also included the uncertainties corresponding to using e^+e^- data for those contributions not covered by tau decay measurements and to the inclusion of narrow resonances and the perturbative QCD part.

Adding errors in quadrature, an uncertainty of $^{+4.0}_{-4.1}$ ($^{+6.1}_{-5.2}$) is obtained at $\mathcal{O}(p^4)$ ($\mathcal{O}(p^6)$). These numbers (all in units of 10^{-10}) have to be compared with the error of 4.0 in ref. [2].

When all other (QED, EW and subleading hadronic) contributions are added to eqs. (81) and (82) according to ref. [2], the 3.7σ [2] deficit of the SM prediction with respect to the *BNL* measurement [45] is reduced to

$$\Delta a_{\mu} \equiv a_{\mu}^{exp} - a_{\mu}^{SM} = (15.3 \pm 7.7) \cdot 10^{-10}, \quad (83)$$

at $\mathcal{O}(p^4)$, and

$$\Delta a_{\mu} \equiv a_{\mu}^{exp} - a_{\mu}^{SM} = (20.3^{+8.3}_{-8.9}) \cdot 10^{-10}, \quad (84)$$

at $\mathcal{O}(p^6)$, which are 2.0 and 2.3σ , respectively.

4 Conclusions

In this work we have revisited the resonance chiral Lagrangian computation of the isospin-breaking and radiative corrections to the $\tau^- \rightarrow \pi^- \pi^0 \nu_{\tau} \gamma$ decays in ref. [62], by including the terms that start to contribute to the $\mathcal{O}(p^6)$ chiral LECs. Our main motivation for that was to revisit the determination of $a_{\mu}^{HVP,LO}$ using tau decay data, so that it could -when combined with the e^+e^- measurements- reduce the Standard Model error on a_{μ} , thus enhancing the sensitivity to new physics of the current BNL and future FNAL and J-PARC measurements.

Our isospin breaking corrections improve the agreement between τ and e^+e^- di-pion data (both in the spectrum and its integral), which endorses our evaluation of $a_{\mu}^{HVP,LO|\tau \text{ data}}$. Our main results are $a_{\mu}^{HVP,LO|\tau \text{ data}} = (705.7^{+4.0}_{-4.1}) \cdot 10^{-10}$ (including the same contributions as in ref. [62]), and $a_{\mu}^{HVP,LO|\tau \text{ data}} = (700.7^{+6.1}_{-5.2}) \cdot 10^{-10}$ (when the operators starting to contribute to the $\mathcal{O}(p^6)$ LECs are also considered). These reduce the anomaly $\Delta a_{\mu} \equiv a_{\mu}^{exp} - a_{\mu}^{SM}$ to 2.0 and 2.3σ , respectively.

We also provide with a detailed study of the $\pi\pi$ spectrum, E_{γ} distribution and branching ratio, for different cuts on the photon energy. These $\tau^- \rightarrow \pi^- \pi^0 \nu_{\tau} \gamma$ decays observables have the potential to reduce drastically the error of our predictions, so we eagerly await their measurement

at Belle-II.

Acknowledgements

A. M. acknowledges Conacyt support through his Ph. D. scholarship. P. R. thanks the funding of Fondo SEP-Cinvestav 2018 (project number 142). A. M. and P. R. have benefitted from enriching discussions on this topic with Gabriel López Castro and Genaro Toledo Sánchez. We thank Vincenzo Cirigliano, Antonio Pich and Jorge Portolés for helpful suggestions regarding the presentation and discussion of our results, and Antonio Rojas, Eduard de la Cruz Burelo and Iván Heredia de la Cruz for their valuable help. We are indebted to Alex Keshavarzi, Bogdan Malaescu, Hisaki Hayashii and Jorge Portolés for providing us with the BaBar, Belle and OPAL data sets.

A Fit results

Since the κ_i^V couplings are related with the ω exchange which is known to give an important contribution to the $\tau \rightarrow \pi\pi\gamma\nu_\tau$ decays, we perform a global fit using the relations for the resonance saturation of the anomalous sector LECs at NLO [88], the eqs. (10)-(18) in section 1.5 and the estimation of the LECs in [168].

Neglecting all the other contributions, we get

$$\kappa_1^V = (-2.1 \pm 0.7) \cdot 10^{-2} \text{ GeV}^{-1}, \quad (85a)$$

$$\kappa_2^V = (-8.8 \pm 9.1) \cdot 10^{-3} \text{ GeV}^{-1}, \quad (85b)$$

$$\kappa_3^V = (2.2 \pm 5.8) \cdot 10^{-3} \text{ GeV}^{-1}, \quad (85c)$$

$$\kappa_6^V = (-2.1 \pm 0.3) \cdot 10^{-2} \text{ GeV}^{-1}, \quad (85d)$$

$$\kappa_7^V = (1.2 \pm 0.5) \cdot 10^{-2} \text{ GeV}^{-1}, \quad (85e)$$

$$\kappa_8^V = (3.1 \pm 0.9) \cdot 10^{-2} \text{ GeV}^{-1}, \quad (85f)$$

$$\kappa_9^V = (-0.1 \pm 5.9) \cdot 10^{-3} \text{ GeV}^{-1}, \quad (85g)$$

$$\kappa_{10}^V = (-5.9 \pm 9.6) \cdot 10^{-3} \text{ GeV}^{-1}, \quad (85h)$$

$$\kappa_{11}^V = (-3.0 \pm 0.6) \cdot 10^{-2} \text{ GeV}^{-1}, \quad (85i)$$

$$\kappa_{12}^V = (1.0 \pm 0.8) \cdot 10^{-2} \text{ GeV}^{-1}, \quad (85j)$$

$$\kappa_{13}^V = (-5.3 \pm 1.1) \cdot 10^{-3} \text{ GeV}^{-1}, \quad (85k)$$

$$\kappa_{18}^V = (4.7 \pm 0.8) \cdot 10^{-3} \text{ GeV}^{-1}. \quad (85l)$$

These values are in good agreement with our earlier estimation in section 1.5, $|\kappa_i^V| \lesssim 0.025 \text{ GeV}^{-1}$.

B Kinematics

B.1 $\tau^-(P) \rightarrow \pi^-(p_-)\pi^0(p_0)\gamma(k)\nu_\tau(q)$ kinematics

In order to describe this type of decays we need five independent variables. We choose $s = (p_- + p_0)^2$, $u = (P - p_-)^2$, $x = (k + q)^2$, θ_ν which is the angle between the direction of the $\pi^-\pi^0$ CM frame in the τ lepton rest frame and the direction of \vec{q} in the $\pi^-\pi^0$ CM frame (see fig. 19) and ϕ_- , which is angle between the plane of the $\pi^-\pi^0$ CM frame and the plane of the $\gamma\nu_\tau$ CM frame.

We can write the invariants in terms of these variables

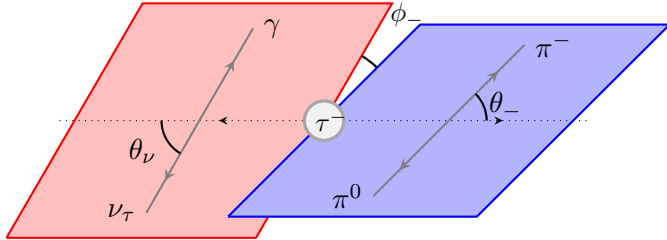


Figure 19: The $\tau^- \rightarrow \pi^-\pi^0\gamma\nu_\tau$ decay in the τ -lepton rest frame.

$$P \cdot p_0 = \frac{s + u - x - m_{\pi^0}^2}{2}, \quad (86a)$$

$$q \cdot k = \frac{x - M_\gamma^2}{2}, \quad (86b)$$

$$p_- \cdot p_0 = \frac{s - m_{\pi^-}^2 - m_{\pi^0}^2}{2}, \quad (86c)$$

$$p_- \cdot (q + k) = \frac{u - x - m_{\pi^0}^2}{2}, \quad (86d)$$

$$P \cdot (q + k) = \frac{x - s + m_\tau^2}{2}, \quad (86e)$$

$$\begin{aligned} P \cdot p_- &= \frac{(m_{\pi^-}^2 - m_{\pi^0}^2 + s)(m_\tau^2 + s - x)}{4s} + \frac{\lambda^{1/2}(s, x, m_\tau^2)\lambda^{1/2}(m_\tau^2, m_{\pi^-}^2, m_{\pi^0}^2)}{4s} \cos \theta_- \\ &= \frac{m_\tau^2 + m_{\pi^-}^2 - u}{2}, \end{aligned} \quad (87)$$

$$P \cdot k = \frac{(m_\tau^2 - s + x)(x + M_\gamma^2)}{4x} - \frac{(x - M_\gamma^2)\lambda^{1/2}(s, x, m_\tau^2)}{4x} \cos \theta_\nu, \quad (88)$$

$$\begin{aligned} p_- \cdot k &= \frac{(x + M_\gamma^2)(m_\tau^2 - s - u + m_{\pi^0}^2)}{4x} - \frac{(x - M_\gamma^2) \cos \theta_\nu}{4x \lambda^{1/2}(s, x, m_\tau^2)} A(s, u, x) \\ &\quad - \frac{(x - M_\gamma^2) \lambda^{1/2}(s, m_{\pi^-}^2, m_{\pi^0}^2)}{4\sqrt{x}\sqrt{s}} \sin \theta_\nu \sin \theta_- \cos \phi_-, \end{aligned} \quad (89)$$

$$\epsilon^{\mu\nu\alpha\beta} k_\mu P_\nu p_{-\alpha} q_\beta = \frac{(x - M_\gamma^2) \lambda^{1/2} (s, m_{\pi^-}^2, m_{\pi^0}^2) \lambda^{1/2} (s, x, m_\tau^2)}{8\sqrt{s}\sqrt{x}} \times \\ \sin \theta_\nu \sin \theta_- \sin \phi_-, \quad (90)$$

$$\epsilon^{\mu\nu\alpha\beta} k_\mu P_\nu p_{-\alpha} p_{0\beta} = \epsilon^{\mu\nu\alpha\beta} k_\mu P_\nu p_{0\alpha} q_\beta = \epsilon^{\mu\nu\alpha\beta} k_\mu p_{-\nu} p_{0\alpha} q_\beta = \epsilon^{\mu\nu\alpha\beta} P_\mu p_{-\nu} p_{0\alpha} q_\beta \\ = -\epsilon^{\mu\nu\alpha\beta} k_\mu P_\nu p_{-\alpha} q_\beta, \quad (91)$$

where

$$A(s, u, x) = m_\tau^4 + s(s+u) + x(u-s-2m_{\pi^-}^2) + m_{\pi^0}^2(m_\tau^2 - s+x) - m_\tau^2(2s+u+x). \quad (92)$$

Working in the τ -lepton rest frame, we have

$$E_\gamma = \frac{(m_\tau^2 - s + x)(x + M_\gamma^2)}{4m_\tau x} - \frac{(x - M_\gamma^2) \lambda^{1/2} (s, x, m_\tau^2)}{4m_\tau x} \cos \theta_\nu, \quad (93)$$

$$E_\nu = |\vec{q}| = \frac{(m_\tau^2 - s + x)(x - M_\gamma^2)}{4m_\tau x} + \frac{(x - M_\gamma^2) \lambda^{1/2} (s, x, m_\tau^2)}{4m_\tau x} \cos \theta_\nu, \quad (94)$$

$$\vec{k} = \left(-\frac{(x + M_\gamma^2) \lambda^{1/2} (s, x, m_\tau^2)}{4m_\tau x} + \frac{(m_\tau^2 - s + x)(x - M_\gamma^2)}{4m_\tau x} \cos \theta_\nu \right) \hat{e}_z \\ + \frac{x - M_\gamma^2}{2\sqrt{x}} \sin \theta_\nu \hat{e}_x, \quad (95)$$

$$\vec{q} = \left(-\frac{(x - M_\gamma^2) \lambda^{1/2} (s, x, m_\tau^2)}{4m_\tau x} - \frac{(m_\tau^2 - s + x)(x - M_\gamma^2)}{4m_\tau x} \cos \theta_\nu \right) \hat{e}_z \\ - \frac{x - M_\gamma^2}{2\sqrt{x}} \sin \theta_\nu \hat{e}_x, \quad (96)$$

$$E_- = \frac{(m_\tau^2 + s - x)(s + m_{\pi^-}^2 - m_{\pi^0}^2)}{4m_\tau s} + \frac{\lambda^{1/2} (s, x, m_\tau^2) \lambda^{1/2} (s, m_{\pi^-}^2, m_{\pi^0}^2)}{4m_\tau s} \cos \theta_- \\ = \frac{m_\tau^2 + m_{\pi^-}^2 - u}{2m_\tau}, \quad (97)$$

$$\begin{aligned} E_0 &= \frac{(m_\tau^2 + s - x)(s - m_{\pi^-}^2 + m_{\pi^0}^2)}{4m_\tau s} - \frac{\lambda^{1/2}(s, x, m_\tau^2) \lambda^{1/2}(s, m_{\pi^-}^2, m_{\pi^0}^2)}{4m_\tau s} \cos \theta_- \\ &= \frac{s + u - x - m_{\pi^-}^2}{2m_\tau}, \end{aligned} \quad (98)$$

$$|\vec{p}_-| = \frac{\lambda^{1/2}(u, m_\tau^2, m_{\pi^-}^2)}{2m_\tau}, \quad (99)$$

$$\begin{aligned} \vec{p}_- &= \left(\frac{(s + m_{\pi^-}^2 - m_{\pi^0}^2)\lambda^{1/2}(s, x, m_\tau^2)}{4m_\tau s} + \frac{(m_\tau^2 + s - x)\lambda^{1/2}(s, m_{\pi^-}^2, m_{\pi^0}^2)}{4m_\tau s} \cos \theta_- \right) \hat{e}_z \\ &\quad + \frac{\lambda^{1/2}(s, m_{\pi^-}^2, m_{\pi^0}^2)}{2\sqrt{s}} \sin \theta_- \hat{e}_\rho, \end{aligned} \quad (100)$$

$$\begin{aligned} \vec{p}_0 &= \left(\frac{(s - m_{\pi^-}^2 + m_{\pi^0}^2)\lambda^{1/2}(s, x, m_\tau^2)}{4m_\tau s} - \frac{(m_\tau^2 + s - x)\lambda^{1/2}(s, m_{\pi^-}^2, m_{\pi^0}^2)}{4m_\tau s} \cos \theta_- \right) \hat{e}_z \\ &\quad - \frac{\lambda^{1/2}(s, m_{\pi^-}^2, m_{\pi^0}^2)}{2\sqrt{s}} \sin \theta_- \hat{e}_\rho, \end{aligned} \quad (101)$$

$$\cos \theta_- = \frac{2s(m_\tau^2 + m_{\pi^-}^2 - u) - (m_\tau^2 + s - x)(s + m_{\pi^-}^2 - m_{\pi^0}^2)}{\lambda^{1/2}(s, x, m_\tau^2) \lambda^{1/2}(s, m_{\pi^-}^2, m_{\pi^0}^2)}, \quad (102)$$

$$\cos \theta_\nu = \frac{(m_\tau^2 - s + x)(x + M_\gamma^2) - 4m_\tau E_\gamma x}{(x - M_\gamma^2) \lambda^{1/2}(s, x, m_\tau^2)}, \quad (103)$$

where $\lambda(x, y, z) = x^2 + y^2 + z^2 - 2xy - 2xz - 2yz$ is the Kallen function, and $\hat{e}_\rho = \cos \phi_- \hat{e}_x + \sin \phi_- \hat{e}_y$.

From eq. (102), we get

$$\begin{aligned} x_\pm(s, u) &= \frac{-m_{\pi^-}^4 + (m_{\pi^0}^2 - s)(m_\tau^2 - u) + m_{\pi^-}^2(m_\tau^2 + m_{\pi^0}^2 + s + u)}{2m_{\pi^-}^2} \\ &\pm \frac{\lambda^{1/2}(u, m_\tau^2, m_{\pi^-}^2) \lambda^{1/2}(s, m_{\pi^-}^2, m_{\pi^0}^2)}{2m_{\pi^-}^2}, \end{aligned} \quad (104)$$

and

$$\begin{aligned} u_\pm(s, x) &= m_\tau^2 + m_{\pi^-}^2 - \frac{(m_\tau^2 + s - x)(s + m_{\pi^-}^2 - m_{\pi^0}^2)}{2s} \\ &\pm \frac{\lambda^{1/2}(s, x, m_\tau^2) \lambda^{1/2}(s, m_{\pi^-}^2, m_{\pi^0}^2)}{2s}, \end{aligned} \quad (105)$$

these bounds on u and x correspond to the forward and backward direction, i.e. by taking $\theta_- = 0, \pi$.

For the non-radiative decay, we have

$$\mathcal{D}^{III} = \left\{ u_{-}(s, 0) \leq u \leq u_{+}(s, 0), (m_{\pi^{-}} + m_{\pi^0})^2 \leq s \leq m_{\tau}^2 \right\}, \quad (106)$$

this region is plotted in fig. 20 which corresponds to the projection \mathcal{R}^{III} onto the su -plane.

In the case of the radiative decay, we have

$$\begin{aligned} \mathcal{D}^{IV} = & \{ x_{min}(s, u) \leq x \leq x_{max}(s, u), u_{min}(s) \leq u \leq u_{max}(s), \\ & (m_{\pi^{-}} + m_{\pi^{-}})^2 \leq s \leq (m_{\tau} - M_{\gamma})^2 \} \end{aligned} \quad (107)$$

with

$$x_{min}(s, u) = \begin{cases} x_{-}(s, u) & u_{+}(s, M_{\gamma}^2) \leq u \leq (m_{\tau} - m_{\pi^{-}})^2, (m_{\pi^{-}} + m_{\pi^0})^2 \leq s \leq s^{*} \\ M_{\gamma}^2 & u_{-}(s, M_{\gamma}^2) \leq u \leq u_{+}(s, M_{\gamma}^2), s^{*} \leq s \leq (m_{\tau} - M_{\gamma})^2, \end{cases} \quad (108)$$

$$x_{max}(s, u) = x_{+}(s, u), \quad (109)$$

$$u_{min}(s) = u_{-}(s, M_{\gamma}^2), \quad (110)$$

$$u_{max}(s) = \begin{cases} (m_{\tau} - m_{\pi^{-}})^2 & (m_{\pi^{-}} + m_{\pi^0})^2 \leq s \leq s^{*}, \\ u_{+}(s, M_{\gamma}^2) & s^{*} \leq s \leq (m_{\tau} - M_{\gamma})^2, \end{cases} \quad (111)$$

where $s^{*} = \frac{m_{\tau}(m_{\tau}m_{\pi^{-}} + m_{\pi^0}^2 - m_{\pi^{-}}^2) - M_{\gamma}^2m_{\pi^{-}}}{m_{\tau} - m_{\pi^{-}}}$ is the value that maximizes $u_{+}(s, M_{\gamma}^2)$. We will be working in the isospin-limit ($m_u = m_d$), i.e. $m_{\pi^{-}}^2 = m_{\pi^0}^2$ and thus many of the last expressions will be simplified.

We use a non-vanishing M_{γ} in order to deal with the IR divergences, at the end these divergences are canceled out by those divergences of the non-radiative decay so we can take the limit $M_{\gamma} \rightarrow 0$. The projection $\mathcal{R}^{IV} = \mathcal{R}^{IV/III} \cup \mathcal{R}^{III}$ of the \mathcal{D}^{IV} is plotted in fig. 20 for $M_{\gamma} \rightarrow 0$.

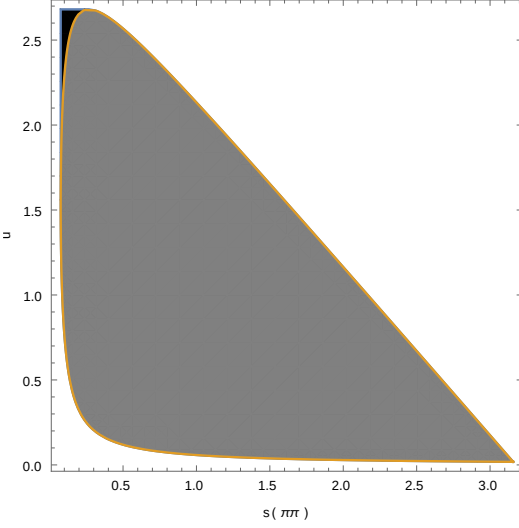


Figure 20: Projection of the kinematic region for the non-radiative decay \mathcal{R}^{III} (gray) and the radiative decay $\mathcal{R}^{IV} = \mathcal{R}^{IV/III} \cup \mathcal{R}^{III}$ (black and gray) onto the su -plane. $\mathcal{R}^{IV/III}$ (black) is the kinematic region which is only accessible to the radiative decay.

C Vector Form Factors

$$\begin{aligned}
v_1^R = & \frac{1}{F^2} \left(\frac{16k \cdot p_0 (2\kappa_{12}^V + \kappa_{16}^V) (-2k \cdot p_- + s) (2\kappa_{12}^V + \kappa_{16}^V) + 2(P - q)^2 \kappa_{17}^V}{D_\omega [(k + p_0)^2]} \right. \\
& + \frac{\sqrt{2}F_V}{M_\rho^2} \left(2s\lambda_{12}^V - (4k \cdot p_0 + s)(\lambda_{13}^V + \lambda_{14}^V - \lambda_{15}^V) + (2k \cdot p_- + s)\lambda_{16}^V - 4k \cdot p_- \lambda_{17}^V \right. \\
& + 4k \cdot p_- \lambda_{18}^V + s\lambda_{18}^V + 4k \cdot p_- \lambda_{19}^V + 2s\lambda_{19}^V + 4k \cdot p_0 \lambda_{21}^V + 2k \cdot p_0 \lambda_{22}^V - 2k \cdot p_- \lambda_{22}^V \Big) \\
& + \frac{1}{M_{a_1}^2 D_{a_1} [(k + p_-)^2]} \left(-8(-2k \cdot p_0 M_{a_1}^2 s + (k \cdot p_- - M_{a_1}^2) s^2 + 2(k \cdot p_0)(k \cdot p_-) \right. \\
& (2M_{a_1}^2 + s))(\lambda_{12}^A)^2 - 8k \cdot p_- (2k \cdot p_0 + s)(2M_{a_1}^2 + s)(\lambda_{13}^A)^2 - 2\sqrt{2}F_A (k \cdot p_0) s\lambda_{15}^A \\
& - 2\sqrt{2}F_A (k \cdot p_-) s\lambda_{15}^A - \sqrt{2}F_A s^2 \lambda_{15}^A - 8\sqrt{2}F_A k \cdot p_- M_{a_1}^2 \lambda_{17}^A - 4\sqrt{2}F_A (k \cdot p_-) s\lambda_{17}^A \\
& + 16(k \cdot p_0)(k \cdot p_-) s\lambda_{15}^A \lambda_{17}^A + 16(k \cdot p_-)^2 s\lambda_{15}^A \lambda_{17}^A + 8(k \cdot p_-) s^2 \lambda_{15}^A \lambda_{17}^A \\
& + 32(k \cdot p_-)^2 M_{a_1}^2 (\lambda_{17}^A)^2 + 16(k \cdot p_-)^2 s(\lambda_{17}^A)^2 + \lambda_{13}^A (8(k \cdot p_-) s(P - q)^2 \lambda_{15}^A \\
& + (2k \cdot p_0 - 2k \cdot p_- + s)(2M_{a_1}^2 + s)(\sqrt{2}F_A - 8k \cdot p_- \lambda_{17}^A)) + \lambda_{12}^A (-8(s(2k \cdot p_-(M_{a_1}^2 - s) \\
& + M_{a_1}^2 s) + 2k \cdot p_0 (4k \cdot p_- M_{a_1}^2 - 2(k \cdot p_-) s + M_{a_1}^2 s)) \lambda_{13}^A - 8(k \cdot p_- - M_{a_1}^2) s(P - q)^2 \lambda_{15}^A \\
& \left. \left. + (k \cdot p_0 (4M_{a_1}^2 - 2s) - s(2M_{a_1}^2 + s) + k \cdot p_- (-4M_{a_1}^2 + 2s)) (\sqrt{2}F_A - 8k \cdot p_- \lambda_{17}^A)) \right) \right) \quad (112)
\end{aligned}$$

$$\begin{aligned}
v_1^{RR} = & \frac{1}{2\sqrt{2}F^2} \left(\frac{64k \cdot p_0 F_V(-(2k \cdot p_- + s)(2\kappa_{12}^V + \kappa_{16}^V) + 2(P - q)^2 \kappa_{17}^V) \kappa_3^{VV}}{M_\rho^2 D_\omega [(k + p_0)^2]} \right. \\
& - \frac{64k \cdot p_0 (4k \cdot p_0 + 2k \cdot p_- + s)(2\kappa_{12}^V + \kappa_{16}^V) \kappa_3^{VV} (-F_V + 2\sqrt{2}(P - q)^2 \lambda_{22}^V)}{D_\rho [(P - q)^2] D_\omega [(k + p_0)^2]} \\
& + \frac{2F_V}{M_{a_1}^2 M_\rho^2 D_{a_1} [(k + p_-)^2]} \left(2(2\sqrt{2}F_A k \cdot p_- M_{a_1}^2 - \sqrt{2}F_A (k \cdot p_-) s + \sqrt{2}F_A M_{a_1}^2 s \right. \\
& + 4(-2k \cdot p_0 M_{a_1}^2 s + (k \cdot p_- - M_{a_1}^2) s^2 + 2(k \cdot p_0)(k \cdot p_-)(2M_{a_1}^2 + s)) \lambda_{12}^A \\
& + 4(2k \cdot p_0 + s)(2k \cdot p_- M_{a_1}^2 - (k \cdot p_-) s + M_{a_1}^2 s) \lambda_{13}^A + 8(k \cdot p_0)(k \cdot p_-) s \lambda_{15}^A \\
& + 8(k \cdot p_-)^2 s \lambda_{15}^A - 8k \cdot p_0 M_{a_1}^2 s \lambda_{15}^A - 8k \cdot p_- M_{a_1}^2 s \lambda_{15}^A + 4(k \cdot p_-) s^2 \lambda_{15}^A \\
& - 4M_{a_1}^2 s^2 \lambda_{15}^A - 16(k \cdot p_-)^2 M_{a_1}^2 \lambda_{17}^A + 8(k \cdot p_-)^2 s \lambda_{17}^A - 8k \cdot p_- M_{a_1}^2 s \lambda_{17}^A \lambda_2^{VA} \\
& - k \cdot p_- (2\sqrt{2}F_A M_{a_1}^2 + \sqrt{2}F_A s + 4(4k \cdot p_0 M_{a_1}^2 - 2(k \cdot p_0) s - s^2) \lambda_{12}^A \\
& + 4(2k \cdot p_0 + s)(2M_{a_1}^2 + s) \lambda_{13}^A - 8(k \cdot p_0) s \lambda_{15}^A - 8(k \cdot p_-) s \lambda_{15}^A - 4s^2 \lambda_{15}^A \\
& - 16k \cdot p_- M_{a_1}^2 \lambda_{17}^A - 8(k \cdot p_-) s \lambda_{17}^A (\lambda_4^{VA} + 2\lambda_5^{VA}) \Big) \\
& + \frac{(\sqrt{2}F_V - 4(P - q)^2 \lambda_{22}^V)}{M_{a_1}^2 D_{a_1} [(k + p_-)^2] D_\rho [(P - q)^2]} \left(-2(-4\sqrt{2}(-2k \cdot p_0 M_{a_1}^2 s + (k \cdot p_- - M_{a_1}^2) s^2 \right. \\
& + 2(k \cdot p_0)(k \cdot p_-)(2M_{a_1}^2 + s)) \lambda_{12}^A + (4k \cdot p_0 M_{a_1}^2 - 2(k \cdot p_0) s - s^2) \\
& (F_A - 4\sqrt{2}k \cdot p_- \lambda_{13}^A - 4\sqrt{2}k \cdot p_- \lambda_{17}^A) \lambda_2^{VA} - 2s(P - q)^2 (F_A + 4\sqrt{2}(k \cdot p_- - M_{a_1}^2) \lambda_{12}^A \\
& - 4\sqrt{2}k \cdot p_- \lambda_{13}^A - 4\sqrt{2}k \cdot p_- \lambda_{17}^A) \lambda_3^{VA} + (2k \cdot p_0 + s)(-4\sqrt{2}(2k \cdot p_- M_{a_1}^2 - (k \cdot p_-) s \\
& + M_{a_1}^2 s) \lambda_{12}^A + (2M_{a_1}^2 + s)(F_A - 4\sqrt{2}k \cdot p_- \lambda_{13}^A - 4\sqrt{2}k \cdot p_- \lambda_{17}^A) (\lambda_4^{VA} + 2\lambda_5^{VA})) \Big) \\
& + \frac{2F_V}{M_\rho^2 D_\rho [(P - q)^2]} \left(-2(P - q)^2 \lambda_{22}^V ((P - q)^2 - 8s \lambda_2^{VV} \right. \\
& - 2(4k \cdot p_0 + s) \lambda_3^{VV} + 8k \cdot p_0 \lambda_4^{VV} + 2s \lambda_4^{VV} - 16k \cdot p_0 \lambda_5^{VV} - 4s \lambda_5^{VV}) \\
& + \sqrt{2}F_V (-4s \lambda_2^{VV} - (4k \cdot p_0 + s)(\lambda_3^{VV} - \lambda_4^{VV} + 2\lambda_5^{VV})) \Big) \\
& \left. - \frac{4F_V (\sqrt{2}(4k \cdot p_0 + s) G_V \lambda_7^{VV} + s \lambda_{21}^V (s - 2(4k \cdot p_0 + s) \lambda_7^{VV}))}{M_\rho^2 D_\rho [s]} \right) \tag{113}
\end{aligned}$$

$$\begin{aligned}
v_1^{RRR} = & - \frac{F_V(-\sqrt{2}F_V + 4(P-q)^2\lambda_{22}^V)}{\sqrt{2}F^2M_{a_1}^2M_\rho^2D_{a_1}[(k+p_-)^2]D_\rho[(P-q)^2]} (-4(-2k \cdot p_0 M_{a_1}^2 s \\
& + (k \cdot p_- - M_{a_1}^2)s^2 + 2(k \cdot p_0)(k \cdot p_-)(2M_{a_1}^2 + s))(\lambda_2^{VA})^2 \\
& - k \cdot p_-(\lambda_4^{VA} + 2\lambda_5^{VA})(-2s(P-q)^2\lambda_3^{VA} + (2k \cdot p_0 + s)(2M_{a_1}^2 + s)(\lambda_4^{VA} + 2\lambda_5^{VA})) \\
& + 2\lambda_2^{VA}(2(k \cdot p_- - M_{a_1}^2)s(P-q)^2\lambda_3^{VA} + (s(2k \cdot p_-(M_{a_1}^2 - s) + M_{a_1}^2 s) \\
& + 2k \cdot p_0(4k \cdot p_- M_{a_1}^2 - 2(k \cdot p_-)s + M_{a_1}^2 s)(\lambda_4^{VA} + 2\lambda_5^{VA}))) \\
\end{aligned} \tag{114}$$

$$\begin{aligned}
v_{GI1}^{R+RR} = & \frac{1}{F^2 D_\rho [(P-q)^2] D_\rho [s]} \left(\sqrt{2} F_V (2(M_\rho^2 - s)s\lambda_{12}^V - (M_\rho^2 - s)(4k \cdot p_0 + s)\lambda_{13}^V \right. \\
& - 4k \cdot p_0 M_\rho^2 \lambda_{14}^V + 4(k \cdot p_0)s\lambda_{14}^V - M_\rho^2 s\lambda_{14}^V + s^2 \lambda_{14}^V + 4k \cdot p_0 M_\rho^2 \lambda_{15}^V - 4(k \cdot p_0)s\lambda_{15}^V \\
& + M_\rho^2 s\lambda_{15}^V - s^2 \lambda_{15}^V - 2k \cdot p_0 M_\rho^2 \lambda_{16}^V + 2(k \cdot p_0)s\lambda_{16}^V + 4k \cdot p_0 M_\rho^2 \lambda_{17}^V - 4(k \cdot p_0)s\lambda_{17}^V \\
& + 2M_\rho^2 s\lambda_{17}^V - 2s^2 \lambda_{17}^V - 4k \cdot p_0 M_\rho^2 \lambda_{18}^V + 4(k \cdot p_0)s\lambda_{18}^V - M_\rho^2 s\lambda_{18}^V + s^2 \lambda_{18}^V \\
& - 2k \cdot p_0 M_\rho^2 \lambda_{19}^V + 2(k \cdot p_0)s\lambda_{19}^V - 4k \cdot p_- M_\rho^2 \lambda_{21}^V + 4(k \cdot p_-)s\lambda_{21}^V - 2M_\rho^2 s\lambda_{21}^V \\
& + s^2 \lambda_{21}^V + 6k \cdot p_0 M_\rho^2 \lambda_{22}^V + 2k \cdot p_- M_\rho^2 \lambda_{22}^V - 6(k \cdot p_0)s\lambda_{22}^V - 2(k \cdot p_-)s\lambda_{22}^V \\
& + 2M_\rho^2 s\lambda_{22}^V - 2s^2 \lambda_{22}^V + 8(k \cdot p_0)s\lambda_{21}^V \lambda_7^{VV} + 2s^2 \lambda_{21}^V \lambda_7^{VV}) + 2G_V(\sqrt{2}(4k \cdot p_0 + s) \\
& ((P-q)^2 - M_\rho^2)\lambda_7^V - (4k \cdot p_0 + s)F_V \lambda_7^{VV} + \sqrt{2}\lambda_{22}^V(-16(k \cdot p_0)^2 - (2M_\rho^2 - s) \\
& (2k \cdot p_- + s) - 2k \cdot p_0(8k \cdot p_- - 2M_\rho^2 + 3s) + 2(4k \cdot p_0 + s)(P-q)^2 \lambda_7^{VV})) \\
\end{aligned}$$

$$\begin{aligned}
& -4(s(4k \cdot p_0 + s)((P - q)^2 - M_\rho^2)\lambda_7^V \lambda_{21}^V + \lambda_{22}^V(2(M_\rho^2 - s)s(P - q)^2\lambda_{12}^V \\
& - (M_\rho^2 - s)(4k \cdot p_0 + s)(P - q)^2\lambda_{13}^V - 8(k \cdot p_0)^2 M_\rho^2 \lambda_{14}^V - 8(k \cdot p_0)(k \cdot p_-) M_\rho^2 \lambda_{14}^V \\
& + 8(k \cdot p_0)^2 s \lambda_{14}^V + 8(k \cdot p_0)(k \cdot p_-) s \lambda_{14}^V - 6k \cdot p_0 M_\rho^2 s \lambda_{14}^V - 2k \cdot p_- M_\rho^2 s \lambda_{14}^V \\
& + 6(k \cdot p_0) s^2 \lambda_{14}^V + 2(k \cdot p_-) s^2 \lambda_{14}^V - M_\rho^2 s^2 \lambda_{14}^V + s^3 \lambda_{14}^V + 8(k \cdot p_0)^2 M_\rho^2 \lambda_{15}^V \\
& + 8(k \cdot p_0)(k \cdot p_-) M_\rho^2 \lambda_{15}^V - 8(k \cdot p_0)^2 s \lambda_{15}^V - 8(k \cdot p_0)(k \cdot p_-) s \lambda_{15}^V \\
& + 6k \cdot p_0 M_\rho^2 s \lambda_{15}^V + 2k \cdot p_- M_\rho^2 s \lambda_{15}^V - 6(k \cdot p_0) s^2 \lambda_{15}^V - 2(k \cdot p_-) s^2 \lambda_{15}^V + M_\rho^2 s^2 \lambda_{15}^V \\
& - s^3 \lambda_{15}^V - 4(k \cdot p_0)^2 M_\rho^2 \lambda_{16}^V - 4(k \cdot p_0)(k \cdot p_-) M_\rho^2 \lambda_{16}^V + 4(k \cdot p_0)^2 s \lambda_{16}^V \\
& + 4(k \cdot p_0)(k \cdot p_-) s \lambda_{16}^V - 2k \cdot p_0 M_\rho^2 s \lambda_{16}^V + 2(k \cdot p_0) s^2 \lambda_{16}^V + 8(k \cdot p_0)^2 M_\rho^2 \lambda_{17}^V \\
& + 8(k \cdot p_0)(k \cdot p_-) M_\rho^2 \lambda_{17}^V - 8(k \cdot p_0)^2 s \lambda_{17}^V - 8(k \cdot p_0)(k \cdot p_-) s \lambda_{17}^V \\
& + 8k \cdot p_0 M_\rho^2 s \lambda_{17}^V + 4k \cdot p_- M_\rho^2 s \lambda_{17}^V - 8(k \cdot p_0) s^2 \lambda_{17}^V - 4(k \cdot p_-) s^2 \lambda_{17}^V \\
& + 2M_\rho^2 s^2 \lambda_{17}^V - 2s^3 \lambda_{17}^V - 8(k \cdot p_0)^2 M_\rho^2 \lambda_{18}^V - 8(k \cdot p_0)(k \cdot p_-) M_\rho^2 \lambda_{18}^V \\
& + 8(k \cdot p_0)^2 s \lambda_{18}^V + 8(k \cdot p_0)(k \cdot p_-) s \lambda_{18}^V - 6k \cdot p_0 M_\rho^2 s \lambda_{18}^V - 2k \cdot p_- M_\rho^2 s \lambda_{18}^V \\
& + 6(k \cdot p_0) s^2 \lambda_{18}^V + 2(k \cdot p_-) s^2 \lambda_{18}^V - M_\rho^2 s^2 \lambda_{18}^V + s^3 \lambda_{18}^V - 4(k \cdot p_0)^2 M_\rho^2 \lambda_{19}^V \\
& - 4(k \cdot p_0)(k \cdot p_-) M_\rho^2 \lambda_{19}^V + 4(k \cdot p_0)^2 s \lambda_{19}^V + 4(k \cdot p_0)(k \cdot p_-) s \lambda_{19}^V \\
& - 2k \cdot p_0 M_\rho^2 s \lambda_{19}^V + 2(k \cdot p_0) s^2 \lambda_{19}^V - 8(k \cdot p_0)(k \cdot p_-) M_\rho^2 \lambda_{21}^V - 8(k \cdot p_-)^2 M_\rho^2 \lambda_{21}^V \\
& - 16(k \cdot p_0)^2 s \lambda_{21}^V - 8(k \cdot p_0)(k \cdot p_-) s \lambda_{21}^V + 8(k \cdot p_-)^2 s \lambda_{21}^V + 4k \cdot p_0 M_\rho^2 s \lambda_{21}^V \\
& - 8k \cdot p_- M_\rho^2 s \lambda_{21}^V - 6(k \cdot p_0) s^2 \lambda_{21}^V + 6(k \cdot p_-) s^2 \lambda_{21}^V - 2M_\rho^2 s^2 \lambda_{21}^V + s^3 \lambda_{21}^V \\
& + 8(k \cdot p_0)^2 M_\rho^2 \lambda_{22}^V + 8(k \cdot p_0)(k \cdot p_-) M_\rho^2 \lambda_{22}^V - 8(k \cdot p_0)^2 s \lambda_{22}^V \\
& - 8(k \cdot p_0)(k \cdot p_-) s \lambda_{22}^V + 6k \cdot p_0 M_\rho^2 s \lambda_{22}^V + 2k \cdot p_- M_\rho^2 s \lambda_{22}^V - 6(k \cdot p_0) s^2 \lambda_{22}^V \\
& - 2(k \cdot p_-) s^2 \lambda_{22}^V + M_\rho^2 s^2 \lambda_{22}^V - s^3 \lambda_{22}^V + 16(k \cdot p_0)^2 s \lambda_{21}^V \lambda_7^{VV} \\
& + 16(k \cdot p_0)(k \cdot p_-) s \lambda_{21}^V \lambda_7^{VV} + 12(k \cdot p_0) s^2 \lambda_{21}^V \lambda_7^{VV} + 4(k \cdot p_-) s^2 \lambda_{21}^V \lambda_7^{VV} \\
& + 2s^3 \lambda_{21}^V \lambda_7^{VV})) \Big)
\end{aligned} \tag{115}$$

$$\begin{aligned}
v_2^R = & \frac{1}{F^2} \left(\frac{8(2k \cdot p_- + s)}{M_\omega^2 D_\omega [(k + p_0)^2]} \left(-4(k \cdot p_0 - M_\omega^2)(2k \cdot p_- + s)(\kappa_{12}^V)^2 + k \cdot p_0 \kappa_{16}^V \right. \right. \\
& ((4k \cdot p_0 + 2k \cdot p_- - 2M_\omega^2 + s)\kappa_{16}^V - 2(P - q)^2 \kappa_{17}^V) + \kappa_{12}^V((-8(k \cdot p_0)^2 + 4k \cdot p_0 M_\omega^2 \\
& + 2M_\omega^2(2k \cdot p_- + s))\kappa_{16}^V + 4(k \cdot p_0 - M_\omega^2)(P - q)^2 \kappa_{17}^V) \Big) + \frac{\sqrt{2}F_V}{M_\rho^2} \left(2s\lambda_{12}^V - s\lambda_{13}^V \right. \\
& + 4k \cdot p_- \lambda_{14}^V + s\lambda_{14}^V - 4k \cdot p_- \lambda_{15}^V - s\lambda_{15}^V - 4k \cdot p_- \lambda_{17}^V + 2k \cdot p_- \lambda_{18}^V - 4k \cdot p_- \lambda_{21}^V \\
& \left. \left. + 2k \cdot p_0 \lambda_{22}^V - 2k \cdot p_- \lambda_{22}^V \right) + \frac{2\sqrt{2}}{M_{a_1}^2 D_{a_1} [(k + p_-)^2]} \left(4\sqrt{2}(k \cdot p_-)^2 (2k \cdot p_0 + 2M_{a_1}^2 + s) \right. \right. \\
& (\lambda_{12}^A)^2 + \lambda_{12}^A(4\sqrt{2}k \cdot p_-(-4(k \cdot p_0)(k \cdot p_-) + 2k \cdot p_0 M_{a_1}^2 + 2k \cdot p_- M_{a_1}^2 - 2(k \cdot p_-)s \\
& + M_{a_1}^2 s)\lambda_{13}^A + 4\sqrt{2}(k \cdot p_-)^2 (P - q)^2 \lambda_{15}^A + (-2(k \cdot p_0)(k \cdot p_-) + 2(k \cdot p_-)^2 \\
& + 2k \cdot p_0 M_{a_1}^2 + 2k \cdot p_- M_{a_1}^2 - (k \cdot p_-)s + M_{a_1}^2 s)(-F_A + 4\sqrt{2}k \cdot p_- \lambda_{17}^A)) \\
& - (k \cdot p_- - M_{a_1}^2)(-4\sqrt{2}k \cdot p_-(2k \cdot p_0 + s)(\lambda_{13}^A)^2 - 4k \cdot p_- \lambda_{17}^A(F_A - 2\sqrt{2}k \cdot p_- \lambda_{17}^A)) \\
& \left. \left. + (P - q)^2 \lambda_{15}^A(-F_A + 4\sqrt{2}k \cdot p_- \lambda_{17}^A) + \lambda_{13}^A(4\sqrt{2}k \cdot p_-(P - q)^2 \lambda_{15}^A \right. \right. \\
& \left. \left. + (2k \cdot p_0 - 2k \cdot p_- + s)(F_A - 4\sqrt{2}k \cdot p_- \lambda_{17}^A))) \right) \right) \\
\end{aligned} \tag{116}$$

$$\begin{aligned}
v_2^{RR} = & \frac{1}{\sqrt{2}F^2} \left(\frac{8F_V(2k \cdot p_- + s)}{M_\rho^2 M_\omega^2 D_\omega [(k + p_0)^2]} \left(2(P - q)^2 \kappa_{17}^V (-M_\omega^2 \kappa_3^{VV} + (2k \cdot p_0 - M_\omega^2) \kappa_4^{VV}) \right. \right. \\
& + \kappa_{16}^V (M_\omega^2 (2k \cdot p_- + s) \kappa_3^{VV} - (2k \cdot p_0 - M_\omega^2) (4k \cdot p_0 + 2k \cdot p_- + s) \kappa_4^{VV}) \\
& + 2(2k \cdot p_- + s) \kappa_{12}^V (M_\omega^2 \kappa_3^{VV} + D_\omega [(k + p_0)^2] \kappa_4^{VV}) \Big) \\
& + \frac{16(2k \cdot p_- + s)(-F_V + 2\sqrt{2}(P - q)^2 \lambda_{22}^V)}{M_\omega^2 D_\rho [(P - q)^2] D_\omega [(k + p_0)^2]} \left(k \cdot p_0 \kappa_{16}^V (((P - q)^2 + M_\omega^2) \kappa_3^{VV} \right. \\
& + (2k \cdot p_0 - M_\omega^2) \kappa_4^{VV}) + \kappa_{12}^V ((-4(k \cdot p_0)^2 + 2M_\omega^2 (2k \cdot p_- + s) \\
& - 2k \cdot p_0 (2k \cdot p_- - 3M_\omega^2 + s)) \kappa_3^{VV} + 2k \cdot p_0 (-2k \cdot p_0 + M_\omega^2) \kappa_4^{VV}) \Big) \\
& - \frac{2k \cdot p_- F_V}{M_{a_1}^2 M_\rho^2 D_{a_1} [(k + p_-)^2]} \left(2k \cdot p_- (-\sqrt{2}F_A + 4(2k \cdot p_0 + 2M_{a_1}^2 + s) \lambda_{12}^A \right. \\
& - 4(2k \cdot p_0 + s) \lambda_{13}^A + 8k \cdot p_0 \lambda_{15}^A + 8k \cdot p_- \lambda_{15}^A + 4s \lambda_{15}^A + 8k \cdot p_- \lambda_{17}^A) \lambda_2^{VA} \\
& - (-4(2k \cdot p_0 (k \cdot p_- - M_{a_1}^2) - M_{a_1}^2 s + k \cdot p_- (-2M_{a_1}^2 + s)) \lambda_{12}^A + (k \cdot p_- - M_{a_1}^2) \\
& \left. \left. (\sqrt{2}F_A + 4(2k \cdot p_0 + s) \lambda_{13}^A - 4(P - q)^2 \lambda_{15}^A - 8k \cdot p_- \lambda_{17}^A)) (\lambda_4^{VA} + 2\lambda_5^{VA}) \right) \right)
\end{aligned}$$

$$\begin{aligned}
& - \frac{(\sqrt{2}F_V - 4(P-q)^2\lambda_{22}^V)}{M_{a_1}^2 D_{a_1} [(k+p_-)^2] D_\rho [(P-q)^2]} \left(2(4\sqrt{2}(k \cdot p_-)^2 (2k \cdot p_0 + 2M_{a_1}^2 + s)\lambda_{12}^A \right. \\
& + (2k \cdot p_0(k \cdot p_- - M_{a_1}^2) - M_{a_1}^2 s + k \cdot p_-(-2M_{a_1}^2 + s))(F_A - 4\sqrt{2}k \cdot p_- \lambda_{13}^A \\
& - 4\sqrt{2}k \cdot p_- \lambda_{17}^A) - (4\sqrt{2}(k \cdot p_-)^2 \lambda_{12}^A + (k \cdot p_- - M_{a_1}^2)(F_A - 4\sqrt{2}k \cdot p_- \lambda_{13}^A \\
& - 4\sqrt{2}k \cdot p_- \lambda_{17}^A))(2(P-q)^2 \lambda_3^{VA} - (2k \cdot p_0 + s)(\lambda_4^{VA} + 2\lambda_5^{VA})) \Big) \\
& + \frac{F_V}{M_\rho^2 D_\rho [(P-q)^2]} \left(\sqrt{2}F_V(-4s\lambda_2^{VV} + (4k \cdot p_- + s)(\lambda_3^{VV} - \lambda_4^{VV}) - 2s\lambda_5^{VV}) \right. \\
& + 2(P-q)^2 \lambda_{22}^V ((P-q)^2 + 8s\lambda_2^{VV} - 2(4k \cdot p_- + s)(\lambda_3^{VV} - \lambda_4^{VV}) + 4s\lambda_5^{VV}) \Big) \\
& \left. + \frac{2F_V(\sqrt{2}(4k \cdot p_- + s)G_V \lambda_7^{VV} + s\lambda_{21}^V(s - 2(4k \cdot p_- + s)\lambda_7^{VV}))}{M_\rho^2 D_\rho [s]} \right) \tag{117}
\end{aligned}$$

$$\begin{aligned}
v_2^{RRR} = & - \frac{\sqrt{2}k \cdot p_- F_V (-\sqrt{2}F_V + 4(P-q)^2 \lambda_{22}^V)}{F^2 M_{a_1}^2 M_\rho^2 D_{a_1} [(k+p_-)^2] D_\rho [(P-q)^2]} \left(4k \cdot p_- (2k \cdot p_0 + 2M_{a_1}^2 + s)(\lambda_2^{VA})^2 \right. \\
& - (k \cdot p_- - M_{a_1}^2)(\lambda_4^{VA} + 2\lambda_5^{VA})(2(P-q)^2 \lambda_3^{VA} - (2k \cdot p_0 + s)(\lambda_4^{VA} + 2\lambda_5^{VA})) \tag{118} \\
& - 2\lambda_2^{VA}(2k \cdot p_-(P-q)^2 \lambda_3^{VA} + (-4(k \cdot p_0)(k \cdot p_-) + 2k \cdot p_0 M_{a_1}^2 \\
& \left. + 2k \cdot p_- M_{a_1}^2 - 2(k \cdot p_-)s + M_{a_1}^2 s)(\lambda_4^{VA} + 2\lambda_5^{VA})) \right)
\end{aligned}$$

$$\begin{aligned}
v_{GI2}^{R+RR} = & \frac{\sqrt{2}F_V}{F^2 D_\rho [(P-q)^2] D_\rho [s]} \left(2(M_\rho^2 - s)s\lambda_{12}^V + s(-M_\rho^2 + s)\lambda_{13}^V + 4k \cdot p_- M_\rho^2 \lambda_{14}^V \right. \\
& - 4(k \cdot p_-)s\lambda_{14}^V + M_\rho^2 s\lambda_{14}^V - s^2 \lambda_{14}^V - 4k \cdot p_- M_\rho^2 \lambda_{15}^V + 4(k \cdot p_-)s\lambda_{15}^V - M_\rho^2 s\lambda_{15}^V \\
& + s^2 \lambda_{15}^V - 2k \cdot p_0 M_\rho^2 \lambda_{16}^V - 2k \cdot p_- M_\rho^2 \lambda_{16}^V + 2(k \cdot p_0)s\lambda_{16}^V + 2(k \cdot p_-)s\lambda_{16}^V \\
& - M_\rho^2 s\lambda_{16}^V + s^2 \lambda_{16}^V + 4k \cdot p_0 M_\rho^2 \lambda_{17}^V - 4(k \cdot p_0)s\lambda_{17}^V + 2M_\rho^2 s\lambda_{17}^V - 2s^2 \lambda_{17}^V \\
& + 2k \cdot p_- M_\rho^2 \lambda_{18}^V - 2(k \cdot p_-)s\lambda_{18}^V + 2k \cdot p_0 M_\rho^2 \lambda_{19}^V + 2k \cdot p_- M_\rho^2 \lambda_{19}^V - 2(k \cdot p_0)s\lambda_{19}^V \\
& - 2(k \cdot p_-)s\lambda_{19}^V + M_\rho^2 s\lambda_{19}^V - s^2 \lambda_{19}^V - 4k \cdot p_- M_\rho^2 \lambda_{21}^V + 4(k \cdot p_-)s\lambda_{21}^V + s^2 \lambda_{21}^V \\
& + 6k \cdot p_0 M_\rho^2 \lambda_{22}^V + 2k \cdot p_- M_\rho^2 \lambda_{22}^V - 6(k \cdot p_0)s\lambda_{22}^V - 2(k \cdot p_-)s\lambda_{22}^V + 2M_\rho^2 s\lambda_{22}^V \\
& - 2s^2 \lambda_{22}^V - 8(k \cdot p_-)s\lambda_{21}^V \lambda_7^{VV} - 2s^2 \lambda_{21}^V \lambda_7^{VV}) - 2G_V(\sqrt{2}(4k \cdot p_- + s) \\
& ((P-q)^2 - M_\rho^2)\lambda_7^V - (4k \cdot p_- + s)F_V \lambda_7^{VV} + \sqrt{2}\lambda_{22}^V(-16(k \cdot p_-)^2 + 8k \cdot p_- M_\rho^2 \\
& - 10(k \cdot p_-)s - s^2 - 2k \cdot p_0(8k \cdot p_- + s) + 2(P-q)^2(4k \cdot p_- + s)\lambda_7^{VV})) \\
& + 4(s(4k \cdot p_- + s)((P-q)^2 - M_\rho^2)\lambda_7^V \lambda_{21}^V + \lambda_{22}^V(-2(M_\rho^2 - s)s(P-q)^2 \lambda_{12}^V \\
& + (M_\rho^2 - s)s(P-q)^2 \lambda_{13}^V - 8(k \cdot p_0)(k \cdot p_-)M_\rho^2 \lambda_{14}^V - 8(k \cdot p_-)^2 M_\rho^2 \lambda_{14}^V
\end{aligned}$$

$$\begin{aligned}
& + 8(k \cdot p_0)(k \cdot p_-)s\lambda_{14}^V + 8(k \cdot p_-)^2s\lambda_{14}^V - 2k \cdot p_0 M_\rho^2 s\lambda_{14}^V - 6k \cdot p_- M_\rho^2 s\lambda_{14}^V \\
& + 2(k \cdot p_0)s^2\lambda_{14}^V + 6(k \cdot p_-)s^2\lambda_{14}^V - M_\rho^2 s^2\lambda_{14}^V + s^3\lambda_{14}^V + 8(k \cdot p_0)(k \cdot p_-)M_\rho^2\lambda_{15}^V \\
& + 8(k \cdot p_-)^2M_\rho^2\lambda_{15}^V - 8(k \cdot p_0)(k \cdot p_-)s\lambda_{15}^V - 8(k \cdot p_-)^2s\lambda_{15}^V + 2k \cdot p_0 M_\rho^2 s\lambda_{15}^V \\
& + 6k \cdot p_- M_\rho^2 s\lambda_{15}^V - 2(k \cdot p_0)s^2\lambda_{15}^V - 6(k \cdot p_-)s^2\lambda_{15}^V + M_\rho^2 s^2\lambda_{15}^V - s^3\lambda_{15}^V \\
& + 4(k \cdot p_0)^2M_\rho^2\lambda_{16}^V + 8(k \cdot p_0)(k \cdot p_-)M_\rho^2\lambda_{16}^V + 4(k \cdot p_-)^2M_\rho^2\lambda_{16}^V - 4(k \cdot p_0)^2s\lambda_{16}^V \\
& - 8(k \cdot p_0)(k \cdot p_-)s\lambda_{16}^V - 4(k \cdot p_-)^2s\lambda_{16}^V + 4k \cdot p_0 M_\rho^2 s\lambda_{16}^V + 4k \cdot p_- M_\rho^2 s\lambda_{16}^V \\
& - 4(k \cdot p_0)s^2\lambda_{16}^V - 4(k \cdot p_-)s^2\lambda_{16}^V + M_\rho^2 s^2\lambda_{16}^V - s^3\lambda_{16}^V - 8(k \cdot p_0)^2M_\rho^2\lambda_{17}^V \\
& - 8(k \cdot p_0)(k \cdot p_-)M_\rho^2\lambda_{17}^V + 8(k \cdot p_0)^2s\lambda_{17}^V + 8(k \cdot p_0)(k \cdot p_-)s\lambda_{17}^V \\
& - 8k \cdot p_0 M_\rho^2 s\lambda_{17}^V - 4k \cdot p_- M_\rho^2 s\lambda_{17}^V + 8(k \cdot p_0)s^2\lambda_{17}^V + 4(k \cdot p_-)s^2\lambda_{17}^V \\
& - 2M_\rho^2 s^2\lambda_{17}^V + 2s^3\lambda_{17}^V - 4(k \cdot p_0)(k \cdot p_-)M_\rho^2\lambda_{18}^V - 4(k \cdot p_-)^2M_\rho^2\lambda_{18}^V \\
& + 4(k \cdot p_0)(k \cdot p_-)s\lambda_{18}^V + 4(k \cdot p_-)^2s\lambda_{18}^V - 2k \cdot p_- M_\rho^2 s\lambda_{18}^V + 2(k \cdot p_-)s^2\lambda_{18}^V \quad (119) \\
& - 4(k \cdot p_0)^2M_\rho^2\lambda_{19}^V - 8(k \cdot p_0)(k \cdot p_-)M_\rho^2\lambda_{19}^V - 4(k \cdot p_-)^2M_\rho^2\lambda_{19}^V + 4(k \cdot p_0)^2s\lambda_{19}^V \\
& + 8(k \cdot p_0)(k \cdot p_-)s\lambda_{19}^V + 4(k \cdot p_-)^2s\lambda_{19}^V - 4k \cdot p_0 M_\rho^2 s\lambda_{19}^V - 4k \cdot p_- M_\rho^2 s\lambda_{19}^V \\
& + 4(k \cdot p_0)s^2\lambda_{19}^V + 4(k \cdot p_-)s^2\lambda_{19}^V - M_\rho^2 s^2\lambda_{19}^V + s^3\lambda_{19}^V + 8(k \cdot p_0)(k \cdot p_-)M_\rho^2\lambda_{21}^V \\
& + 8(k \cdot p_-)^2M_\rho^2\lambda_{21}^V - 24(k \cdot p_0)(k \cdot p_-)s\lambda_{21}^V - 24(k \cdot p_-)^2s\lambda_{21}^V + 12k \cdot p_- M_\rho^2 s\lambda_{21}^V \\
& - 2(k \cdot p_0)s^2\lambda_{21}^V - 14(k \cdot p_-)s^2\lambda_{21}^V - s^3\lambda_{21}^V - 8(k \cdot p_0)^2M_\rho^2\lambda_{22}^V \\
& - 8(k \cdot p_0)(k \cdot p_-)M_\rho^2\lambda_{22}^V + 8(k \cdot p_0)^2s\lambda_{22}^V + 8(k \cdot p_0)(k \cdot p_-)s\lambda_{22}^V \\
& - 6k \cdot p_0 M_\rho^2 s\lambda_{22}^V - 2k \cdot p_- M_\rho^2 s\lambda_{22}^V + 6(k \cdot p_0)s^2\lambda_{22}^V + 2(k \cdot p_-)s^2\lambda_{22}^V - M_\rho^2 s^2\lambda_{22}^V \\
& + s^3\lambda_{22}^V + 16(k \cdot p_0)(k \cdot p_-)s\lambda_{21}^V\lambda_7^{VV} + 16(k \cdot p_-)^2s\lambda_{21}^V\lambda_7^{VV} + 4(k \cdot p_0)s^2\lambda_{21}^V\lambda_7^{VV} \\
& + 12(k \cdot p_-)s^2\lambda_{21}^V\lambda_7^{VV} + 2s^3\lambda_{21}^V\lambda_7^{VV}) \Big)
\end{aligned}$$

$$\begin{aligned}
v_3^R = & \frac{2}{F^2} \left(\frac{8}{M_\omega^2 D_\omega [(k+p_0)^2]} \left(-4(4(k \cdot p_0)^2 - M_\omega^2 (2k \cdot p_- + s)) + k \cdot p_0 \right. \right. \\
& (2k \cdot p_- - 2M_\omega^2 + s)(\kappa_{12}^V)^2 + k \cdot p_0 \kappa_{16}^V ((2k \cdot p_- + s) \kappa_{16}^V - 2(P-q)^2 \kappa_{17}^V) \\
& + 2\kappa_{12}^V ((4(k \cdot p_0)^2 - 2k \cdot p_0 M_\omega^2 + M_\omega^2 (2k \cdot p_- + s)) \kappa_{16}^V + 2(k \cdot p_0 - M_\omega^2) \\
& (P-q)^2 \kappa_{17}^V) \Big) + \frac{\sqrt{2} F_V (2\lambda_{13}^V + \lambda_{16}^V + \lambda_{18}^V + 2\lambda_{19}^V)}{M_\rho^2} \\
& + \frac{8}{M_{a_1}^2 D_{a_1} [(k+p_-)^2]} \left((-2(k \cdot p_0)(k \cdot p_-) + 2k \cdot p_0 M_{a_1}^2 + 2k \cdot p_- M_{a_1}^2 - (k \cdot p_-) s \right. \\
& + M_{a_1}^2 s)(\lambda_{12}^A)^2 - 8k \cdot p_- (2k \cdot p_0 + s)(\lambda_{13}^A)^2 - 2\sqrt{2} F_A k \cdot p_0 \lambda_{15}^A - 2\sqrt{2} F_A k \cdot p_- \lambda_{15}^A \\
& - \sqrt{2} F_A s \lambda_{15}^A - 4\sqrt{2} F_A k \cdot p_- \lambda_{17}^A + 16(k \cdot p_0)(k \cdot p_-) \lambda_{15}^A \lambda_{17}^A + 16(k \cdot p_-)^2 \lambda_{15}^A \lambda_{17}^A \\
& + 8(k \cdot p_-) s \lambda_{15}^A \lambda_{17}^A + 16(k \cdot p_-)^2 (\lambda_{17}^A)^2 + \lambda_{13}^A (8k \cdot p_- (P-q)^2 \lambda_{15}^A + (2k \cdot p_0 \\
& - 2k \cdot p_- + s)(\sqrt{2} F_A - 8k \cdot p_- \lambda_{17}^A)) + \lambda_{12}^A (8(k \cdot p_0 (4k \cdot p_- - 2M_{a_1}^2) - M_{a_1}^2 s \\
& + 2k \cdot p_- (M_{a_1}^2 + s)) \lambda_{13}^A - 8(k \cdot p_- - M_{a_1}^2) (P-q)^2 \lambda_{15}^A + (2k \cdot p_0 - 2k \cdot p_- + 4M_{a_1}^2 \\
& + s)(-\sqrt{2} F_A + 8k \cdot p_- \lambda_{17}^A)) \Big) \Big)
\end{aligned} \tag{120}$$

$$\begin{aligned}
v_3^{RR} = & \frac{1}{\sqrt{2}F^2} \left(-\frac{16F_V}{M_\rho^2 M_\omega^2 D_\omega [(k+p_0)^2]} \left(2\kappa_{12}^V (-M_\omega^2 (2k \cdot p_- + s) \kappa_3^{VV} + (2k \cdot p_0 - M_\omega^2) \right. \right. \\
& (4k \cdot p_0 + 2k \cdot p_- + s) \kappa_4^{VV}) - ((2k \cdot p_- + s) \kappa_{16}^V - 2(P-q)^2 \kappa_{17}^V) (M_\omega^2 \kappa_3^{VV} \\
& + D_\omega [(k+p_0)^2] \kappa_4^{VV}) \Big) + \frac{32(-F_V + 2\sqrt{2}(P-q)^2 \lambda_{22}^V)}{M_\omega^2 D_\rho [(P-q)^2] D_\omega [(k+p_0)^2]} \left(-2\kappa_{12}^V ((2(k \cdot p_0)^2 \right. \\
& - M_\omega^2 (2k \cdot p_- + s) + k \cdot p_0 (2k \cdot p_- - 3M_\omega^2 + s)) \kappa_3^{VV} + k \cdot p_0 (-2k \cdot p_0 + M_\omega^2) \kappa_4^{VV}) \\
& + k \cdot p_0 \kappa_{16}^V (((P-q)^2 + M_\omega^2) \kappa_3^{VV} + D_\omega [(k+p_0)^2] \kappa_4^{VV}) \Big) \\
& + \frac{2F_V}{M_{a_1}^2 M_\rho^2 D_{a_1} [(k+p_-)^2]} \left(-2(-4(2k \cdot p_0 (k \cdot p_- - M_{a_1}^2) - M_{a_1}^2 s + k \cdot p_- \right. \\
& (-2M_{a_1}^2 + s)) \lambda_{12}^A + (k \cdot p_- - M_{a_1}^2) (\sqrt{2}F_A + 4(2k \cdot p_0 + s) \lambda_{13}^A - 4(P-q)^2 \lambda_{15}^A \\
& - 8k \cdot p_- \lambda_{17}^A) \lambda_2^{VA} + k \cdot p_- (-\sqrt{2}F_A + 4(2k \cdot p_0 + 2M_{a_1}^2 + s) \lambda_{12}^A - 4(2k \cdot p_0 + s) \lambda_{13}^A \\
& + 8k \cdot p_0 \lambda_{15}^A + 8k \cdot p_- \lambda_{15}^A + 4s \lambda_{15}^A + 8k \cdot p_- \lambda_{17}^A) (\lambda_4^{VA} + 2\lambda_5^{VA}) \Big) \\
& + \frac{(-\sqrt{2}F_V + 4(P-q)^2 \lambda_{22}^V)}{M_{a_1}^2 D_{a_1} [(k+p_-)^2] D_\rho [(P-q)^2]} \left(-2(4\sqrt{2}(2k \cdot p_0 (k \cdot p_- - M_{a_1}^2) - M_{a_1}^2 s \right. \\
& + k \cdot p_- (-2M_{a_1}^2 + s)) \lambda_{12}^A + (2k \cdot p_0 + 2M_{a_1}^2 + s) (F_A - 4\sqrt{2}k \cdot p_- \lambda_{13}^A \\
& - 4\sqrt{2}k \cdot p_- \lambda_{17}^A) \lambda_2^{VA} + (F_A + 4\sqrt{2}(k \cdot p_- - M_{a_1}^2) \lambda_{12}^A - 4\sqrt{2}k \cdot p_- \lambda_{13}^A \\
& - 4\sqrt{2}k \cdot p_- \lambda_{17}^A) (2(P-q)^2 \lambda_3^{VA} - (2k \cdot p_0 + s) (\lambda_4^{VA} + 2\lambda_5^{VA})) \Big) \\
& \left. + \frac{8F_V (\sqrt{2}F_V - 4(P-q)^2 \lambda_{22}^V) \lambda_5^{VV}}{M_\rho^2 D_\rho [(P-q)^2]} \right) \\
& \tag{121}
\end{aligned}$$

$$\begin{aligned}
v_3^{RRR} = & -\frac{\sqrt{2}F_V (-\sqrt{2}F_V + 4(P-q)^2 \lambda_{22}^V)}{F^2 M_{a_1}^2 M_\rho^2 D_{a_1} [(k+p_-)^2] D_\rho [(P-q)^2]} \left(-4(2k \cdot p_0 (k \cdot p_- - M_{a_1}^2) \right. \\
& - M_{a_1}^2 s + k \cdot p_- (-2M_{a_1}^2 + s)) (\lambda_2^{VA})^2 + k \cdot p_- (\lambda_4^{VA} + 2\lambda_5^{VA}) (2(P-q)^2 \lambda_3^{VA} \\
& - (2k \cdot p_0 + s) (\lambda_4^{VA} + 2\lambda_5^{VA})) + 2\lambda_2^{VA} (2(k \cdot p_- - M_{a_1}^2) (P-q)^2 \lambda_3^{VA} \\
& \left. - (k \cdot p_0 (4k \cdot p_- - 2M_{a_1}^2) - M_{a_1}^2 s + 2k \cdot p_- (M_{a_1}^2 + s)) (\lambda_4^{VA} + 2\lambda_5^{VA})) \right) \\
& \tag{122}
\end{aligned}$$

$$v_{GI3}^{R+RR} = \frac{2\sqrt{2}}{F^2 D_\rho [(P-q)^2]} (F_V - 2\sqrt{2}(P-q)^2 \lambda_{22}^V) (2\lambda_{13}^V + \lambda_{16}^V + \lambda_{18}^V + \lambda_{19}^V) \tag{123}$$

$$\begin{aligned}
v_4^R = & \frac{2}{F^2} \left(\frac{8}{M_\omega^2 D_\omega [(k+p_0)^2]} \left(4(k \cdot p_0 - M_\omega^2)(2k \cdot p_- + s)(\kappa_{12}^V)^2 + k \cdot p_0 \kappa_{16}^V \right. \right. \\
& \left. \left. (-2k \cdot p_- + s)\kappa_{16}^V + 2(2k \cdot p_- + M_\omega^2 + s)\kappa_{17}^V) - 2\kappa_{12}^V(M_\omega^2(2k \cdot p_- + s)\kappa_{16}^V \right. \right. \\
& \left. \left. + 2(-M_\omega^2(2k \cdot p_- + s) + k \cdot p_0(2k \cdot p_- - M_\omega^2 + s))\kappa_{17}^V) \right) \right. \\
& \left. - \frac{\sqrt{2}F_V(\lambda_{13}^V + \lambda_{14}^V - \lambda_{15}^V - \lambda_{21}^V)}{M_\rho^2} \right. \\
& \left. - \frac{\sqrt{2}(2\lambda_{12}^A + \lambda_{15}^A)(-F_A + 4\sqrt{2}k \cdot p_-(\lambda_{12}^A + \lambda_{13}^A + \lambda_{17}^A))}{D_{a_1}[(k+p_-)^2]} \right)
\end{aligned} \tag{124}$$

$$\begin{aligned}
v_4^{RR} = & \frac{\sqrt{2}}{F^2} \left(- \frac{8F_V}{M_\rho^2 M_\omega^2 D_\omega [(k+p_0)^2]} \left((2k \cdot p_- + s)\kappa_{16}^V(M_\omega^2 \kappa_3^{VV} + (-2k \cdot p_0 + M_\omega^2)\kappa_4^{VV}) \right. \right. \\
& \left. \left. - 2\kappa_{17}^V(M_\omega^2(P-q)^2 \kappa_3^{VV} - (2k \cdot p_0 - M_\omega^2)(2k \cdot p_- + s)\kappa_4^{VV}) + 2(2k \cdot p_- + s)\kappa_{12}^V \right. \right. \\
& \left. \left. (M_\omega^2 \kappa_3^{VV} + D_\omega[(k+p_0)^2] \kappa_4^{VV}) \right) - \frac{16\kappa_3^{VV}(-F_V + 2\sqrt{2}(P-q)^2 \lambda_{22}^V)}{M_\omega^2 D_\rho [(P-q)^2] D_\omega [(k+p_0)^2]} \right. \\
& \left. \left((2M_\omega^2(2k \cdot p_- + s) - 2k \cdot p_0(2k \cdot p_- - 2M_\omega^2 + s))\kappa_{12}^V + k \cdot p_0(2k \cdot p_- + 2M_\omega^2 + s)\kappa_{16}^V \right) \right. \\
& \left. + \frac{(\sqrt{2}F_V - 4(P-q)^2 \lambda_{22}^V)(-F_A + 4\sqrt{2}k \cdot p_-(\lambda_{12}^A + \lambda_{13}^A + \lambda_{17}^A))(2\lambda_2^{VA} - \lambda_3^{VA})}{D_{a_1}[(k+p_-)^2] D_\rho [(P-q)^2]} \right. \\
& \left. + \frac{4k \cdot p_- F_V(2\lambda_{12}^A + \lambda_{15}^A)(2\lambda_2^{VA} - \lambda_4^{VA} - 2\lambda_5^{VA})}{M_\rho^2 D_{a_1}[(k+p_-)^2]} - \frac{2F_V(\sqrt{2}G_V - 2s\lambda_{21}^V)\lambda_7^{VV}}{M_\rho^2 D_\rho [s]} \right. \\
& \left. - \frac{F_V(\sqrt{2}F_V(\lambda_3^{VV} - \lambda_4^{VV} + 2\lambda_5^{VV}) - 2(P-q)^2 \lambda_{22}^V(-1 + 2\lambda_3^{VV} - 2\lambda_4^{VV} + 4\lambda_5^{VV}))}{M_\rho^2 D_\rho [(P-q)^2]} \right)
\end{aligned} \tag{125}$$

$$v_4^{RRR} = - \frac{2\sqrt{2}F_V k \cdot p_- (\sqrt{2}F_V - 4(P-q)^2 \lambda_{22}^V)(2\lambda_2^{VA} - \lambda_3^{VA})(2\lambda_2^{VA} - \lambda_4^{VA} - 2\lambda_5^{VA})}{F^2 M_\rho^2 D_{a_1}[(k+p_-)^2] D_\rho [(P-q)^2]} \tag{126}$$

$$\begin{aligned}
v_{GI4}^{R+RR} = & \frac{2\sqrt{2}F_V}{F^2 D_\rho [(P-q)^2] D_\rho [s]} \left(\right. \\
& (-M_\rho^2 + s) (\lambda_{13}^V + \lambda_{14}^V - \lambda_{15}^V + \lambda_{18}^V + \lambda_{19}^V) + 2M_\rho^2 \lambda_{21}^V - s \lambda_{21}^V \\
& + 2s \lambda_{21}^V \lambda_7^{VV}) + 4G_V (\sqrt{2}((P-q)^2 - M_\rho^2) \lambda_7^V - F_V \lambda_7^{VV} + \sqrt{2} \lambda_{22}^V (-4k \cdot p_0 - 4k \cdot p_- \\
& + 3M_\rho^2 - 2s + 2(P-q)^2 \lambda_7^{VV})) - 8(s((P-q)^2 - M_\rho^2) \lambda_7^V \lambda_{21}^V + \lambda_{22}^V (-(M_\rho^2 - s) \\
& (P-q)^2 \lambda_{13}^V - (M_\rho^2 - s)(P-q)^2 \lambda_{14}^V + 2k \cdot p_0 M_\rho^2 \lambda_{15}^V + 2k \cdot p_- M_\rho^2 \lambda_{15}^V - 2(k \cdot p_0) s \lambda_{15}^V \\
& - 2(k \cdot p_-) s \lambda_{15}^V + M_\rho^2 s \lambda_{15}^V - s^2 \lambda_{15}^V - 2k \cdot p_0 M_\rho^2 \lambda_{18}^V - 2k \cdot p_- M_\rho^2 \lambda_{18}^V + 2(k \cdot p_0) s \lambda_{18}^V \\
& + 2(k \cdot p_-) s \lambda_{18}^V - M_\rho^2 s \lambda_{18}^V + s^2 \lambda_{18}^V - 2k \cdot p_0 M_\rho^2 \lambda_{19}^V - 2k \cdot p_- M_\rho^2 \lambda_{19}^V + 2(k \cdot p_0) s \lambda_{19}^V \\
& + 2(k \cdot p_-) s \lambda_{19}^V - M_\rho^2 s \lambda_{19}^V + s^2 \lambda_{19}^V + 4k \cdot p_0 M_\rho^2 \lambda_{21}^V + 4k \cdot p_- M_\rho^2 \lambda_{21}^V - 8(k \cdot p_0) s \lambda_{21}^V \\
& - 8(k \cdot p_-) s \lambda_{21}^V + 5M_\rho^2 s \lambda_{21}^V - 4s^2 \lambda_{21}^V + 4(k \cdot p_0) s \lambda_{21}^V \lambda_7^{VV} + 4(k \cdot p_-) s \lambda_{21}^V \lambda_7^{VV} \\
& \left. + 2s^2 \lambda_{21}^V \lambda_7^{VV} \right)
\end{aligned} \tag{127}$$

D Axial Form Factors

$$\begin{aligned}
a_1^R = & \frac{\sqrt{2}}{3F^2} \left(- \frac{2(P-q)^2 F_V (\kappa_1^V - \kappa_2^V + \kappa_3^V + \kappa_6^V + \kappa_7^V - \kappa_8^V - 2\kappa_{12}^V - \kappa_{16}^V + \kappa_{17}^V)}{M_\omega^2} \right. \\
& + \frac{4((P-q)^2 \kappa_{11}^V + s \kappa_{12}^V - (k \cdot p_0 + k \cdot p_-) \kappa_{16}^V) (-G_V + \sqrt{2}s \lambda_{21}^V)}{D_\rho[s]} \\
& + \frac{1}{M_\rho^2 D_\rho [(k+p_-)^2]} \left(F_V (2k \cdot p_- + s) (2(k \cdot p_- - M_\rho^2) \kappa_{12}^V - k \cdot p_- \kappa_{16}^V) \right. \\
& + G_V (-4(2(k \cdot p_-)^2 + (k \cdot p_-)s - M_\rho^2 s) \kappa_{12}^V + 2k \cdot p_- (2k \cdot p_- - 2M_\rho^2 + s) \kappa_{16}^V) \\
& + \sqrt{2} (-2\kappa_{12}^V ((k \cdot p_- - M_\rho^2) (2k \cdot p_0 + s) (2k \cdot p_- + s) \lambda_{16}^V - 2(k \cdot p_- - M_\rho^2) \\
& (2k \cdot p_0 + s) (2k \cdot p_- + s) \lambda_{17}^V + 8(k \cdot p_0) (k \cdot p_-)^2 \lambda_{18}^V + 8(k \cdot p_-)^3 \lambda_{18}^V \\
& + 4(k \cdot p_0) (k \cdot p_-) s \lambda_{18}^V + 8(k \cdot p_-)^2 s \lambda_{18}^V - 4k \cdot p_0 M_\rho^2 s \lambda_{18}^V - 4k \cdot p_- M_\rho^2 s \lambda_{18}^V \\
& + 2(k \cdot p_-) s^2 \lambda_{18}^V - 2M_\rho^2 s^2 \lambda_{18}^V + 8(k \cdot p_0) (k \cdot p_-)^2 \lambda_{19}^V + 8(k \cdot p_0) (k \cdot p_-) M_\rho^2 \lambda_{19}^V \\
& + 8(k \cdot p_-)^2 M_\rho^2 \lambda_{19}^V + 4(k \cdot p_0) (k \cdot p_-) s \lambda_{19}^V + 4(k \cdot p_-)^2 s \lambda_{19}^V - 4k \cdot p_0 M_\rho^2 s \lambda_{19}^V \\
& + 2(k \cdot p_-) s^2 \lambda_{19}^V - 2M_\rho^2 s^2 \lambda_{19}^V - 8(k \cdot p_-)^3 \lambda_{21}^V - 4(k \cdot p_-)^2 s \lambda_{21}^V + 4k \cdot p_- M_\rho^2 s \lambda_{21}^V \\
& + 8(k \cdot p_-)^3 \lambda_{22}^V - 8(k \cdot p_-)^2 M_\rho^2 \lambda_{22}^V + 4(k \cdot p_-)^2 s \lambda_{22}^V - 4k \cdot p_- M_\rho^2 s \lambda_{22}^V) \\
& + k \cdot p_- \kappa_{16}^V ((2k \cdot p_0 + s) (2k \cdot p_- + s) \lambda_{16}^V + 2(-(2k \cdot p_0 + s) (2k \cdot p_- + s) \lambda_{17}^V \\
& + (P-q)^2 (2k \cdot p_- - 2M_\rho^2 + s) \lambda_{18}^V + 4(k \cdot p_0) (k \cdot p_-) \lambda_{19}^V - 8k \cdot p_0 M_\rho^2 \lambda_{19}^V \\
& - 4k \cdot p_- M_\rho^2 \lambda_{19}^V + 2(k \cdot p_0) s \lambda_{19}^V + 2(k \cdot p_-) s \lambda_{19}^V - 2M_\rho^2 s \lambda_{19}^V + s^2 \lambda_{19}^V - 4(k \cdot p_-)^2 \\
& \lambda_{21}^V + 4k \cdot p_- M_\rho^2 \lambda_{21}^V - 2(k \cdot p_-) s \lambda_{21}^V + 4(k \cdot p_-)^2 \lambda_{22}^V + 2(k \cdot p_-) s \lambda_{22}^V)) \Big) \\
& + \frac{1}{M_\rho^2 D_\rho [(k+p_0)^2]} \left(F_V (4k \cdot p_0 + 2k \cdot p_- + s) (2(k \cdot p_0 - M_\rho^2) \kappa_{12}^V - k \cdot p_0 \kappa_{16}^V) \right. \\
& + G_V (-4(4(k \cdot p_0)^2 - M_\rho^2 (2k \cdot p_- + s) + k \cdot p_0 (2k \cdot p_- - 2M_\rho^2 + s)) \kappa_{12}^V + 2k \cdot p_0 \\
& (4k \cdot p_0 + 2k \cdot p_- - 2M_\rho^2 + s) \kappa_{16}^V) + \sqrt{2} (k \cdot p_0 \kappa_{16}^V ((2k \cdot p_- + s) (4k \cdot p_0 + 2k \cdot p_- + s) \\
& \lambda_{16}^V + 2(-(2k \cdot p_- + s) (4k \cdot p_0 + 2k \cdot p_- + s) \lambda_{17}^V + (8(k \cdot p_0)^2 + 12(k \cdot p_0) (k \cdot p_-) \\
& + 4(k \cdot p_-)^2 - 4k \cdot p_0 M_\rho^2 - 4k \cdot p_- M_\rho^2 + 6(k \cdot p_0) s + 4(k \cdot p_-) s - 2M_\rho^2 s + s^2) \lambda_{18}^V \\
& + 8(k \cdot p_0) (k \cdot p_-) \lambda_{19}^V + 4(k \cdot p_-)^2 \lambda_{19}^V - 4k \cdot p_- M_\rho^2 \lambda_{19}^V + 4(k \cdot p_0) s \lambda_{19}^V \\
& + 4(k \cdot p_-) s \lambda_{19}^V - 2M_\rho^2 s \lambda_{19}^V + s^2 \lambda_{19}^V - 8(k \cdot p_0)^2 \lambda_{21}^V - 4(k \cdot p_0) (k \cdot p_-) \lambda_{21}^V \\
& + 4k \cdot p_0 M_\rho^2 \lambda_{21}^V - 2(k \cdot p_0) s \lambda_{21}^V + 8(k \cdot p_0)^2 \lambda_{22}^V + 4(k \cdot p_0) (k \cdot p_-) \lambda_{22}^V + 2(k \cdot p_0) s \lambda_{22}^V) \\
& - 2\kappa_{12}^V ((k \cdot p_0 - M_\rho^2) (2k \cdot p_- + s) (4k \cdot p_0 + 2k \cdot p_- + s) \lambda_{16}^V + 2(-(k \cdot p_0 - M_\rho^2) \\
& (2k \cdot p_- + s) (4k \cdot p_0 + 2k \cdot p_- + s) \lambda_{17}^V + (P-q)^2 (4(k \cdot p_0)^2 - M_\rho^2 (2k \cdot p_- + s) \\
& + k \cdot p_0 (2k \cdot p_- - 2M_\rho^2 + s)) \lambda_{18}^V + 8(k \cdot p_0)^2 (k \cdot p_-) \lambda_{19}^V + 4(k \cdot p_0) (k \cdot p_-)^2 \lambda_{19}^V
\end{aligned}$$

$$\begin{aligned}
& -4(k \cdot p_0)(k \cdot p_-) M_\rho^2 \lambda_{19}^V - 4(k \cdot p_-)^2 M_\rho^2 \lambda_{19}^V + 4(k \cdot p_0)^2 s \lambda_{19}^V + 4(k \cdot p_0)(k \cdot p_-) s \lambda_{19}^V \\
& - 2k \cdot p_0 M_\rho^2 s \lambda_{19}^V - 4k \cdot p_- M_\rho^2 s \lambda_{19}^V + (k \cdot p_0) s^2 \lambda_{19}^V - M_\rho^2 s^2 \lambda_{19}^V - 8(k \cdot p_0)^3 \lambda_{21}^V \\
& - 4(k \cdot p_0)^2 (k \cdot p_-) \lambda_{21}^V + 4(k \cdot p_0)^2 M_\rho^2 \lambda_{21}^V + 4(k \cdot p_0)(k \cdot p_-) M_\rho^2 \lambda_{21}^V - 2(k \cdot p_0)^2 s \lambda_{21}^V \\
& + 2k \cdot p_0 M_\rho^2 s \lambda_{21}^V + 8(k \cdot p_0)^3 \lambda_{22}^V + 4(k \cdot p_0)^2 (k \cdot p_-) \lambda_{22}^V - 8(k \cdot p_0)^2 M_\rho^2 \lambda_{22}^V \\
& - 4(k \cdot p_0)(k \cdot p_-) M_\rho^2 \lambda_{22}^V + 2(k \cdot p_0)^2 s \lambda_{22}^V - 2k \cdot p_0 M_\rho^2 s \lambda_{22}^V))) \\
& + \frac{2(P-q)^2(\kappa_5^A - \kappa_6^A + \kappa_7^A)(-F_A + 2\sqrt{2}(P-q)^2 \lambda_{17}^A)}{D_{a_1}[(P-q)^2]} \Big)
\end{aligned} \tag{128}$$

$$\begin{aligned}
a_1^{RR} = & \frac{1}{3\sqrt{2}F^2} \left(\frac{4sF_V \kappa_3^{VV} (-\sqrt{2}G_V + 2s \lambda_{21}^V)}{M_\omega^2 D_\rho[s]} \right. \\
& - \frac{1}{M_\rho^2 M_\omega^2 D_\rho [(k+p_-)^2]} \left(F_V (\sqrt{2}(2k \cdot p_- + s) F_V (M_\rho^2 \kappa_3^{VV} + D_\rho [(k+p_-)^2] \kappa_4^{VV}) \right. \\
& + 2\sqrt{2}G_V (M_\rho^2 (2k \cdot p_- - s) \kappa_3^{VV} - (2k \cdot p_- + s) D_\rho [(k+p_-)^2] \kappa_4^{VV}) \\
& + 2(2k \cdot p_- - M_\rho^2) (2k \cdot p_- + s) \kappa_4^{VV} ((2k \cdot p_0 + s) \lambda_{16}^V - 2(2k \cdot p_0 + s) \lambda_{17}^V + 4k \cdot p_0 \lambda_{18}^V \\
& + 4k \cdot p_- \lambda_{18}^V + 2s \lambda_{18}^V + 4k \cdot p_0 \lambda_{19}^V + 2s \lambda_{19}^V - 4k \cdot p_- \lambda_{21}^V + 4k \cdot p_- \lambda_{22}^V) - 2M_\rho^2 \kappa_3^{VV} \\
& ((2k \cdot p_0 + s) (2k \cdot p_- + s) \lambda_{16}^V - 2(2k \cdot p_0 + s) (2k \cdot p_- + s) \lambda_{17}^V - 2(2k \cdot p_- - s) \\
& (P-q)^2 \lambda_{18}^V - 24(k \cdot p_0)(k \cdot p_-) \lambda_{19}^V - 16(k \cdot p_-)^2 \lambda_{19}^V + 4(k \cdot p_0) s \lambda_{19}^V - 4(k \cdot p_-) s \lambda_{19}^V \\
& + 2s^2 \lambda_{19}^V + 8(k \cdot p_-)^2 \lambda_{21}^V - 4(k \cdot p_-) s \lambda_{21}^V + 8(k \cdot p_-)^2 \lambda_{22}^V + 4(k \cdot p_-) s \lambda_{22}^V)) \\
& + \frac{1}{M_\rho^2 M_\omega^2 D_\rho [(k+p_0)^2]} \left(F_V (-\sqrt{2}F_V (4k \cdot p_0 + 2k \cdot p_- + s) (M_\rho^2 \kappa_3^{VV} + D_\rho [(k+p_0)^2] \right. \\
& \left. \kappa_4^{VV}) + 2\sqrt{2}G_V (M_\rho^2 (2k \cdot p_- + s) \kappa_3^{VV} + (4k \cdot p_0 + 2k \cdot p_- + s) D_\rho [(k+p_0)^2] \kappa_4^{VV}) \right. \\
& - 2(2k \cdot p_0 - M_\rho^2) (4k \cdot p_0 + 2k \cdot p_- + s) \kappa_4^{VV} ((2k \cdot p_- + s) \lambda_{16}^V - 2(2k \cdot p_- + s) \lambda_{17}^V \\
& + 4k \cdot p_0 \lambda_{18}^V + 4k \cdot p_- \lambda_{18}^V + 2s \lambda_{18}^V + 4k \cdot p_- \lambda_{19}^V + 2s \lambda_{19}^V - 4k \cdot p_0 \lambda_{21}^V + 4k \cdot p_0 \lambda_{22}^V) \\
& + 2M_\rho^2 \kappa_3^{VV} ((2k \cdot p_- + s) (4k \cdot p_0 + 2k \cdot p_- + s) \lambda_{16}^V + 2(-(2k \cdot p_- + s) \\
& (4k \cdot p_0 + 2k \cdot p_- + s) \lambda_{17}^V + (2k \cdot p_- + s) (P-q)^2 \lambda_{18}^V + 4(k \cdot p_-)^2 \lambda_{19}^V \\
& + 4(k \cdot p_-) s \lambda_{19}^V + s^2 \lambda_{19}^V - 4(k \cdot p_0)(k \cdot p_-) \lambda_{21}^V - 2(k \cdot p_0) s \lambda_{21}^V + 8(k \cdot p_0)^2 \lambda_{22}^V \\
& + 4(k \cdot p_0)(k \cdot p_-) \lambda_{22}^V + 2(k \cdot p_0) s \lambda_{22}^V))) \\
& + \frac{2(P-q)^2 F_V (\kappa_2^{VA} - \kappa_3^{VA} - \kappa_4^{VA})(-\sqrt{2}F_A + 4(P-q)^2 \lambda_{17}^A)}{M_\omega^2 D_{a_1}[(P-q)^2]} \\
& - \frac{4(P-q)^2 \kappa_5^{VA} (-\sqrt{2}G_V + 2s \lambda_{21}^V) (-F_A + 2\sqrt{2}(P-q)^2 \lambda_{17}^A)}{D_{a_1}[(P-q)^2] D_\rho[s]}
\end{aligned}$$

$$\begin{aligned}
& - \frac{2(F_A - 2\sqrt{2}(P-q)^2\lambda_{17}^A)}{M_\rho^2 D_{a_1} [(P-q)^2] D_\rho [(k+p_-)^2]} \left(k \cdot p_- \kappa_{16}^V (-2(-(2M_\rho^2 - s)(2k \cdot p_- + s) \right. \\
& + 2k \cdot p_0 (2k \cdot p_- - 4M_\rho^2 + s)) \lambda_2^{VA} - 2M_\rho^2 (4k \cdot p_0 + 2k \cdot p_- + s) \lambda_3^{VA} \\
& + (2k \cdot p_- + s)((2k \cdot p_0 + 4k \cdot p_- - 2M_\rho^2 + s) \lambda_4^{VA} + 2(2k \cdot p_0 + s) \lambda_5^{VA})) \\
& + 2\kappa_{12}^V (2((k \cdot p_-) s^2 - M_\rho^2 s^2 + 2(k \cdot p_-)^2 (2M_\rho^2 + s) + 2k \cdot p_0 (2(k \cdot p_-)^2 \\
& - M_\rho^2 s + k \cdot p_- (2M_\rho^2 + s))) \lambda_2^{VA} - 2k \cdot p_- M_\rho^2 (4k \cdot p_0 + 2k \cdot p_- + s) \lambda_3^{VA} \\
& - (2k \cdot p_- + s)((4(k \cdot p_-)^2 - 2k \cdot p_- M_\rho^2 + 2k \cdot p_0 (k \cdot p_- - M_\rho^2) + (k \cdot p_-) s \\
& - M_\rho^2 s) \lambda_4^{VA} + 2(k \cdot p_- - M_\rho^2) (2k \cdot p_0 + s) \lambda_5^{VA})) \Big) \\
& + \frac{2(F_A - 2\sqrt{2}(P-q)^2\lambda_{17}^A)}{M_\rho^2 D_{a_1} [(P-q)^2] D_\rho [(k+p_0)^2]} \left(-k \cdot p_0 \kappa_{16}^V (-2(2k \cdot p_- + s) (4k \cdot p_0 + 2k \cdot p_- \right. \\
& - 2M_\rho^2 + s) \lambda_2^{VA} - 2M_\rho^2 (2k \cdot p_- + s) \lambda_3^{VA} + (4k \cdot p_0 + 2k \cdot p_- + s) ((4k \cdot p_0 + 2k \cdot p_- \\
& - 2M_\rho^2 + s) \lambda_4^{VA} + 2(2k \cdot p_- + s) \lambda_5^{VA}) + 2\kappa_{12}^V (-2(2k \cdot p_- + s) (4(k \cdot p_0)^2 \\
& - M_\rho^2 (2k \cdot p_- + s) + k \cdot p_0 (2k \cdot p_- - 2M_\rho^2 + s)) \lambda_2^{VA} + 2k \cdot p_0 M_\rho^2 (2k \cdot p_- + s) \lambda_3^{VA} \\
& + (4k \cdot p_0 + 2k \cdot p_- + s) ((4(k \cdot p_0)^2 - M_\rho^2 (2k \cdot p_- + s) + k \cdot p_0 (2k \cdot p_- - 2M_\rho^2 + s)) \\
& \left. \lambda_4^{VA} + 2(k \cdot p_0 - M_\rho^2) (2k \cdot p_- + s) \lambda_5^{VA}) \right) \Big) \quad (129)
\end{aligned}$$

$$\begin{aligned}
a_1^{RRR} = & - \frac{F_V (\sqrt{2} F_A - 4(P-q)^2 \lambda_{17}^A)}{3\sqrt{2} F^2 M_\omega^2 M_\rho^2 D_{a_1} [(P-q)^2] D_\rho [(k+p_0)^2] D_\rho [(k+p_-)^2]} \left(-M_\rho^2 (2k \cdot p_- + s) \right. \\
& D_\rho [(k+p_-)^2] \kappa_3^{VV} (2(2k \cdot p_- + s) \lambda_2^{VA} + 4k \cdot p_0 \lambda_3^{VA} - (4k \cdot p_0 + 2k \cdot p_- + s) \\
& (\lambda_4^{VA} + 2\lambda_5^{VA}) + D_\rho [(k+p_0)^2] (2D_\rho [(k+p_-)^2] \kappa_4^{VV} (-2(3k \cdot p_0 + k \cdot p_- + s) \\
& (2k \cdot p_- + s) \lambda_2^{VA} + (8(k \cdot p_0)^2 + 6(k \cdot p_-)^2 + 5(k \cdot p_-) s + s^2 + 5k \cdot p_0 \\
& (2k \cdot p_- + s)) \lambda_4^{VA} + 2(3k \cdot p_0 + k \cdot p_- + s) (2k \cdot p_- + s) \lambda_5^{VA}) + M_\rho^2 \kappa_3^{VV} \\
& (2(12(k \cdot p_0) (k \cdot p_-) + 8(k \cdot p_-)^2 - 2(k \cdot p_0) s + 2(k \cdot p_-) s - s^2) \lambda_2^{VA} \\
& - 4k \cdot p_- (4k \cdot p_0 + 2k \cdot p_- + s) \lambda_3^{VA} + (2k \cdot p_0 + s) (2k \cdot p_- + s) (\lambda_4^{VA} + 2\lambda_5^{VA})) \Big) \quad (130)
\end{aligned}$$

$$\begin{aligned}
a_2^R = & \frac{4\sqrt{2}}{3F^2} \left(-\frac{2(P-q)^2 F_V (\kappa_1^V - \kappa_2^V + \kappa_3^V)}{M_\omega^2 D_\pi [(P-q)^2]} \right. \\
& + \frac{F_V (3\kappa_1^V - 3\kappa_2^V + 3\kappa_3^V + \kappa_6^V + \kappa_7^V - \kappa_8^V - 2\kappa_{12}^V - \kappa_{16}^V + \kappa_{17}^V)}{M_\omega^2} \\
& + \frac{2\sqrt{2}k \cdot p_0 (2\kappa_{12}^V + \kappa_{16}^V) (\lambda_{18}^V + 2\lambda_{19}^V)}{D_\rho [(k+p_0)^2]} - \frac{2k \cdot p_0 (2\kappa_{12}^V + \kappa_{16}^V) (-G_V + 2\sqrt{2}k \cdot p_0 \lambda_{21}^V)}{D_\pi [(P-q)^2] D_\rho [(k+p_0)^2]} \\
& - \frac{2k \cdot p_- (2\kappa_{12}^V + \kappa_{16}^V) (-G_V + 2\sqrt{2}k \cdot p_- \lambda_{21}^V)}{D_\pi [(P-q)^2] D_\rho [(k+p_-)^2]} + \frac{2(\kappa_{11}^V + \kappa_{12}^V) (G_V - \sqrt{2}s \lambda_{21}^V)}{D_\rho [s]} \\
& - \frac{2(k \cdot p_0 + k \cdot p_-) (2\kappa_{12}^V + \kappa_{16}^V) (G_V - \sqrt{2}s \lambda_{21}^V)}{D_\pi [(P-q)^2] D_\rho [s]} + \frac{1}{M_\rho^2 D_\rho [(k+p_-)^2]} \\
& \left(G_V (4(k \cdot p_- - M_\rho^2) \kappa_{12}^V - 2k \cdot p_- \kappa_{16}^V) + F_V (-2(k \cdot p_- - M_\rho^2) \kappa_{12}^V + k \cdot p_- \kappa_{16}^V) \right. \\
& + \sqrt{2} (-k \cdot p_- \kappa_{16}^V ((2k \cdot p_0 + s) \lambda_{16}^V - 2(2k \cdot p_0 + s) \lambda_{17}^V + 4k \cdot p_0 \lambda_{18}^V + 4k \cdot p_- \lambda_{18}^V) \\
& - 2M_\rho^2 \lambda_{18}^V + 2s \lambda_{18}^V + 4k \cdot p_0 \lambda_{19}^V + 2s \lambda_{19}^V - 4k \cdot p_- \lambda_{21}^V + 4k \cdot p_- \lambda_{22}^V) + 2\kappa_{12}^V \\
& ((k \cdot p_- - M_\rho^2) (2k \cdot p_0 + s) \lambda_{16}^V - 2(k \cdot p_- - M_\rho^2) (2k \cdot p_0 + s) \lambda_{17}^V + 2(2(k \cdot p_-)^2 \\
& + 2k \cdot p_0 (k \cdot p_- - M_\rho^2) - M_\rho^2 s + k \cdot p_- (-M_\rho^2 + s)) \lambda_{18}^V + 2(k \cdot p_- - M_\rho^2) \\
& ((2k \cdot p_0 + s) \lambda_{19}^V + 2k \cdot p_- (-\lambda_{21}^V + \lambda_{22}^V))) \Big) + \frac{(\kappa_5^A - \kappa_6^A + \kappa_7^A) (F_A - 2\sqrt{2}(P-q)^2 \lambda_{17}^A)}{D_{a_1} [(P-q)^2]} \Big)
\end{aligned} \tag{131}$$

$$\begin{aligned}
a_2^{RR} = & \frac{2\sqrt{2}}{3F^2} \left(\frac{8k \cdot p_0 F_V \kappa_3^{VV} (\lambda_{18}^V + 2\lambda_{19}^V)}{M_\omega^2 D_\rho [(k+p_0)^2]} + \frac{4k \cdot p_0 F_V \kappa_3^{VV} (\sqrt{2}G_V - 4k \cdot p_0 \lambda_{21}^V)}{M_\omega^2 D_\pi [(P-q)^2] D_\rho [(k+p_0)^2]} \right. \\
& + \frac{4k \cdot p_- F_V \kappa_3^{VV} (\sqrt{2}G_V - 4k \cdot p_- \lambda_{21}^V)}{M_\omega^2 D_\pi [(P-q)^2] D_\rho [(k+p_-)^2]} + \frac{2F_V \kappa_3^{VV} (\sqrt{2}G_V - 2s \lambda_{21}^V)}{M_\omega^2 D_\rho [s]} \\
& + \frac{F_V}{M_\rho^2 M_\omega^2 D_\rho [(k+p_-)^2]} \left(\sqrt{2}F_V (M_\rho^2 \kappa_3^{VV} + D_\rho [(k+p_-)^2] \kappa_4^{VV}) \right. \\
& - 2\sqrt{2}G_V (M_\rho^2 \kappa_3^{VV} + D_\rho [(k+p_-)^2] \kappa_4^{VV}) - 2M_\rho^2 \kappa_3^{VV} ((2k \cdot p_0 + s) \lambda_{16}^V \\
& - 2(2k \cdot p_0 + s) \lambda_{17}^V + 4k \cdot p_0 \lambda_{18}^V + 2s \lambda_{18}^V + 4k \cdot p_0 \lambda_{19}^V + 2s \lambda_{19}^V - 4k \cdot p_- \lambda_{21}^V \\
& + 4k \cdot p_- \lambda_{22}^V) + 2(2k \cdot p_- - M_\rho^2) \kappa_4^{VV} ((2k \cdot p_0 + s) \lambda_{16}^V - 2(2k \cdot p_0 + s) \lambda_{17}^V \\
& + 4k \cdot p_0 \lambda_{18}^V + 4k \cdot p_- \lambda_{18}^V + 2s \lambda_{18}^V + 4k \cdot p_0 \lambda_{19}^V + 2s \lambda_{19}^V - 4k \cdot p_- \lambda_{21}^V \\
& \left. + 4k \cdot p_- \lambda_{22}^V) \right) + \frac{F_V (\kappa_2^{VA} - \kappa_3^{VA} - \kappa_4^{VA}) (\sqrt{2}F_A - 4(P-q)^2 \lambda_{17}^A)}{M_\omega^2 D_{a_1} [(P-q)^2]} \\
& + \frac{2\kappa_5^{VA} (\sqrt{2}G_V - 2s \lambda_{21}^V) (F_A - 2\sqrt{2}(P-q)^2 \lambda_{17}^A)}{D_{a_1} [(P-q)^2] D_\rho [s]} \\
& + \frac{4k \cdot p_0 (2\kappa_{12}^V + \kappa_{16}^V) (F_A - 2\sqrt{2}(P-q)^2 \lambda_{17}^A) (2\lambda_2^{VA} - \lambda_3^{VA})}{D_{a_1} [(P-q)^2] D_\rho [(k+p_0)^2]} \\
& + \frac{2(F_A - 2\sqrt{2}(P-q)^2 \lambda_{17}^A)}{M_\rho^2 D_{a_1} [(P-q)^2] D_\rho [(k+p_-)^2]} \left(k \cdot p_- \kappa_{16}^V (-2(2k \cdot p_0 + s) \lambda_2^{VA} \right. \\
& + (2k \cdot p_0 + 4k \cdot p_- - 2M_\rho^2 + s) \lambda_4^{VA} + 2(2k \cdot p_0 + s) \lambda_5^{VA}) + 2\kappa_{12}^V \\
& (2(k \cdot p_- - M_\rho^2) (2k \cdot p_0 + s) \lambda_2^{VA} + (-2(k \cdot p_0) (k \cdot p_-) - 4(k \cdot p_-)^2 \\
& + 2k \cdot p_0 M_\rho^2 + 2k \cdot p_- M_\rho^2 - (k \cdot p_-) s + M_\rho^2 s) \lambda_4^{VA} - 2(k \cdot p_- - M_\rho^2) \\
& \left. (2k \cdot p_0 + s) \lambda_5^{VA}) \right) \Bigg) \quad (132)
\end{aligned}$$

$$\begin{aligned}
a_2^{RRR} = & - \frac{2\sqrt{2}F_V (\sqrt{2}F_A - 4(P-q)^2 \lambda_{17}^A)}{3F^2 M_\rho^2 M_\omega^2 D_{a_1} [(P-q)^2] D_\rho [(k+p_0)^2] D_\rho [(k+p_-)^2]} \left(4k \cdot p_0 M_\rho^2 \right. \\
& D_\rho [(k+p_-)^2] \kappa_3^{VV} (-2\lambda_2^{VA} + \lambda_3^{VA}) + D_\rho [(k+p_0)^2] (M_\rho^2 (2k \cdot p_0 + s) \kappa_3^{VV} \\
& (2\lambda_2^{VA} - \lambda_4^{VA} - 2\lambda_5^{VA}) + D_\rho [(k+p_-)^2] \kappa_4^{VV} (2(2k \cdot p_0 + s) \lambda_2^{VA} \\
& \left. - (2k \cdot p_0 + 4k \cdot p_- + s) \lambda_4^{VA} - 2(2k \cdot p_0 + s) \lambda_5^{VA})) \right) \quad (133)
\end{aligned}$$

$$\begin{aligned}
a_3^R = & \frac{\sqrt{2}}{3F^2} \left(- \frac{4F_V(k \cdot p_0 - k \cdot p_-)(\kappa_1^V - \kappa_2^V + \kappa_3^V + \kappa_6^V + \kappa_7^V - \kappa_8^V - \kappa_{17}^V)}{M_\omega^2} \right. \\
& - \frac{4(k \cdot p_0 - k \cdot p_-)(2\kappa_{11}^V - \kappa_{16}^V)(G_V - \sqrt{2}s\lambda_{21}^V)}{D_\rho[s]} \\
& + \frac{1}{M_\rho^2 D_\rho [(k + p_0)^2]} \left(-2G_V(2(4(k \cdot p_0)^2 + M_\rho^2(2k \cdot p_- + s) - k \cdot p_0 \right. \\
& (2k \cdot p_- + 2M_\rho^2 + s))\kappa_{12}^V + k \cdot p_0(-4k \cdot p_0 + 2k \cdot p_- + 2M_\rho^2 + s)\kappa_{16}^V) \\
& + F_V(2(4(k \cdot p_0)^2 - k \cdot p_0(2k \cdot p_- + s) + M_\rho^2(2k \cdot p_- + s))\kappa_{12}^V + k \cdot p_0 \\
& (-4k \cdot p_0 + 2k \cdot p_- + 4M_\rho^2 + s)\kappa_{16}^V) - \sqrt{2}(k \cdot p_0\kappa_{16}^V(-(4k \cdot p_0 - 2k \cdot p_- \\
& - 4M_\rho^2 - s)(2k \cdot p_- + s)\lambda_{16}^V + 2((4k \cdot p_0 - 2k \cdot p_- - 4M_\rho^2 - s)(2k \cdot p_- + s)\lambda_{17}^V \\
& + (-8(k \cdot p_0)^2 + 4(k \cdot p_-)^2 - 2k \cdot p_0(2k \cdot p_- - 2M_\rho^2 + s) + 4k \cdot p_-(M_\rho^2 + s) \\
& + s(2M_\rho^2 + s))\lambda_{18}^V - 8(k \cdot p_0)(k \cdot p_-)\lambda_{19}^V + 4(k \cdot p_-)^2\lambda_{19}^V + 4k \cdot p_- M_\rho^2 \lambda_{19}^V \\
& - 4(k \cdot p_0)s\lambda_{19}^V + 4(k \cdot p_-)s\lambda_{19}^V + 2M_\rho^2 s\lambda_{19}^V + s^2\lambda_{19}^V + 8(k \cdot p_0)^2\lambda_{21}^V \\
& - 4(k \cdot p_0)(k \cdot p_-)\lambda_{21}^V - 4k \cdot p_0 M_\rho^2 \lambda_{21}^V - 2(k \cdot p_0)s\lambda_{21}^V - 8(k \cdot p_0)^2\lambda_{22}^V \\
& + 4(k \cdot p_0)(k \cdot p_-)\lambda_{22}^V + 8k \cdot p_0 M_\rho^2 \lambda_{22}^V + 2(k \cdot p_0)s\lambda_{22}^V) + 2\kappa_{12}^V((2k \cdot p_- + s) \\
& (4(k \cdot p_0)^2 - k \cdot p_0(2k \cdot p_- + s) + M_\rho^2(2k \cdot p_- + s))\lambda_{16}^V + 2(-(2k \cdot p_- + s) \\
& (4(k \cdot p_0)^2 - k \cdot p_0(2k \cdot p_- + s) + M_\rho^2(2k \cdot p_- + s))\lambda_{17}^V + (8(k \cdot p_0)^3 - k \cdot p_0 \\
& (2k \cdot p_- + s)^2 + M_\rho^2(2k \cdot p_- + s)^2 + 2(k \cdot p_0)^2(2k \cdot p_- - 2M_\rho^2 + s))\lambda_{18}^V \\
& + 8(k \cdot p_0)^2(k \cdot p_-)\lambda_{19}^V - 4(k \cdot p_0)(k \cdot p_-)^2\lambda_{19}^V - 4(k \cdot p_0)(k \cdot p_-)M_\rho^2 \lambda_{19}^V \\
& + 4(k \cdot p_-)^2 M_\rho^2 \lambda_{19}^V + 4(k \cdot p_0)^2 s\lambda_{19}^V - 4(k \cdot p_0)(k \cdot p_-)s\lambda_{19}^V - 2k \cdot p_0 M_\rho^2 s\lambda_{19}^V \\
& + 4k \cdot p_- M_\rho^2 s\lambda_{19}^V - (k \cdot p_0)s^2\lambda_{19}^V + M_\rho^2 s^2\lambda_{19}^V - 8(k \cdot p_0)^3\lambda_{21}^V + 4(k \cdot p_0)^2(k \cdot p_-)\lambda_{21}^V \\
& + 4(k \cdot p_0)^2 M_\rho^2 \lambda_{21}^V - 4(k \cdot p_0)(k \cdot p_-)M_\rho^2 \lambda_{21}^V + 2(k \cdot p_0)^2 s\lambda_{21}^V - 2k \cdot p_0 M_\rho^2 s\lambda_{21}^V \\
& + 8(k \cdot p_0)^3\lambda_{22}^V - 4(k \cdot p_0)^2(k \cdot p_-)\lambda_{22}^V + 4(k \cdot p_0)(k \cdot p_-)M_\rho^2 \lambda_{22}^V - 2(k \cdot p_0)^2 s\lambda_{22}^V \\
& + 2k \cdot p_0 M_\rho^2 s\lambda_{22}^V)) \Big) + \frac{1}{M_\rho^2 D_\rho [(k + p_-)^2]} \left(2G_V(2(2(k \cdot p_-)^2 - (k \cdot p_-)s + M_\rho^2 s)\kappa_{12}^V \right. \\
& + k \cdot p_-(-2k \cdot p_- + 2M_\rho^2 + s)\kappa_{16}^V) - F_V(2(2(k \cdot p_-)^2 + 2k \cdot p_- M_\rho^2 - (k \cdot p_-)s \\
& + M_\rho^2 s)\kappa_{12}^V + k \cdot p_-(-2k \cdot p_- + 4M_\rho^2 + s)\kappa_{16}^V) + \sqrt{2}(k \cdot p_- \kappa_{16}^V(-(2k \cdot p_- - 4M_\rho^2 - s) \\
& (2k \cdot p_0 + s)\lambda_{16}^V + 2((2k \cdot p_- - 4M_\rho^2 - s)(2k \cdot p_0 + s)\lambda_{17}^V - (2k \cdot p_- - 2M_\rho^2 - s) \\
& (P - q)^2 \lambda_{18}^V - 4(k \cdot p_0)(k \cdot p_-)\lambda_{19}^V + 4k \cdot p_- M_\rho^2 \lambda_{19}^V + 2(k \cdot p_0)s\lambda_{19}^V - 2(k \cdot p_-)s\lambda_{19}^V \\
& + 2M_\rho^2 s\lambda_{19}^V + s^2\lambda_{19}^V + 4(k \cdot p_-)^2\lambda_{21}^V - 4k \cdot p_- M_\rho^2 \lambda_{21}^V - 2(k \cdot p_-)s\lambda_{21}^V - 4(k \cdot p_-)^2\lambda_{22}^V
\end{aligned}$$

$$\begin{aligned}
& + 8k \cdot p_- M_\rho^2 \lambda_{22}^V + 2(k \cdot p_-) s \lambda_{22}^V)) + 2\kappa_{12}^V ((2k \cdot p_0 + s)(2(k \cdot p_-)^2 + 2k \cdot p_- M_\rho^2 \\
& - (k \cdot p_-) s + M_\rho^2 s) \lambda_{16}^V + 2((2k \cdot p_0 + s)(-2(k \cdot p_-)^2 - M_\rho^2 s + k \cdot p_- (-2M_\rho^2 + s)) \lambda_{17}^V \\
& + (P - q)^2 (2(k \cdot p_-)^2 - (k \cdot p_-) s + M_\rho^2 s) \lambda_{18}^V + 4(k \cdot p_0) (k \cdot p_-)^2 \lambda_{19}^V - 4(k \cdot p_0) \\
& (k \cdot p_-) M_\rho^2 \lambda_{19}^V + 4(k \cdot p_-)^2 M_\rho^2 \lambda_{19}^V - 2(k \cdot p_0) (k \cdot p_-) s \lambda_{19}^V + 2(k \cdot p_-)^2 s \lambda_{19}^V \\
& + 2k \cdot p_0 M_\rho^2 s \lambda_{19}^V - (k \cdot p_-) s^2 \lambda_{19}^V + M_\rho^2 s^2 \lambda_{19}^V - 4(k \cdot p_-)^3 \lambda_{21}^V + 2(k \cdot p_-)^2 s \lambda_{21}^V \\
& - 2k \cdot p_- M_\rho^2 s \lambda_{21}^V + 4(k \cdot p_-)^3 \lambda_{22}^V + 4(k \cdot p_-)^2 M_\rho^2 \lambda_{22}^V - 2(k \cdot p_-)^2 s \lambda_{22}^V \\
& + 2k \cdot p_- M_\rho^2 s \lambda_{22}^V))) \Big) + \frac{4(-k \cdot p_0 + k \cdot p_-)(\kappa_5^A - \kappa_6^A + \kappa_7^A)(F_A - 2\sqrt{2}(P - q)^2 \lambda_{17}^A)}{D_{a_1} [(P - q)^2]} \\
\end{aligned} \tag{134}$$

$$\begin{aligned}
a_3^{RR} = & \frac{1}{3\sqrt{2}F^2} \left(\frac{F_V}{M_\rho^2 M_\omega^2 D_\rho [(k + p_0)^2]} \left(\sqrt{2}F_V (M_\rho^2 (4k \cdot p_0 + 2k \cdot p_- + s) \kappa_3^{VV} \right. \right. \\
& + (-4k \cdot p_0 + 2k \cdot p_- + s) D_\rho [(k + p_0)^2] \kappa_4^{VV}) - 2(\sqrt{2}G_V (M_\rho^2 (2k \cdot p_- + s) \kappa_3^{VV} \\
& + (-4k \cdot p_0 + 2k \cdot p_- + s) D_\rho [(k + p_0)^2] \kappa_4^{VV}) + (2k \cdot p_0 - M_\rho^2) (4k \cdot p_0 \\
& - 2k \cdot p_- - s) \kappa_4^{VV} ((2k \cdot p_- + s) \lambda_{16}^V - 2(2k \cdot p_- + s) \lambda_{17}^V + 4k \cdot p_0 \lambda_{18}^V \\
& + 4k \cdot p_- \lambda_{18}^V + 2s \lambda_{18}^V + 4k \cdot p_- \lambda_{19}^V + 2s \lambda_{19}^V - 4k \cdot p_0 \lambda_{21}^V + 4k \cdot p_0 \lambda_{22}^V) \\
& + M_\rho^2 \kappa_3^{VV} ((2k \cdot p_- + s) (4k \cdot p_0 + 2k \cdot p_- + s) \lambda_{16}^V + 2(-(2k \cdot p_- + s) \\
& (4k \cdot p_0 + 2k \cdot p_- + s) \lambda_{17}^V + (2k \cdot p_- + s) (P - q)^2 \lambda_{18}^V + 4(k \cdot p_-)^2 \lambda_{19}^V \\
& + 4(k \cdot p_-) s \lambda_{19}^V + s^2 \lambda_{19}^V - 4(k \cdot p_0) (k \cdot p_-) \lambda_{21}^V - 2(k \cdot p_0) s \lambda_{21}^V + 8(k \cdot p_0)^2 \lambda_{22}^V \\
& \left. \left. + 4(k \cdot p_0) (k \cdot p_-) \lambda_{22}^V + 2(k \cdot p_0) s \lambda_{22}^V)) \right) + \frac{F_V}{M_\rho^2 M_\omega^2 D_\rho [(k + p_-)^2]} \right. \\
& \left(-\sqrt{2}F_V (M_\rho^2 (6k \cdot p_- + s) \kappa_3^{VV} + (-2k \cdot p_- + s) D_\rho [(k + p_-)^2] \kappa_4^{VV}) \right. \\
& + 2(\sqrt{2}G_V (M_\rho^2 (2k \cdot p_- + s) \kappa_3^{VV} + (-2k \cdot p_- + s) D_\rho [(k + p_-)^2] \kappa_4^{VV}) \\
& + (2k \cdot p_- - M_\rho^2) (2k \cdot p_- - s) \kappa_4^{VV} ((2k \cdot p_0 + s) \lambda_{16}^V - 2(2k \cdot p_0 + s) \lambda_{17}^V \\
& + 4k \cdot p_0 \lambda_{18}^V + 4k \cdot p_- \lambda_{18}^V + 2s \lambda_{18}^V + 4k \cdot p_0 \lambda_{19}^V + 2s \lambda_{19}^V - 4k \cdot p_- \lambda_{21}^V \\
& + 4k \cdot p_- \lambda_{22}^V) + M_\rho^2 \kappa_3^{VV} ((2k \cdot p_0 + s) (6k \cdot p_- + s) \lambda_{16}^V + 2(-(2k \cdot p_0 + s) \\
& (6k \cdot p_- + s) \lambda_{17}^V + (2k \cdot p_- + s) (P - q)^2 \lambda_{18}^V - 4(k \cdot p_0) (k \cdot p_-) \lambda_{19}^V \\
& + 8(k \cdot p_-)^2 \lambda_{19}^V + 2(k \cdot p_0) s \lambda_{19}^V + 2(k \cdot p_-) s \lambda_{19}^V + s^2 \lambda_{19}^V - 4(k \cdot p_-)^2 \lambda_{21}^V \\
& \left. \left. - 2(k \cdot p_-) s \lambda_{21}^V + 12(k \cdot p_-)^2 \lambda_{22}^V + 2(k \cdot p_-) s \lambda_{22}^V)) \right) + \frac{4F_V}{M_\omega^2 D_{a_1} [(P - q)^2]} \right)
\end{aligned}$$

$$\begin{aligned}
& \left((-k \cdot p_0 + k \cdot p_-)(\kappa_2^{VA} - \kappa_3^{VA} - \kappa_4^{VA})(\sqrt{2}F_A - 4(P-q)^2\lambda_{17}^A) \right) \\
& + \frac{8(-k \cdot p_0 + k \cdot p_-)\kappa_5^{VA}(\sqrt{2}G_V - 2s\lambda_{21}^V)(F_A - 2\sqrt{2}(P-q)^2\lambda_{17}^A)}{D_{a_1}[(P-q)^2]D_\rho[s]} \\
& + \frac{2(F_A - 2\sqrt{2}(P-q)^2\lambda_{17}^A)}{M_\rho^2 D_{a_1}[(P-q)^2]D_\rho[(k+p_-)^2]} \left(k \cdot p_- \kappa_{16}^V ((-8(k \cdot p_0)(k \cdot p_-) + 8k \cdot p_- M_\rho^2 \right. \\
& + 4(k \cdot p_0)s - 4(k \cdot p_-)s + 4M_\rho^2 s + 2s^2)\lambda_2^{VA} + 2M_\rho^2(4k \cdot p_0 - 2k \cdot p_- + s)\lambda_3^{VA} \\
& + 4(k \cdot p_0)(k \cdot p_-)\lambda_4^{VA} + 8(k \cdot p_-)^2\lambda_4^{VA} - 8k \cdot p_0 M_\rho^2 \lambda_4^{VA} - 4k \cdot p_- M_\rho^2 \lambda_4^{VA} \\
& - 2(k \cdot p_0)s\lambda_4^{VA} - 2(k \cdot p_-)s\lambda_4^{VA} - 2M_\rho^2 s\lambda_4^{VA} - s^2\lambda_4^{VA} + 8(k \cdot p_0)(k \cdot p_-)\lambda_5^{VA} \\
& - 16k \cdot p_0 M_\rho^2 \lambda_5^{VA} - 4(k \cdot p_0)s\lambda_5^{VA} + 4(k \cdot p_-)s\lambda_5^{VA} - 8M_\rho^2 s\lambda_5^{VA} - 2s^2\lambda_5^{VA}) \\
& + 2\kappa_{12}^V(2(2k \cdot p_0(k \cdot p_- - M_\rho^2))(2k \cdot p_- - s) - (k \cdot p_-)s^2 + M_\rho^2 s^2 \\
& + 2(k \cdot p_-)^2(2M_\rho^2 + s))\lambda_2^{VA} + 2k \cdot p_- M_\rho^2(4k \cdot p_0 - 2k \cdot p_- + s)\lambda_3^{VA} \\
& - 4(k \cdot p_0)(k \cdot p_-)^2\lambda_4^{VA} - 8(k \cdot p_-)^3\lambda_4^{VA} - 4(k \cdot p_0)(k \cdot p_-)M_\rho^2 \lambda_4^{VA} \\
& + 4(k \cdot p_-)^2 M_\rho^2 \lambda_4^{VA} + 2(k \cdot p_0)(k \cdot p_-)s\lambda_4^{VA} + 2(k \cdot p_-)^2 s\lambda_4^{VA} \\
& - 2k \cdot p_0 M_\rho^2 s\lambda_4^{VA} - 4k \cdot p_- M_\rho^2 s\lambda_4^{VA} + (k \cdot p_-)s^2\lambda_4^{VA} - M_\rho^2 s^2\lambda_4^{VA} \\
& - 8(k \cdot p_0)(k \cdot p_-)^2\lambda_5^{VA} - 8(k \cdot p_0)(k \cdot p_-)M_\rho^2 \lambda_5^{VA} + 4(k \cdot p_0)(k \cdot p_-)s\lambda_5^{VA} \\
& - 4(k \cdot p_-)^2 s\lambda_5^{VA} - 4k \cdot p_0 M_\rho^2 s\lambda_5^{VA} - 4k \cdot p_- M_\rho^2 s\lambda_5^{VA} + 2(k \cdot p_-)s^2\lambda_5^{VA} \\
& - 2M_\rho^2 s^2\lambda_5^{VA}) \Big) + \frac{2(F_A - 2\sqrt{2}(P-q)^2\lambda_{17}^A)}{M_\rho^2 D_{a_1}[(P-q)^2]D_\rho[(k+p_0)^2]} \left(k \cdot p_0 \kappa_{16}^V (2(4k \cdot p_0 - 2k \cdot p_- \right. \\
& - 2M_\rho^2 - s)(2k \cdot p_- + s)\lambda_2^{VA} - 2M_\rho^2(2k \cdot p_- + s)\lambda_3^{VA} - 16(k \cdot p_0)^2\lambda_4^{VA} \\
& + 4(k \cdot p_-)^2\lambda_4^{VA} + 8k \cdot p_0 M_\rho^2 \lambda_4^{VA} + 4k \cdot p_- M_\rho^2 \lambda_4^{VA} + 4(k \cdot p_-)s\lambda_4^{VA} \\
& + 2M_\rho^2 s\lambda_4^{VA} + s^2\lambda_4^{VA} - 16(k \cdot p_0)(k \cdot p_-)\lambda_5^{VA} + 8(k \cdot p_-)^2\lambda_5^{VA} \\
& + 16k \cdot p_- M_\rho^2 \lambda_5^{VA} - 8(k \cdot p_0)s\lambda_5^{VA} + 8(k \cdot p_-)s\lambda_5^{VA} + 8M_\rho^2 s\lambda_5^{VA} + 2s^2\lambda_5^{VA}) \\
& + 2\kappa_{12}^V(-2(2k \cdot p_- + s)(4(k \cdot p_0)^2 + M_\rho^2(2k \cdot p_- + s) - k \cdot p_0 \\
& (2k \cdot p_- + 2M_\rho^2 + s))\lambda_2^{VA} - 2k \cdot p_0 M_\rho^2(2k \cdot p_- + s)\lambda_3^{VA} + 16(k \cdot p_0)^3\lambda_4^{VA} \\
& - 4(k \cdot p_0)(k \cdot p_-)^2\lambda_4^{VA} - 8(k \cdot p_0)^2 M_\rho^2 \lambda_4^{VA} + 4(k \cdot p_0)(k \cdot p_-)M_\rho^2 \lambda_4^{VA} \\
& + 4(k \cdot p_-)^2 M_\rho^2 \lambda_4^{VA} - 4(k \cdot p_0)(k \cdot p_-)s\lambda_4^{VA} + 2k \cdot p_0 M_\rho^2 s\lambda_4^{VA} \\
& + 4k \cdot p_- M_\rho^2 s\lambda_4^{VA} - (k \cdot p_0)s^2\lambda_4^{VA} + M_\rho^2 s^2\lambda_4^{VA} + 16(k \cdot p_0)^2(k \cdot p_-)\lambda_5^{VA} \\
& - 8(k \cdot p_0)(k \cdot p_-)^2\lambda_5^{VA} + 8(k \cdot p_-)^2 M_\rho^2 \lambda_5^{VA} + 8(k \cdot p_0)^2 s\lambda_5^{VA} \\
& - 8(k \cdot p_0)(k \cdot p_-)s\lambda_5^{VA} + 8k \cdot p_- M_\rho^2 s\lambda_5^{VA} - 2(k \cdot p_0)s^2\lambda_5^{VA} + 2M_\rho^2 s^2\lambda_5^{VA}) \Big) \Big)
\end{aligned} \tag{135}$$

$$\begin{aligned}
a_3^{RRR} = & \frac{F_V(\sqrt{2}F_A - 4(P-q)^2\lambda_{17}^A)}{3\sqrt{2}F^2M_\rho^2M_\omega^2D_{a_1}[(P-q)^2]D_\rho[(k+p_0)^2]D_\rho[(k+p_-)^2]} \left(-M_\rho^2(2k \cdot p_- + s) \right. \\
& D_\rho[(k+p_-)^2]\kappa_3^{VV}(2(2k \cdot p_- + s)\lambda_2^{VA} + 4k \cdot p_0\lambda_3^{VA} - (4k \cdot p_0 + 2k \cdot p_- + s) \\
& (\lambda_4^{VA} + 2\lambda_5^{VA}) - D_\rho[(k+p_0)^2](2(k \cdot p_0 - k \cdot p_-)D_\rho[(k+p_-)^2]\kappa_4^{VV} \\
& (-2(2k \cdot p_- + 3s)\lambda_2^{VA} + (8k \cdot p_0 + 6k \cdot p_- + s)\lambda_4^{VA} + 2(2k \cdot p_- + 3s)\lambda_5^{VA}) \\
& + M_\rho^2\kappa_3^{VV}(2(4(k \cdot p_0)(k \cdot p_-) - 8(k \cdot p_-)^2 - 2(k \cdot p_0)s - 2(k \cdot p_-)s - s^2)\lambda_2^{VA} \\
& \left. - 4k \cdot p_-(4k \cdot p_0 - 2k \cdot p_- + s)\lambda_3^{VA} + (2k \cdot p_0 + s)(6k \cdot p_- + s)(\lambda_4^{VA} + 2\lambda_5^{VA})) \right) \\
& \quad (136)
\end{aligned}$$

$$\begin{aligned}
a_4^R = & \frac{4\sqrt{2}}{3F^2M_\rho^2} \left(\frac{1}{D_\rho[(k+p_0)^2]} \left(G_V(4(k \cdot p_0 - M_\rho^2)\kappa_{12}^V - 2k \cdot p_0\kappa_{16}^V) \right. \right. \\
& + F_V(-2(k \cdot p_0 - M_\rho^2)\kappa_{12}^V + k \cdot p_0\kappa_{16}^V) + \sqrt{2}(-k \cdot p_0\kappa_{16}^V((2k \cdot p_- + s)\lambda_{16}^V \\
& - 2(2k \cdot p_- + s)\lambda_{17}^V + 4k \cdot p_0\lambda_{18}^V + 4k \cdot p_-\lambda_{18}^V + 2s\lambda_{18}^V + 4k \cdot p_-\lambda_{19}^V + 4M_\rho^2\lambda_{19}^V \\
& + 2s\lambda_{19}^V - 4k \cdot p_0\lambda_{21}^V + 4k \cdot p_0\lambda_{22}^V) + 2\kappa_{12}^V((k \cdot p_0 - M_\rho^2)(2k \cdot p_- + s)\lambda_{16}^V \\
& - 2(k \cdot p_0 - M_\rho^2)(2k \cdot p_- + s)\lambda_{17}^V + 4(k \cdot p_0)^2\lambda_{18}^V + 4(k \cdot p_0)(k \cdot p_-)\lambda_{18}^V \\
& - 4k \cdot p_0M_\rho^2\lambda_{18}^V - 4k \cdot p_-M_\rho^2\lambda_{18}^V + 2(k \cdot p_0)s\lambda_{18}^V - 2M_\rho^2s\lambda_{18}^V + 4(k \cdot p_0)(k \cdot p_-)\lambda_{19}^V \\
& - 4k \cdot p_0M_\rho^2\lambda_{19}^V - 4k \cdot p_-M_\rho^2\lambda_{19}^V + 2(k \cdot p_0)s\lambda_{19}^V - 2M_\rho^2s\lambda_{19}^V - 4(k \cdot p_0)^2\lambda_{21}^V \\
& \left. + 4k \cdot p_0M_\rho^2\lambda_{21}^V + 4(k \cdot p_0)^2\lambda_{22}^V - 4k \cdot p_0M_\rho^2\lambda_{22}^V) \right) + \frac{1}{D_\rho[(k+p_-)^2]} \\
& \left(F_V(2(k \cdot p_- - M_\rho^2)\kappa_{12}^V - k \cdot p_-\kappa_{16}^V) + G_V(-4(k \cdot p_- - M_\rho^2)\kappa_{12}^V + 2k \cdot p_-\kappa_{16}^V) \right. \\
& + \sqrt{2}(k \cdot p_-\kappa_{16}^V((2k \cdot p_0 + s)\lambda_{16}^V - 2(2k \cdot p_0 + s)\lambda_{17}^V + 4k \cdot p_0\lambda_{18}^V + 4k \cdot p_-\lambda_{18}^V \\
& + 2s\lambda_{18}^V + 4k \cdot p_0\lambda_{19}^V + 4M_\rho^2\lambda_{19}^V + 2s\lambda_{19}^V - 4k \cdot p_-\lambda_{21}^V + 4k \cdot p_-\lambda_{22}^V) \\
& + \kappa_{12}^V(-2(k \cdot p_- - M_\rho^2)(2k \cdot p_0 + s)\lambda_{16}^V + 4(k \cdot p_- - M_\rho^2)(2k \cdot p_0 + s)\lambda_{17}^V \\
& - 4(k \cdot p_- - M_\rho^2)(P-q)^2\lambda_{18}^V - 8(k \cdot p_0)(k \cdot p_-)\lambda_{19}^V + 8k \cdot p_0M_\rho^2\lambda_{19}^V + 8k \cdot p_-M_\rho^2\lambda_{19}^V \\
& - 4(k \cdot p_-)s\lambda_{19}^V + 4M_\rho^2s\lambda_{19}^V + 8(k \cdot p_-)^2\lambda_{21}^V - 8k \cdot p_-M_\rho^2\lambda_{21}^V - 8(k \cdot p_-)^2\lambda_{22}^V \\
& \left. + 8k \cdot p_-M_\rho^2\lambda_{22}^V) \right) \right) \\
& \quad (137)
\end{aligned}$$

$$\begin{aligned}
a_4^{RR} = & \frac{2\sqrt{2}}{3F^2M_\rho^2} \left(\frac{F_V}{M_\omega^2 D_\rho [(k+p_0)^2]} \left(\sqrt{2}F_V(M_\rho^2 \kappa_3^{VV} + D_\rho [(k+p_0)^2] \kappa_4^{VV}) \right. \right. \\
& - 2\sqrt{2}G_V(M_\rho^2 \kappa_3^{VV} + D_\rho [(k+p_0)^2] \kappa_4^{VV}) + 2(2k \cdot p_0 - M_\rho^2) \kappa_4^{VV} \\
& ((2k \cdot p_- + s) \lambda_{16}^V - 2(2k \cdot p_- + s) \lambda_{17}^V + 4k \cdot p_0 \lambda_{18}^V + 4k \cdot p_- \lambda_{18}^V + 2s \lambda_{18}^V \\
& + 4k \cdot p_- \lambda_{19}^V + 2s \lambda_{19}^V - 4k \cdot p_0 \lambda_{21}^V + 4k \cdot p_0 \lambda_{22}^V) - 2M_\rho^2 \kappa_3^{VV} ((2k \cdot p_- + s) \lambda_{16}^V \\
& - 2(2k \cdot p_- + s) \lambda_{17}^V + 4k \cdot p_0 \lambda_{18}^V + 4k \cdot p_- \lambda_{18}^V + 2s \lambda_{18}^V + 8k \cdot p_0 \lambda_{19}^V + 4k \cdot p_- \lambda_{19}^V \\
& + 2s \lambda_{19}^V - 4k \cdot p_0 \lambda_{21}^V + 4k \cdot p_0 \lambda_{22}^V) \Big) + \frac{F_V}{M_\omega^2 D_\rho [(k+p_-)^2]} \left(-\sqrt{2}F_V(M_\rho^2 \kappa_3^{VV} \right. \\
& \left. \left. + D_\rho [(k+p_-)^2] \kappa_4^{VV}) + 2\sqrt{2}G_V(M_\rho^2 \kappa_3^{VV} + D_\rho [(k+p_-)^2] \kappa_4^{VV}) \right. \right. \\
& - 2(2k \cdot p_- - M_\rho^2) \kappa_4^{VV} ((2k \cdot p_0 + s) \lambda_{16}^V - 2(2k \cdot p_0 + s) \lambda_{17}^V + 4k \cdot p_0 \lambda_{18}^V \\
& + 4k \cdot p_- \lambda_{18}^V + 2s \lambda_{18}^V + 4k \cdot p_0 \lambda_{19}^V + 2s \lambda_{19}^V - 4k \cdot p_- \lambda_{21}^V + 4k \cdot p_- \lambda_{22}^V) \\
& + 2M_\rho^2 \kappa_3^{VV} ((2k \cdot p_0 + s) \lambda_{16}^V - 2(2k \cdot p_0 + s) \lambda_{17}^V + 4k \cdot p_0 \lambda_{18}^V + 4k \cdot p_- \lambda_{18}^V \\
& \left. \left. + 2s \lambda_{18}^V + 4k \cdot p_0 \lambda_{19}^V + 8k \cdot p_- \lambda_{19}^V + 2s \lambda_{19}^V - 4k \cdot p_- \lambda_{21}^V + 4k \cdot p_- \lambda_{22}^V) \right. \right) \\
& - \frac{2(F_A - 2\sqrt{2}(P-q)^2 \lambda_{17}^A)}{D_{a_1} [(P-q)^2] D_\rho [(k+p_-)^2]} \left(k \cdot p_- \kappa_{16}^V (-2(2k \cdot p_0 + 2M_\rho^2 + s) \lambda_2^{VA} \right. \\
& + 2M_\rho^2 \lambda_3^{VA} + 2k \cdot p_0 \lambda_4^{VA} + 4k \cdot p_- \lambda_4^{VA} - 2M_\rho^2 \lambda_4^{VA} + s \lambda_4^{VA} + 4k \cdot p_0 \lambda_5^{VA} + 2s \lambda_5^{VA}) \\
& + 2\kappa_{12}^V (2(2(k \cdot p_0)(k \cdot p_-) - 2k \cdot p_0 M_\rho^2 - 2k \cdot p_- M_\rho^2 + (k \cdot p_-)s - M_\rho^2 s) \lambda_2^{VA} \\
& + 2k \cdot p_- M_\rho^2 \lambda_3^{VA} - 2(k \cdot p_0)(k \cdot p_-) \lambda_4^{VA} - 4(k \cdot p_-)^2 \lambda_4^{VA} + 2k \cdot p_0 M_\rho^2 \lambda_4^{VA} \\
& + 2k \cdot p_- M_\rho^2 \lambda_4^{VA} - (k \cdot p_-)s \lambda_4^{VA} + M_\rho^2 s \lambda_4^{VA} - 4(k \cdot p_0)(k \cdot p_-) \lambda_5^{VA} \\
& \left. \left. + 4k \cdot p_0 M_\rho^2 \lambda_5^{VA} - 2(k \cdot p_-)s \lambda_5^{VA} + 2M_\rho^2 s \lambda_5^{VA}) \right) + \frac{2(F_A - 2\sqrt{2}(P-q)^2 \lambda_{17}^A)}{D_{a_1} [(P-q)^2] D_\rho [(k+p_0)^2]} \quad (138) \right. \\
& \left. \left(k \cdot p_0 \kappa_{16}^V (-2(2k \cdot p_- + 2M_\rho^2 + s) \lambda_2^{VA} + 2M_\rho^2 \lambda_3^{VA} + 4k \cdot p_0 \lambda_4^{VA} + 2k \cdot p_- \lambda_4^{VA} \right. \right. \\
& - 2M_\rho^2 \lambda_4^{VA} + s \lambda_4^{VA} + 4k \cdot p_- \lambda_5^{VA} + 2s \lambda_5^{VA}) + \kappa_{12}^V (4(-M_\rho^2(2k \cdot p_- + s) \\
& + k \cdot p_0(2k \cdot p_- - 2M_\rho^2 + s)) \lambda_2^{VA} + 4k \cdot p_0 M_\rho^2 \lambda_3^{VA} - 8(k \cdot p_0)^2 \lambda_4^{VA} \\
& - 4(k \cdot p_0)(k \cdot p_-) \lambda_4^{VA} + 4k \cdot p_0 M_\rho^2 \lambda_4^{VA} + 4k \cdot p_- M_\rho^2 \lambda_4^{VA} - 2(k \cdot p_0)s \lambda_4^{VA} \\
& + 2M_\rho^2 s \lambda_4^{VA} - 8(k \cdot p_0)(k \cdot p_-) \lambda_5^{VA} + 8k \cdot p_- M_\rho^2 \lambda_5^{VA} - 4(k \cdot p_0)s \lambda_5^{VA} \\
& \left. \left. + 4M_\rho^2 s \lambda_5^{VA}) \right) \right)
\end{aligned}$$

$$a_4^{RRR} = - \frac{4\sqrt{2}F_V(k \cdot p_0 - k \cdot p_-)(\sqrt{2}F_A - 4(P - q)^2\lambda_{17}^A)}{3F^2M_\rho^2M_\omega^2D_{a_1}[(P - q)^2]D_\rho[(k + p_0)^2]D_\rho[(k + p_-)^2]} \\ \left(- D_\rho[(k + p_0)^2]D_\rho[(k + p_-)^2]\kappa_4^{VV}(2\lambda_2^{VA} + \lambda_4^{VA} - 2\lambda_5^{VA}) \right. \\ \left. + M_\rho^2\kappa_3^{VV}(2(M_\rho^2 + (P - q)^2)\lambda_2^{VA} - 2M_\rho^2\lambda_3^{VA} + D_\rho[(P - q)^2](\lambda_4^{VA} + 2\lambda_5^{VA})) \right) \quad (139)$$

References

- [1] J. Grange et al. Muon (g-2) Technical Design Report. 1 2015, 1501.06858.
- [2] T. Aoyama et al. The anomalous magnetic moment of the muon in the Standard Model. 2006.04822.
- [3] Michel Davier, Andreas Hoecker, Bogdan Malaescu, and Zhiqing Zhang. Reevaluation of the hadronic vacuum polarisation contributions to the Standard Model predictions of the muon $g - 2$ and $\alpha(m_Z^2)$ using newest hadronic cross-section data. *Eur. Phys. J.*, C77(12):827, 2017, 1706.09436.
- [4] Alexander Keshavarzi, Daisuke Nomura, and Thomas Teubner. Muon $g - 2$ and $\alpha(M_Z^2)$: a new data-based analysis. *Phys. Rev.*, D97(11):114025, 2018, 1802.02995.
- [5] Gilberto Colangelo, Martin Hoferichter, and Peter Stoffer. Two-pion contribution to hadronic vacuum polarization. *JHEP*, 02:006, 2019, 1810.00007.
- [6] Martin Hoferichter, Bai-Long Hoid, and Bastian Kubis. Three-pion contribution to hadronic vacuum polarization. *JHEP*, 08:137, 2019, 1907.01556.
- [7] M. Davier, A. Hoecker, B. Malaescu, and Z. Zhang. A new evaluation of the hadronic vacuum polarisation contributions to the muon anomalous magnetic moment and to $\alpha(m_Z^2)$. *Eur. Phys. J.*, C80(3):241, 2020, 1908.00921.
- [8] Alexander Keshavarzi, Daisuke Nomura, and Thomas Teubner. The $g - 2$ of charged leptons, $\alpha(M_Z^2)$ and the hyperfine splitting of muonium. *Phys. Rev.*, D101:014029, 2020, 1911.00367.
- [9] Alexander Kurz, Tao Liu, Peter Marquard, and Matthias Steinhauser. Hadronic contribution to the muon anomalous magnetic moment to next-to-next-to-leading order. *Phys. Lett.*, B734:144–147, 2014, 1403.6400.
- [10] B. Chakraborty et al. Strong-Isospin-Breaking Correction to the Muon Anomalous Magnetic Moment from Lattice QCD at the Physical Point. *Phys. Rev. Lett.*, 120(15):152001, 2018, 1710.11212.

- [11] Sz. Borsanyi et al. Hadronic vacuum polarization contribution to the anomalous magnetic moments of leptons from first principles. *Phys. Rev. Lett.*, 121(2):022002, 2018, 1711.04980.
- [12] T. Blum, P. A. Boyle, V. Gülpers, T. Izubuchi, L. Jin, C. Jung, A. Jüttner, C. Lehner, A. Portelli, and J. T. Tsang. Calculation of the hadronic vacuum polarization contribution to the muon anomalous magnetic moment. *Phys. Rev. Lett.*, 121(2):022003, 2018, 1801.07224.
- [13] D. Giusti, V. Lubicz, G. Martinelli, F. Sanfilippo, and S. Simula. Electromagnetic and strong isospin-breaking corrections to the muon $g - 2$ from Lattice QCD+QED. *Phys. Rev. D*, 99(11):114502, 2019, 1901.10462.
- [14] Eigo Shintani and Yoshinobu Kuramashi. Study of systematic uncertainties in hadronic vacuum polarization contribution to muon $g - 2$ with 2+1 flavor lattice QCD. *Phys. Rev.*, D100(3):034517, 2019, 1902.00885.
- [15] C. T. H. Davies et al. Hadronic-vacuum-polarization contribution to the muon's anomalous magnetic moment from four-flavor lattice QCD. *Phys. Rev.*, D101(3):034512, 2020, 1902.04223.
- [16] Antoine Gérardin, Marco Cè, Georg von Hippel, Ben Hörz, Harvey B. Meyer, Daniel Mohler, Konstantin Ottnad, Jonas Wilhelm, and Hartmut Wittig. The leading hadronic contribution to $(g - 2)_\mu$ from lattice QCD with $N_f = 2 + 1$ flavours of $O(a)$ improved Wilson quarks. *Phys. Rev. D*, 100(1):014510, 2019, 1904.03120.
- [17] Christopher Aubin, Thomas Blum, Cheng Tu, Maarten Golterman, Chulwoo Jung, and Santiago Peris. Light quark vacuum polarization at the physical point and contribution to the muon $g - 2$. *Phys. Rev.*, D101(1):014503, 2020, 1905.09307.
- [18] D. Giusti and S. Simula. Lepton anomalous magnetic moments in Lattice QCD+QED. *PoS*, LATTICE2019:104, 2019, 1910.03874.
- [19] Kirill Melnikov and Arkady Vainshtein. Hadronic light-by-light scattering contribution to the muon anomalous magnetic moment revisited. *Phys. Rev.*, D70:113006, 2004, hep-ph/0312226.
- [20] Pere Masjuan and Pablo Sánchez-Puertas. Pseudoscalar-pole contribution to the $(g_\mu - 2)$: a rational approach. *Phys. Rev.*, D95(5):054026, 2017, 1701.05829.
- [21] Gilberto Colangelo, Martin Hoferichter, Massimiliano Procura, and Peter Stoffer. Dispersion relation for hadronic light-by-light scattering: two-pion contributions. *JHEP*, 04:161, 2017, 1702.07347.
- [22] Martin Hoferichter, Bai-Long Hoid, Bastian Kubis, Stefan Leupold, and Sebastian P. Schneider. Dispersion relation for hadronic light-by-light scattering: pion pole. *JHEP*, 10:141, 2018, 1808.04823.

- [23] Antoine Gérardin, Harvey B. Meyer, and Andreas Nyffeler. Lattice calculation of the pion transition form factor with $N_f = 2 + 1$ Wilson quarks. *Phys. Rev.*, D100(3):034520, 2019, 1903.09471.
- [24] Johan Bijnens, Nils Hermansson-Truedsson, and Antonio Rodríguez-Sánchez. Short-distance constraints for the HLbL contribution to the muon anomalous magnetic moment. *Phys. Lett.*, B798:134994, 2019, 1908.03331.
- [25] Gilberto Colangelo, Franziska Hagelstein, Martin Hoferichter, Laetitia Laub, and Peter Stoffer. Longitudinal short-distance constraints for the hadronic light-by-light contribution to $(g - 2)_\mu$ with large- N_c Regge models. *JHEP*, 03:101, 2020, 1910.13432.
- [26] Vladyslav Pauk and Marc Vanderhaeghen. Single meson contributions to the muon's anomalous magnetic moment. *Eur. Phys. J.*, C74(8):3008, 2014, 1401.0832.
- [27] Igor Danilkin and Marc Vanderhaeghen. Light-by-light scattering sum rules in light of new data. *Phys. Rev.*, D95(1):014019, 2017, 1611.04646.
- [28] Friedrich Jegerlehner. The Anomalous Magnetic Moment of the Muon. *Springer Tracts Mod. Phys.*, 274:1–693, 2017.
- [29] M. Knecht, S. Narison, A. Rabemananjara, and D. Rabetiarivony. Scalar meson contributions to a_μ from hadronic light-by-light scattering. *Phys. Lett.*, B787:111–123, 2018, 1808.03848.
- [30] Gernot Eichmann, Christian S. Fischer, and Richard Williams. Kaon-box contribution to the anomalous magnetic moment of the muon. *Phys. Rev.*, D101(5):054015, 2020, 1910.06795.
- [31] Pablo Roig and Pablo Sánchez-Puertas. Axial-vector exchange contribution to the hadronic light-by-light piece of the muon anomalous magnetic moment. *Phys. Rev.*, D101(7):074019, 2020, 1910.02881.
- [32] Gilberto Colangelo, Martin Hoferichter, Andreas Nyffeler, Massimo Passera, and Peter Stoffer. Remarks on higher-order hadronic corrections to the muon $g - 2$. *Phys. Lett.*, B735:90–91, 2014, 1403.7512.
- [33] Thomas Blum, Norman Christ, Masashi Hayakawa, Taku Izubuchi, Luchang Jin, Chulwoo Jung, and Christoph Lehner. The hadronic light-by-light scattering contribution to the muon anomalous magnetic moment from lattice QCD. *Phys. Rev. Lett.*, 124(13):132002, 2020, 1911.08123.
- [34] Tatsumi Aoyama, Masashi Hayakawa, Toichiro Kinoshita, and Makiko Nio. Complete Tenth-Order QED Contribution to the Muon g-2. *Phys. Rev. Lett.*, 109:111808, 2012, 1205.5370.
- [35] Tatsumi Aoyama, Toichiro Kinoshita, and Makiko Nio. Theory of the Anomalous Magnetic Moment of the Electron. *Atoms*, 7(1):28, 2019.

- [36] Andrzej Czarnecki, William J. Marciano, and Arkady Vainshtein. Refinements in electroweak contributions to the muon anomalous magnetic moment. *Phys. Rev.*, D67:073006, 2003, hep-ph/0212229. [Erratum: Phys. Rev. **D73**, 119901 (2006)].
- [37] C. Gnendiger, D. Stöckinger, and H. Stöckinger-Kim. The electroweak contributions to $(g - 2)_\mu$ after the Higgs boson mass measurement. *Phys. Rev.*, D88:053005, 2013, 1306.5546.
- [38] Marc Knecht. On some short-distance properties of the fourth-rank hadronic vacuum polarization tensor and the anomalous magnetic moment of the muon. *JHEP*, 08:056, 2020, 2005.09929.
- [39] Pere Masjuan, Pablo Roig, and Pablo Sánchez-Puertas. A different viewpoint on the Hadronic light-by-light tensor short-distance constraints. 2005.11761.
- [40] Jan Lüdtke and Massimiliano Procura. Effects of Longitudinal Short-Distance Constraints on the Hadronic Light-by-Light Contribution to the Muon $g - 2$. 2006.00007.
- [41] Bai-Long Hoid, Martin Hoferichter, and Bastian Kubis. Hadronic vacuum polarization and vector-meson resonance parameters from $e^+e^- \rightarrow \pi^0\gamma$. 2007.12696.
- [42] B. Ananthanarayan, Irinel Caprini, and Diganta Das. Test of analyticity and unitarity for the pion form-factor data around the ρ resonance. 2008.00669.
- [43] Christopher Aubin, Thomas Blum, Maarten Golterman, and Santiago Peris. On the application of Effective Field Theory to finite-volume effects in a_μ^{HVP} . 2008.03809.
- [44] Johan Bijnens, Nils Hermansson-Truedsson, Laetitia Laub, and Antonio Rodríguez-Sánchez. Short-distance HLbL contributions to the muon anomalous magnetic moment beyond perturbation theory. 2008.13487.
- [45] G. W. Bennett et al. Final Report of the Muon E821 Anomalous Magnetic Moment Measurement at BNL. *Phys. Rev.*, D73:072003, 2006, hep-ex/0602035.
- [46] M. Abe et al. A New Approach for Measuring the Muon Anomalous Magnetic Moment and Electric Dipole Moment. *PTEP*, 2019(5):053C02, 2019, 1901.03047.
- [47] V. M. Aul'chenko et al. Measurement of the pion form-factor in the range 1.04-GeV to 1.38-GeV with the CMD-2 detector. *JETP Lett.*, 82:743–747, 2005, hep-ex/0603021. [*Pisma Zh. Eksp. Teor. Fiz.* **82**, 841 (2005)].
- [48] M. N. Achasov et al. Update of the $e^+ e^- \rightarrow \pi^+ \pi^-$ cross-section measured by SND detector in the energy region 400-MeV < $s^{**}(1/2) < \text{file1000-MeV}$. *J. Exp. Theor. Phys.*, 103:380–384, 2006, hep-ex/0605013. [*Zh. Eksp. Teor. Fiz.* **130**, 437 (2006)].
- [49] V. M. Aul'chenko et al. Measurement of the $e^+ e^- \rightarrow \pi^+ \pi^-$ cross section with the CMD-2 detector in the 370 - 520-MeV c.m. energy range. *JETP Lett.*, 84:413–417, 2006, hep-ex/0610016. [*Pisma Zh. Eksp. Teor. Fiz.* **84**, 491 (2006)].

- [50] R. R. Akhmetshin et al. High-statistics measurement of the pion form factor in the rho-meson energy range with the CMD-2 detector. *Phys. Lett.*, B648:28–38, 2007, hep-ex/0610021.
- [51] F. Ambrosino et al. Measurement of $\sigma(e^+e^- \rightarrow \pi^+\pi^-\gamma(\gamma))$ and the dipion contribution to the muon anomaly with the KLOE detector. *Phys. Lett.*, B670:285–291, 2009, 0809.3950.
- [52] Bernard Aubert et al. Precise measurement of the $e^+ e^- \rightarrow \pi^+ \pi^- (\gamma)$ cross section with the Initial State Radiation method at BABAR. *Phys. Rev. Lett.*, 103:231801, 2009, 0908.3589.
- [53] F. Ambrosino et al. Measurement of $\sigma(e^+e^- \rightarrow \pi^+\pi^-)$ from threshold to 0.85 GeV² using Initial State Radiation with the KLOE detector. *Phys. Lett.*, B700:102–110, 2011, 1006.5313.
- [54] J. P. Lees et al. Precise Measurement of the $e^+e^- \rightarrow \pi^+\pi^-(\gamma)$ Cross Section with the Initial-State Radiation Method at BABAR. *Phys. Rev.*, D86:032013, 2012, 1205.2228.
- [55] M. Ablikim et al. Measurement of the $e^+e^- \rightarrow \pi^+\pi^-$ cross section between 600 and 900 MeV using initial state radiation. *Phys. Lett.*, B753:629–638, 2016, 1507.08188.
- [56] A. Anastasi et al. Combination of KLOE $\sigma(e^+e^- \rightarrow \pi^+\pi^-\gamma(\gamma))$ measurements and determination of $a_\mu^{\pi^+\pi^-}$ in the energy range $0.10 < s < 0.95$ GeV². *JHEP*, 03:173, 2018, 1711.03085.
- [57] Stanley J. Brodsky and Eduardo De Rafael. SUGGESTED BOSON - LEPTON PAIR COUPLINGS AND THE ANOMALOUS MAGNETIC MOMENT OF THE MUON. *Phys. Rev.*, 168:1620–1622, 1968.
- [58] B.E. Lautrup and E. De Rafael. Calculation of the sixth-order contribution from the fourth-order vacuum polarization to the difference of the anomalous magnetic moments of muon and electron. *Phys. Rev.*, 174:1835–1842, 1968.
- [59] Ricard Alemany, Michel Davier, and Andreas Hocker. Improved determination of the hadronic contribution to the muon (g-2) and to alpha (M(z)) using new data from hadronic tau decays. *Eur. Phys. J. C*, 2:123–135, 1998, hep-ph/9703220.
- [60] Sz. Borsanyi et al. Leading-order hadronic vacuum polarization contribution to the muon magnetic moment from lattice QCD. 2002.12347.
- [61] V. Cirigliano, G. Ecker, and H. Neufeld. Isospin violation and the magnetic moment of the muon. *Phys. Lett.*, B513:361–370, 2001, hep-ph/0104267.
- [62] V. Cirigliano, G. Ecker, and H. Neufeld. Radiative tau decay and the magnetic moment of the muon. *JHEP*, 08:002, 2002, hep-ph/0207310.
- [63] G. Ecker, J. Gasser, A. Pich, and E. de Rafael. The Role of Resonances in Chiral Perturbation Theory. *Nucl. Phys.*, B321:311–342, 1989.

- [64] G. Ecker, J. Gasser, H. Leutwyler, A. Pich, and E. de Rafael. Chiral Lagrangians for Massive Spin 1 Fields. *Phys. Lett.*, B223:425–432, 1989.
- [65] F. Flores-Báez, A. Flores-Tlalpa, G. López Castro, and G. Toledo Sánchez. Long-distance radiative corrections to the di-pion tau lepton decay. *Phys. Rev.*, D74:071301, 2006, hep-ph/0608084.
- [66] A. Flores-Tlalpa, F. Flores-Báez, G. López Castro, and G. Toledo Sánchez. Model-dependent radiative corrections to $\tau^- \rightarrow \pi^- \pi^0 \nu$ revisited. *Nucl. Phys. Proc. Suppl.*, 169:250–254, 2007, hep-ph/0611226. [,250(2006)].
- [67] M. Davier, A. Hoecker, G. López Castro, B. Malaescu, X. H. Mo, G. Toledo Sánchez, P. Wang, C. Z. Yuan, and Z. Zhang. The Discrepancy Between tau and e+e- Spectral Functions Revisited and the Consequences for the Muon Magnetic Anomaly. *Eur. Phys. J.*, C66:127–136, 2010, 0906.5443.
- [68] Michel Davier, Andreas Hoecker, Bogdan Malaescu, and Zhiqing Zhang. Reevaluation of the Hadronic Contributions to the Muon g-2 and to alpha(MZ). *Eur. Phys. J.*, C71:1515, 2011, 1010.4180. [Erratum: Eur. Phys. J.C72,1874(2012)].
- [69] Michel Davier, Andreas Höcker, Bogdan Malaescu, Chang-Zheng Yuan, and Zhiqing Zhang. Update of the ALEPH non-strange spectral functions from hadronic τ decays. *Eur. Phys. J. C*, 74(3):2803, 2014, 1312.1501.
- [70] J.A. Miranda and P. Roig. Effective-field theory analysis of the $\tau^- \rightarrow \pi^- \pi^0 \nu_\tau$ decays. *JHEP*, 11:038, 2018, 1806.09547.
- [71] Vincenzo Cirigliano, Adam Falkowski, Martín González-Alonso, and Antonio Rodríguez-Sánchez. Hadronic τ Decays as New Physics Probes in the LHC Era. *Phys. Rev. Lett.*, 122(22):221801, 2019, 1809.01161.
- [72] Sergi González-Solís, Alejandro Miranda, Javier Rendón, and Pablo Roig. Exclusive hadronic tau decays as probes of non-SM interactions. *Phys. Lett. B*, 804:135371, 2020, 1912.08725.
- [73] Andreas Crivellin, Martin Hoferichter, Claudio Andrea Manzari, and Marc Montull. Hadronic vacuum polarization: $(g-2)_\mu$ versus global electroweak fits. *Phys. Rev. Lett.*, 125(9):091801, 2020, 2003.04886.
- [74] Alexander Keshavarzi, William J. Marciano, Massimo Passera, and Alberto Sirlin. Muon $g-2$ and $\Delta\alpha$ connection. *Phys. Rev. D*, 102(3):033002, 2020, 2006.12666.
- [75] Eduardo de Rafael. On Constraints Between $\Delta\alpha_{\text{had}}(M_Z^2)$ and $(g_\mu - 2)_{\text{HVP}}$. *Phys. Rev. D*, 102(5):056025, 2020, 2006.13880.
- [76] Bogdan Malaescu and Matthias Schott. Impact of correlations between a_μ and α_{QED} on the EW fit. 2008.08107.

- [77] Fred Jegerlehner and Robert Szafron. $\rho^0 - \gamma$ mixing in the neutral channel pion form factor F_π^e and its role in comparing e^+e^- with τ spectral functions. *Eur. Phys. J. C*, 71:1632, 2011, 1101.2872.
- [78] Mattia Bruno, Taku Izubuchi, Christoph Lehner, and Aaron Meyer. On isospin breaking in τ decays for $(g-2)_\mu$ from Lattice QCD. *PoS*, LATTICE2018:135, 2018, 1811.00508.
- [79] Fred Jegerlehner. Muon $g-2$ theory: The hadronic part. *EPJ Web Conf.*, 166:00022, 2018, 1705.00263.
- [80] P. D. Ruiz-Femenía, A. Pich, and J. Portolés. Odd intrinsic parity processes within the resonance effective theory of QCD. *JHEP*, 07:003, 2003, hep-ph/0306157.
- [81] V. Cirigliano, G. Ecker, M. Eidemuller, A. Pich, and J. Portolés. The $< \text{VAP} >$ Green function in the resonance region. *Phys. Lett.*, B596:96–106, 2004, hep-ph/0404004.
- [82] V. Cirigliano, G. Ecker, M. Eidemuller, Roland Kaiser, A. Pich, and J. Portolés. The $< \text{SPP} >$ Green function and SU(3) breaking in K(13) decays. *JHEP*, 04:006, 2005, hep-ph/0503108.
- [83] V. Cirigliano, G. Ecker, M. Eidemuller, Roland Kaiser, A. Pich, and J. Portolés. Towards a consistent estimate of the chiral low-energy constants. *Nucl. Phys.*, B753:139–177, 2006, hep-ph/0603205.
- [84] Zhi-Hui Guo. Study of $\tau \rightarrow V P \nu(\tau)$ in the framework of resonance chiral theory. *Phys. Rev. D*, 78:033004, 2008, 0806.4322.
- [85] D. Gómez Dumm, P. Roig, A. Pich, and J. Portolés. Hadron structure in $\tau \rightarrow KK \pi \nu(\tau)$ decays. *Phys. Rev.*, D81:034031, 2010, 0911.2640.
- [86] D. Gómez Dumm, P. Roig, A. Pich, and J. Portolés. $\tau \rightarrow \pi \pi \pi \nu(\tau)$ decays and the $a_1(1260)$ off-shell width revisited. *Phys. Lett.*, B685:158–164, 2010, 0911.4436.
- [87] Zhi-Hui Guo and Pablo Roig. One meson radiative tau decays. *Phys. Rev.*, D82:113016, 2010, 1009.2542.
- [88] Karol Kampf and Jiri Novotný. Resonance saturation in the odd-intrinsic parity sector of low-energy QCD. *Phys. Rev.*, D84:014036, 2011, 1104.3137.
- [89] Daniel Gómez Dumm and Pablo Roig. Resonance Chiral Lagrangian analysis of $\tau^- \rightarrow \eta^{(\prime)} \pi^- \pi^0 \nu_\tau$ decays. *Phys. Rev. D*, 86:076009, 2012, 1208.1212.
- [90] Yun-Hua Chen, Zhi-Hui Guo, and Han-Qing Zheng. Study of $\eta - \eta'$ mixing from radiative decay processes. *Phys. Rev.*, D85:054018, 2012, 1201.2135.
- [91] P. Colangelo, J.J. Sanz-Cillero, and F. Zuo. Holography, chiral Lagrangian and form factor relations. *JHEP*, 11:012, 2012, 1207.5744.
- [92] L.Y. Dai, J. Portolés, and O. Shekhovtsova. Three pseudoscalar meson production in e^+e^- annihilation. *Phys. Rev. D*, 88:056001, 2013, 1305.5751.

- [93] A. Guevara, G. López Castro, and P. Roig. Weak radiative pion vertex in $\tau^- \rightarrow \pi^- \nu_\tau \ell^+ \ell^-$ decays. *Phys. Rev. D*, 88(3):033007, 2013, 1306.1732.
- [94] Pablo Roig and Juan José Sanz Cillero. Consistent high-energy constraints in the anomalous QCD sector. *Phys. Lett.*, B733:158–163, 2014, 1312.6206.
- [95] Yun-Hua Chen, Zhi-Hui Guo, and Han-Qing Zheng. Radiative transition processes of light vector resonances in a chiral framework. *Phys. Rev.*, D90(3):034013, 2014, 1311.3366.
- [96] P. Roig, A. Guevara, and G. López Castro. $VV'P$ form factors in resonance chiral theory and the $\pi - \eta - \eta'$ light-by-light contribution to the muon $g-2$. *Phys. Rev. D*, 89(7):073016, 2014, 1401.4099.
- [97] Yun-Hua Chen, De-Liang Yao, and Han-Qing Zheng. A study of $\rho - \omega$ mixing in resonance chiral theory. *Commun. Theor. Phys.*, 69(1):50, 2018, 1710.11448.
- [98] A. Guevara, P. Roig, and J. J. Sanz-Cillero. Pseudoscalar pole light-by-light contributions to the muon ($g-2$) in Resonance Chiral Theory. *JHEP*, 06:160, 2018, 1803.08099.
- [99] Ling-Yun Dai, Javier Fuentes-Martín, and Jorge Portolés. Scalar-involved three-point Green functions and their phenomenology. *Phys. Rev. D*, 99(11):114015, 2019, 1902.10411.
- [100] Tomas Kadavý, Karol Kampf, and Jiri Novotný. OPE of Green Functions of Chiral Currents. 2006.13006.
- [101] V. Mateu and J. Portolés. Form-factors in radiative pion decay. *Eur. Phys. J. C*, 52:325–338, 2007, 0706.1039.
- [102] B. Moussallam. A Sum rule approach to the violation of Dashen's theorem. *Nucl. Phys. B*, 504:381–414, 1997, hep-ph/9701400.
- [103] Santiago Peris, Michel Perrottet, and Eduardo de Rafael. Matching long and short distances in large N(c) QCD. *JHEP*, 05:011, 1998, hep-ph/9805442.
- [104] M. Knecht, S. Peris, M. Perrottet, and E. de Rafael. Decay of pseudoscalars into lepton pairs and large N(c) QCD. *Phys. Rev. Lett.*, 83:5230–5233, 1999, hep-ph/9908283.
- [105] S. Peris, B. Phily, and E. de Rafael. Tests of large N(c) QCD from hadronic tau decay. *Phys. Rev. Lett.*, 86:14–17, 2001, hep-ph/0007338.
- [106] Marc Knecht and Andreas Nyffeler. Resonance estimates of $O(p^{**6})$ low-energy constants and QCD short distance constraints. *Eur. Phys. J. C*, 21:659–678, 2001, hep-ph/0106034.
- [107] Johan Bijnens, Elvira Gámiz, Edisher Lipartia, and Joaquim Prades. QCD short distance constraints and hadronic approximations. *JHEP*, 04:055, 2003, hep-ph/0304222.
- [108] B. Ananthanarayan and B. Moussallam. Four-point correlator constraints on electromagnetic chiral parameters and resonance effective Lagrangians. *JHEP*, 06:047, 2004, hep-ph/0405206.

- [109] A. Guevara, G. López-Castro, and P. Roig. $\tau^- \rightarrow \eta^{(\prime)}\pi^-\nu_\tau\gamma$ decays as backgrounds in the search for second class currents. *Phys. Rev.*, D95(5):054015, 2017, 1612.03291.
- [110] J. Bijnens, G. Ecker, and J. Gasser. Radiative semileptonic kaon decays. *Nucl. Phys.*, B396:81–118, 1993, hep-ph/9209261.
- [111] F. E. Low. Bremsstrahlung of very low-energy quanta in elementary particle collisions. *Phys. Rev.*, 110:974–977, 1958.
- [112] Gerard 't Hooft. A Planar Diagram Theory for Strong Interactions. *Nucl. Phys. B*, 72:461, 1974.
- [113] Gerard 't Hooft. A Two-Dimensional Model for Mesons. *Nucl. Phys. B*, 75:461–470, 1974.
- [114] Edward Witten. Baryons in the $1/n$ Expansion. *Nucl. Phys. B*, 160:57–115, 1979.
- [115] D. Gómez Dumm, A. Pich, and J. Portolés. The Hadronic off-shell width of meson resonances. *Phys. Rev. D*, 62:054014, 2000, hep-ph/0003320.
- [116] I.M. Nugent, T. Przedzinski, P. Roig, O. Shekhovtsova, and Z. Was. Resonance chiral Lagrangian currents and experimental data for $\tau^- \rightarrow \pi^-\pi^-\pi^+\nu_\tau$. *Phys. Rev. D*, 88:093012, 2013, 1310.1053.
- [117] I. Rosell, J.J. Sanz-Cillero, and A. Pich. Quantum loops in the resonance chiral theory: The Vector form-factor. *JHEP*, 08:042, 2004, hep-ph/0407240.
- [118] I. Rosell, P. Ruiz-Femenía, and J. Portolés. One-loop renormalization of resonance chiral theory: Scalar and pseudoscalar resonances. *JHEP*, 12:020, 2005, hep-ph/0510041.
- [119] Ignasi Rosell, Juan José Sanz-Cillero, and Antonio Pich. Towards a determination of the chiral couplings at NLO in $1/N(C)$: $L^{**}r(8)(\mu)$. *JHEP*, 01:039, 2007, hep-ph/0610290.
- [120] Jorge Portolés, Ignasi Rosell, and Pedro Ruiz-Femenía. Vanishing chiral couplings in the large- $N(C)$ resonance theory. *Phys. Rev. D*, 75:114011, 2007, hep-ph/0611375.
- [121] A. Pich, I. Rosell, and J.J. Sanz-Cillero. Form-factors and current correlators: Chiral couplings $L(10)\mu$ $^{**}r(\mu)$ and $C(87)^{**}r(\mu)$ at NLO in $1/N(C)$. *JHEP*, 07:014, 2008, 0803.1567.
- [122] J.J. Sanz-Cillero. Renormalization group equations in resonance chiral theory. *Phys. Lett. B*, 681:100–104, 2009, 0905.3676.
- [123] Antonio Pich, Ignasi Rosell, and Juan José Sanz-Cillero. The vector form factor at the next-to-leading order in $1/N(C)$: chiral couplings $L9(\mu)$ and $C88(\mu) - C90(\mu)$. *JHEP*, 02:109, 2011, 1011.5771.
- [124] D. Gómez Dumm and P. Roig. Dispersive representation of the pion vector form factor in $\tau \rightarrow \pi\pi\nu_\tau$ decays. *Eur. Phys. J.*, C73(8):2528, 2013, 1301.6973.
- [125] Sergi González-Solís and Pablo Roig. A dispersive analysis of the pion vector form factor and $\tau^- \rightarrow K^-K_S\nu_\tau$ decay. *Eur. Phys. J. C*, 79(5):436, 2019, 1902.02273.

- [126] Steven Weinberg. Phenomenological Lagrangians. *Physica A*, 96(1-2):327–340, 1979.
- [127] J. Gasser and H. Leutwyler. Chiral Perturbation Theory to One Loop. *Annals Phys.*, 158:142, 1984.
- [128] J. Gasser and H. Leutwyler. Chiral Perturbation Theory: Expansions in the Mass of the Strange Quark. *Nucl. Phys. B*, 250:465–516, 1985.
- [129] Johan Bijnens, Gilberto Colangelo, and Gerhard Ecker. The Mesonic chiral Lagrangian of order p^{**6} . *JHEP*, 02:020, 1999, hep-ph/9902437.
- [130] J. Bijnens, L. Girlanda, and P. Talavera. The Anomalous chiral Lagrangian of order p^{**6} . *Eur. Phys. J. C*, 23:539–544, 2002, hep-ph/0110400.
- [131] J. Wess and B. Zumino. Consequences of anomalous Ward identities. *Phys. Lett.*, 37B:95–97, 1971.
- [132] Edward Witten. Global Aspects of Current Algebra. *Nucl. Phys.*, B223:422–432, 1983.
- [133] A. Pich. Colorless mesons in a polychromatic world. In *Phenomenology of large $N(c)$ QCD. Proceedings, Tempe, USA, January 9-11, 2002*, pages 239–258, 2002, hep-ph/0205030.
- [134] Steven Weinberg. Precise relations between the spectra of vector and axial vector mesons. *Phys. Rev. Lett.*, 18:507–509, 1967.
- [135] Maarten F. L. Golterman and Santiago Peris. The 7/11 Rule: An Estimate of $m(\rho) / f(\pi)$. *Phys. Rev.*, D61:034018, 2000, hep-ph/9908252.
- [136] Matthias Jamin, José Antonio Oller, and Antonio Pich. S wave $K\pi$ scattering in chiral perturbation theory with resonances. *Nucl. Phys.*, B587:331–362, 2000, hep-ph/0006045.
- [137] Matthias Jamin, José Antonio Oller, and Antonio Pich. Strangeness changing scalar form-factors. *Nucl. Phys.*, B622:279–308, 2002, hep-ph/0110193.
- [138] Stanley J. Brodsky and Glennys R. Farrar. Scaling Laws at Large Transverse Momentum. *Phys. Rev. Lett.*, 31:1153–1156, 1973.
- [139] G. Peter Lepage and Stanley J. Brodsky. Exclusive Processes in Perturbative Quantum Chromodynamics. *Phys. Rev.*, D22:2157, 1980.
- [140] Yun-Hua Chen, Zhi-Hui Guo, and Bing-Song Zou. Unified study of $J/\psi \rightarrow PV$, $P\gamma^{(*)}$ and light hadron radiative processes. *Phys. Rev.*, D91:014010, 2015, 1411.1159.
- [141] T. H. Burnett and Norman M. Kroll. Extension of the low soft photon theorem. *Phys. Rev. Lett.*, 20:86, 1968.
- [142] Alain Flores-Tlalpa. *Modelo de dominancia de mesones para decaimientos semileptónicos de sabores pesados*. PhD thesis, CINVESTAV, IPN, 2008.
- [143] Francisco Guerrero and Antonio Pich. Effective field theory description of the pion form-factor. *Phys. Lett. B*, 412:382–388, 1997, hep-ph/9707347.

- [144] J. J. Sakurai. Theory of strong interactions. *Annals Phys.*, 11:1–48, 1960.
- [145] M. Gourdin and E. De Rafael. Hadronic contributions to the muon g-factor. *Nucl. Phys.*, B10:667–674, 1969.
- [146] A. Sirlin. Radiative corrections to $g(v)/g(\mu)$ in simple extensions of the $su(2) \times u(1)$ gauge model. *Nucl. Phys. B*, 71:29–51, 1974.
- [147] A. Sirlin. Current Algebra Formulation of Radiative Corrections in Gauge Theories and the Universality of the Weak Interactions. *Rev. Mod. Phys.*, 50:573, 1978. [Erratum: Rev.Mod.Phys. 50, 905 (1978)].
- [148] A. Sirlin. Large $m(W)$, $m(Z)$ Behavior of the $O(\alpha)$ Corrections to Semileptonic Processes Mediated by W . *Nucl. Phys. B*, 196:83–92, 1982.
- [149] W.J. Marciano and A. Sirlin. Radiative Corrections to beta Decay and the Possibility of a Fourth Generation. *Phys. Rev. Lett.*, 56:22, 1986.
- [150] W.J. Marciano and A. Sirlin. Electroweak Radiative Corrections to tau Decay. *Phys. Rev. Lett.*, 61:1815–1818, 1988.
- [151] Eric Braaten and Chong-Sheng Li. Electroweak radiative corrections to the semihadronic decay rate of the tau lepton. *Phys. Rev. D*, 42:3888–3891, 1990.
- [152] William J. Marciano and A. Sirlin. Radiative corrections to $\pi(\text{lepton } 2)$ decays. *Phys. Rev. Lett.*, 71:3629–3632, 1993.
- [153] Jens Erler. Electroweak radiative corrections to semileptonic tau decays. *Rev. Mex. Fis.*, 50:200–202, 2004, hep-ph/0211345.
- [154] Julian S. Schwinger. *PARTICLES, SOURCES, AND FIELDS. VOL. 3.* 10 1989.
- [155] Manuel Drees and Ken-ichi Hikasa. Scalar top production in $e^+ e^-$ annihilation. *Phys. Lett. B*, 252:127–134, 1990.
- [156] M. Tanabashi et al. Review of Particle Physics. *Phys. Rev.*, D98(3):030001, 2018.
- [157] P.A. Zyla et al. Review of Particle Physics. *To be published at Prog. Theor. Exp. Phys.*, 2020, 2020. 083C01.
- [158] M. Fujikawa et al. High-Statistics Study of the $\tau^- \rightarrow \pi^- \pi^0 \nu(\tau)$ Decay. *Phys. Rev. D*, 78:072006, 2008, 0805.3773.
- [159] S. Schael et al. Branching ratios and spectral functions of tau decays: Final ALEPH measurements and physics implications. *Phys. Rept.*, 421:191–284, 2005, hep-ex/0506072.
- [160] D. Babusci et al. Precision measurement of $\sigma(e^+ e^- \rightarrow \pi^+ \pi^- \gamma)/\sigma(e^+ e^- \rightarrow \mu^+ \mu^- \gamma)$ and determination of the $\pi^+ \pi^-$ contribution to the muon anomaly with the KLOE detector. *Phys. Lett.*, B720:336–343, 2013, 1212.4524.

- [161] M. Ablikim et al. Erratum to "Measurement of the $e^+e^- \rightarrow \pi^+\pi^-$ cross section between 600 and 900 MeV using initial state radiation". 2009.05011.
- [162] M. Benayoun, P. David, L. DelBuono, and F. Jegerlehner. Upgraded Breaking Of The HLS Model: A Full Solution to the $\tau^-e^+e^-$ and ϕ Decay Issues And Its Consequences On g-2 VMD Estimates. *Eur. Phys. J. C*, 72:1848, 2012, 1106.1315.
- [163] M. Benayoun, P. David, L. DelBuono, and F. Jegerlehner. An Update of the HLS Estimate of the Muon g-2. *Eur. Phys. J. C*, 73:2453, 2013, 1210.7184.
- [164] M. Benayoun, P. David, L. DelBuono, and F. Jegerlehner. Muon $g - 2$ estimates: can one trust effective Lagrangians and global fits? *Eur. Phys. J. C*, 75(12):613, 2015, 1507.02943.
- [165] M. Benayoun, L. Delbuono, and F. Jegerlehner. BHLS₂, a New Breaking of the HLS Model and its Phenomenology. *Eur. Phys. J. C*, 80(2):81, 2020, 1903.11034. [Erratum: Eur.Phys.J.C 80, 244 (2020)].
- [166] S. Anderson et al. Hadronic structure in the decay $\tau^- \rightarrow \pi^- \pi^0$ neutrino(τ). *Phys. Rev. D*, 61:112002, 2000, hep-ex/9910046.
- [167] K. Ackerstaff et al. Measurement of the strong coupling constant alpha(s) and the vector and axial vector spectral functions in hadronic tau decays. *Eur. Phys. J. C*, 7:571–593, 1999, hep-ex/9808019.
- [168] Shao-Zhou Jiang, Zhen-Long Wei, Qing-Sen Chen, and Qing Wang. Computation of the $O(p^6)$ order low-energy constants: An update. *Phys. Rev. D*, 92:025014, 2015, 1502.05087.